Investigations of the UV-induced DNA damage response in human cells and zebrafish embryos

Dissertation

Zur Erlangung des Grades Doktor

der Naturwissenschaften

Am Fachbereich Biologie

Der Johannes Gutenberg-Universität Mainz

Claudia Scalera

geb. am 21.03.1992 in Altamura, Italien

Mainz, Juni 2024

Summary

Organisms are constantly exposed to ultraviolet (UV) light by the sun, resulting in different DNA lesions. Thus, cells have developed DNA repair pathways such as nucleotide excision repair (NER) to efficiently repair UV light-induced DNA damage. Defects in the NER pathway are associated with the development of diseases such as Cockayne syndrome and melanoma. Many studies investigated the signaling pathways that are triggered by UV light irradiation in human cancer cell lines. However, only a few studies investigated these signaling pathways in whole organisms. Zebrafish experience UV-B light exposure in the wild, since UV-B light passes through clear water [1]. Zebrafish develop cancers that resemble human tumors both at molecular and histopathological level, and possess conserved DNA repair mechanisms, including NER pathway [2]. Therefore, zebrafish display a well-suited model organism to study the DNA damage response to UV light. In our study, we used UV-C irradiation since it generates DNA adducts, in particular cyclobutane pyrimidine dimers (CPDs) and 6-4 photoproducts (6-4PPs), which inhibit RNA polymerase II elongation.

We explored the gene regulatory mechanisms that allow zebrafish embryos to oppose UV-C-induced DNA damage. We applied state-of-the-art quantitative proteomics and genomics approaches to study the response of zebrafish embryos to UV-C radiation. We compared the changes in protein levels, phosohorylation- and ubiquitylation-dependent signaling and gene expression at early and late response to UV-C irradiation.

Using quantitative phosphoproteomics, we identified increased phosphorylation of proteins involved in translation and DNA repair. Moreover, UV-C-induced phosphorylation occurred on a specific sequence motif (S/TQ) targeted by protein kinases ATM and ATR. We detected sites that are present in human and to also be conserved in zebrafish embryos, such as VCP (S784) and nucks1a (S52). We found increased phosphorylation of Serine 115 in NELFE, which we have previously shown to be important for transcription regulation after UV-C light-induced DNA damage [3]. The prominent difference between the protein kinases that we could predict to be activated in human cells and zebrafish embryos upon UV-C stress includes G protein-coupled receptor kinases (GRKs) and transforming growth factor receptors (TGFBR). Furthermore, the exposure to UV-C radiation induces the decrease of total level of proteins involved in DNA replication and ATP production. Increased levels were found for proteins belonging to paraspeckles, mRNA processing and splicing factors. Differentially expressed genes were enriched for cell cycle arrest and DNA damage response. Finally, to investigate the changes in ubiquitin signaling induced by UV-C irradiation, we combined a pulldown using a high-affinity ubiquitin-binding domain (UBD) with quantitative proteomics in zebrafish embryos [4]. We found increased ubiquitylation of proteins involved in RNA processing and DNA repair, in particular the factors involved in Fanconi anemia (FA) repair pathway, FANCI and FANCD2, and in RNA processing.

In conclusion, this study provides the first overview of the UV-C-induced DNA damage response in zebrafish embryos.

Zusammenfassung

Organismen sind durch die Sonne ständig ultraviolettem (UV) Licht ausgesetzt, was zu verschiedenen DNA-Schäden führt. Daher haben die Zellen DNA-Reparaturwege wie die Nukleotid-Exzisionsreparatur (NER) entwickelt, um durch UV-Licht verursachte DNA-Schäden effizient zu reparieren. Defekte im NER-Signalweg werden mit der Entstehung von Krankheiten wie dem Cockayne-Syndrom und Melanomen in Verbindung gebracht. Viele Studien untersuchten die Signalwege, die durch UV-Licht-Bestrahlung in menschlichen Krebszelllinien ausgelöst werden, doch nur wenige Studien untersuchten diese Signalwege in ganzen Organismen. Zebrafische sind in freier Wildbahn UV-B-Licht ausgesetzt, da UV-B-Licht durch klares Wasser dringt [1]. Zebrafische entwickeln Krebsarten, die menschlichen Tumoren sowohl auf molekularer als auch auf histopathologischer Ebene ähneln, und verfügen über konservierte DNA-Reparaturmechanismen, einschließlich des NER-Signalwegs [2]. Daher sind Zebrafische ein gut geeigneter Modellorganismus zur Untersuchung der DNA-Schadensreaktion auf UV-Licht. In unserer Studie verwendeten wir UV-C-Bestrahlung, da sie DNA-Addukte, insbesondere Cyclobutan-Pyrimidin-Dimere (CPDs) und 6-4-Photoprodukte (6-4PPs), erzeugt welche die Elongation der RNA-Polymerase II hemmen. Wir untersuchten die genregulatorischen Mechanismen, die es Zebrafisch-Embryonen ermöglichen, sich gegen UV-C-induzierte DNA-Schäden zu wehren. Wir haben modernste quantitative Proteomik- und Genomikansätze angewandt, um die Reaktion von Zebrafischembryonen auf UV-C-Strahlung zu untersuchen. Wir verglichen die Veränderungen der Proteinkonzentrationen, der von Phosphorylierung und Ubiquitylierung abhängigen Signalübertragung und der Genexpression bei der frühen und späten Reaktion auf UV-C-Bestrahlung. Mithilfe der quantitativen Phosphoproteomik konnten wir eine erhöhte Phosphorylierung von Proteinen feststellen, die an der Translation und DNA-Reparatur beteiligt sind. Darüber hinaus erfolgte die UV-C-induzierte Phosphorylierung an einem spezifischen Sequenzmotiv (S/TQ), das von den Proteinkinasen ATM und ATR gesteuert wird. Wir entdeckten Stellen, die beim Menschen vorkommen und auch in Zebrafisch-Embryonen konserviert sind, wie VCP (S784) und nucks1a (S52). Wir fanden eine erhöhte Phosphorylierung von Serin 115 in NELFE, von dem wir zuvor gezeigt haben, dass es für die Transkriptionsregulation nach UV-C-Licht-induzierten DNA-Schäden wichtig ist [3]. Zu den auffälligen Unterschieden zwischen den Proteinkinasen, die nach UV-C-Belastung in menschlichen Zellen und Zebrafischembryonen aktiviert werden, gehören G-Protein-gekoppelte Rezeptorkinasen (GRKs) und transformierende Wachstumsfaktor-Rezeptoren (TGFBR). Darüber hinaus führt die Exposition gegenüber UV-C-Strahlung zu einer Verringerung des Gesamtniveaus von Proteinen, die an der DNA-Replikation und ATP-Produktion beteiligt sind. Wir fanden eine Anreicherung von Proteinen, die mit Paraspeckles, mRNA-Verarbeitung und Spleißfaktoren in Verbindung gebracht werden. Die von uns gefundenen, differenziell exprimierten Gene sind mit Zellzyklus-Stillstand und DNA-Schadensreaktion assoziiert. Um schließlich die durch UV-C-Bestrahlung induzierten Veränderungen im Ubiquitin-Signalweg zu untersuchen, kombinierten wir einen Pulldown mit einer hochaffinen Ubiquitin-Bindungsdomäne (UBD) mit quantitativer Proteomik in Zebrafischembryonen [4]. Wir fanden eine erhöhte Ubiquitylierung von Proteinen,

die an der RNA-Verarbeitung und DNA-Reparatur beteiligt sind, insbesondere von Faktoren, die am Reparaturweg der Fanconi-Anämie (FA), FANCI und FANCD2, beteiligt sind. Zusammenfassend lässt sich sagen, dass diese Studie den ersten Überblick über die UV-C-induzierte DNA-Schadensreaktion in Zebrafisch-Embryonen liefert.

Table of Contents

1 Introduction

Cells are constantly exposed to sources that can generate DNA lesions. To counteract the impact of the DNA lesions, cells have evolved an intricate DNA damage response (DDR) network that involves various pathways such as cell cycle arrest, DNA repair, apoptosis, senescence and regulation of transcription [5], [6], [7]. Stress conditions and DNA damage lead to the activation of cell cycle checkpoints and reallocating energy from regular cellular maintenance and specialized functions towards the repair process. In fact, a temporary pause of cell growth occurs and serves as a protective measure by preventing the replication and transmission of the damaged genome to future cell generations, thereby maintaining the overall integrity of the genetic and functional information of the cells [8]. Failure to remove DNA lesions can result in genetic mutations, which have the potential to contribute to the development of diseases, including cancer [9]. To maintain the overall health and integrity of the organism, across the evolution, cells developed also a mechanism known as programmed cell death, acting as a safeguard and allowing the elimination of those cells undergoing an extensive damage [10].

1.1 UV-light

The majority of living organisms are exposed to ultraviolet (UV) light, which can result in various effects, such as DNA damage, sunburn, premature skin aging, and an elevated risk of skin cancer [11], [12], [13]. UV radiation is emitted naturally from the sun and artificial sources, such as sunlamps, UV lamps and fluorescent lamps. Depending on the wavelength, UV light can be divided into three categories: UV-A (320-400 nm), UV-B (280-320 nm) and UV-C (100-280 nm). Among them, almost all UV-C and some UV-B are absorbed by the ozone layer and do not affect organisms [14], [15], [16]. The rest of the UV-B can be absorbed by the cells inducing the oxidative stress by generating the reactive oxygen species (ROS), which can lead to premature aging [17], [18], and erythema [19]. On the contrary, UV-A has a higher wavelength that, in human, can cause indirect DNA damage along with collagen and elastin fibre degradation through oxidative stress pathways [20] and is the major responsible of skin aging [21]. Since the maximal absorption of DNA occurs at 260 nm, namely in the UV-C radiation, UV-C induces the most severe DNA damage in the form of cyclobutane pyrimidine dimers (CPDs) and 6-4 photoproducts (6-4PPs), and RNA-protein crosslinks (RPCs) [22], [23], [24], [25].

1.2 Lesions generated in response to UV-C irradiation

1.2.1 Transcription-blocking lesions (TBLs)

The molecular origins of several skin cancers, such as melanoma, is associated to the UV-induced dimerization of adjacent pyrimidine nucleotides in DNA [26], [27], [28]. The exposure of cells to UV-C radiation generates cyclobutane pyrimidine dimers (CPDs) and 6-4 photoproducts (6-4PPs), both of which are DNA adducts that induce conformational alterations to the DNA double helix [29]. These molecular distortions, when accumulated, are implicated in the rise of skin cancers, for example cutaneous squamous cell carcinoma, basal cell carcinoma, and melanoma [30], [31], [32].

The cyclobutane thymine–thymine dimer (T∧T) represents the most cytotoxic of these UV-C-induced lesions, but various pyrimidine bases are susceptible to dimerization yielding a variety of CPDs due to the formation of covalent bonds at the C5-C6 positions. Conversely, 6-4PPs are characterized by a noncyclic bond linkage between the C6 atom of one pyrimidine residue and the C4 atom of the adjacent residue (**Figure 1**).

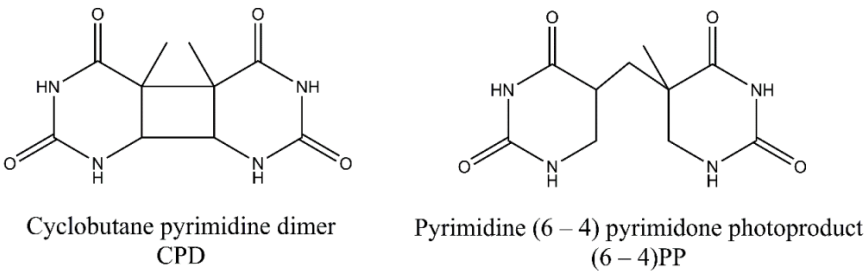

Figure 1. The main UV-induced photoproducts
CPDs and 6-4PPs structures (from [398]).

Although additional photoproducts have been identified, such as the cytosine photohydrate, which forms by water molecule addition to the cytosine double bond, known as cytosine photohydrate (6-hydroxy-5, 6-dihydrocytosine) [26], and the adenine dimer [27], these lesions are relatively unstable and considered to be less pathogenic.

The accumulation of such photoproducts presents a significant impediment to DNA replication and transcription processes, thus compromising genomic stability [7]. During transcription, RNA polymerase II (Pol II) is able to navigate past minor DNA anomalies, like oxidative lesions [28]. However, it cannot bypass substantial obstructions like CPDs and 6-4PPs, which are, for this reason, categorized as transcription-blocking lesions (TBLs). Although individual genes are upregulated, the presence of UV-C-induced lesions typically triggers a global cessation of transcriptional process, with normal transcriptional function only restored upon lesion excision [29], [30], [31]. The impaired cellular ability to remove the UV-induced DNA damages results in persistent transcriptional suppression, as observed in cells from Cockayne syndrome (CS) and Xeroderma Pigmentosum (XP) patients [31]. The primary mechanism employed by cells for the resolution of CPDs and 6-4PPs is the nucleotide excision repair (NER) pathway, which systematically excises the lesions, thus restoring DNA integrity and cellular function [32].

1.2.2 Oxidative damage

UV-C radiation can induce DNA damage indirectly through the generation of reactive free radical species [33]. The hydroxyl radical (OH*), which is the most reactive oxygen species (ROS), can be produced by the interaction of the superoxide radical ($O2^{-}$) with hydrogen peroxide (H_2O_2) in the presence of metal ions such as iron(II) (Fe^{2+}) or copper(I) (Cu^{+}) as catalytic agents [34], [35], [36], [37], [38]. ROS have the potential to compromise DNA integrity by generating oxidized nitrogen bases. Oxidation of pyrimidines can form hydrates and glycol derivatives mutagenic

lesions, instead oxidation of purines generates formamidopyrimidine derivative, 8-oxo derivatives, in particular 7,8 dihydro-8-oxogusnine (also known as 8oxo-guanine or 8-oxo-G) [39] (**Figure 2**).

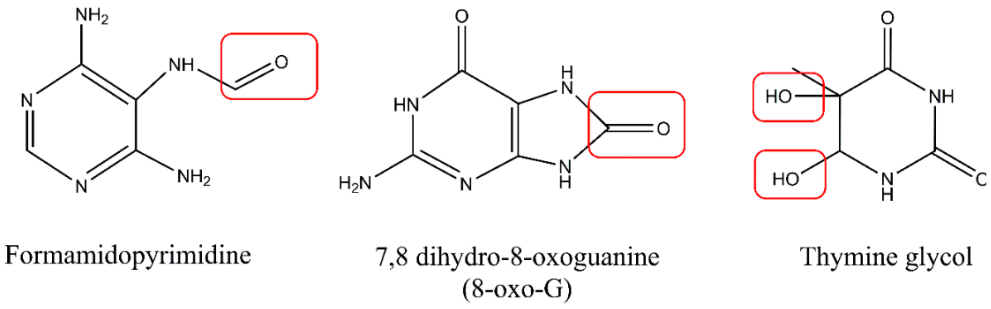

Figure 2. Oxidized DNA bases
Formamidopyrimidine derivative of adenine (Fapy-A), 7,8 dihydro-8-oxoguanine (8-oxo-G) and thymine glycol. The red boxes highlight the modification of the proper base structures by ROS (from [398]).

Such oxidative damage is capable of interfering with DNA replication and transcription by causing base modifications and provoking single-stranded DNA breaks (SSBs) by directly binding the sugar-phosphate backbone of the DNA. If SSBs occur concurrently on opposing strands, they may develop into the more severe double-stranded DNA breaks (DSBs). ROS not only damage nucleic acids but also adversely impact lipids and proteins. Excessive OH* can initiate lipid peroxidation, which in turn compromises cell membranes and lipoproteins [40]. This process may also yield reactive aldehydes as malondialdehyde that can further form DNA adducts with bases such as adenine, cytosine, or guanine [41], [42]. Oxidative stress can also affect proteins by structural changes, potentially leading to the loss of function [35], [43], [44]. It has been shown that UV-C exposure is associated with the inhibition of DNA topoisomerase I (top I), potentially transforming the cleaved top I complex into DSBs [45]. This supports the hypothesis that DSBs may be generated in a top I-dependent fashion following UV-induced replication stress. Similarly, ROS can impair topoisomerase II (top II), leading to DSBs formation [46], [47].To mitigate oxidative DNA damage, cells employ the base excision repair (BER) pathway [35], [43]. Instead, DSBs are typically removed via repair mechanisms such as non-homologous end joining (NHEJ) and homologous recombination (HR) [48].

1.2.3 RNA-protein crosslinks (RPCs)

Our recent publication [23] has revealed that, beyond causing DNA damage, both formaldehyde (FA) and UV-C irradiation are capable of inducing RNA-protein crosslinks (RPCs), which represent significant obstacles to the proper functioning of ribosomes, thereby disrupting the translation process [49], [50]. RPCs lead to ribosome stalling and subsequent collisions, resulting in the formation of di-ribosomes [51]. These di-ribosomes are subsequently targeted by the ubiquitin E3 ligase ZNF598, which ubiquitylates the 40S ribosomal subunits RPS10 and RPS20, a critical step in the activation of the ribosome-associated quality control (RQC) pathway. RQC pathway plays a crucial role in resolving stalled ribosomes [52], [53], [54]. K6-linked ubiquitylation is catalyzed by the E3 ligase RNF14 and targets RPCs proteins driving RPCs resolution. RPCs removal is aided by valosin-containing protein (VCP or p97), the ubiquitin-

dependent protein remodeler. RPCs induction and their resolution appear to be conserved across the organisms. In yeast, FA-induced K6-linked ubiquitylation has been shown to rely on the RNF14 ortholog ITT1, underscoring the evolutionary conservation of this pathway [23], [55] (**Figure 3**).

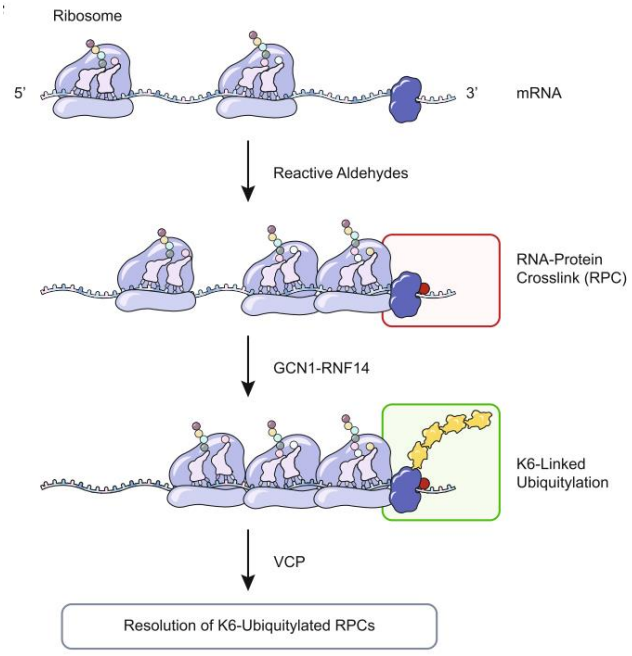

Figure 3. Formation of RPCs
Schematic representation of RPCs resolution. RPCs are formed in cells upon exposure to FA and UV-C. Translating ribosomes stall at the RPC, and subsequent K6-linked ubiquitylation catalyzed by RNF14 marks the RPC. VCP unfoldase is recruited to extract the protein and solved the RPC (from [23]).

1.3 DNA repair systems

Depending on the generated UV-induced DNA damage, different DNA repair mechanisms are employed. The relevant pathways involved in the removal of the UV-induced DNA lesions are the nucleotide excision repair (NER), the base excision repair (BER), the mismatch repair (MMR), and the double-strand break repair (DSBR) that includes homologous recombination (HR) and non-homologous end-joining (NHEJ) mechanisms, but cells employd also mechanisms such as Transletion synthesis (TLS) and Fanconi anemia (FA) repair.

1.3.1 Nucleotide excision repair (NER) pathway

The nucleotide excision repair (NER) is the main pathway employed by the cells to remove CPDs and 6-4PPs. This mechanism is highly conserved and is carried out by Xeroderma Pigmentosum (XP) factors. Indeed earliest studies were performed both in bacteria and in human. In bacteria, although the steps of the process and the protein functions are similar as in mammals, the pathway is less complicated and involves fewer proteins [56]. NER is divided in two subpathways: global-genome nucleotide excision repair (GG-NER) and transcription-coupled nucleotide excision repair (TC-NER). The two subpathways differ in the DNA damage recognition. On the one hand, GG-NER starts with the DNA damage recognition by XPC complex, consisting of XPC, the UV

excision repair protein RAD23 homolog B (RAD23B), and centrin-2 (CEN2) [57], [58], which bind the undamaged strand opposite to the lesion and recruit the transcription factor II H (TFIIH) complex. On the other hand, TC-NER occurs in transcribed active genes. TC-NER is triggered by the stalled-Pol II that functions as sensor for transcription-blocking lesions (TBLs) [59], [60], [61]. When transcribing Pol II encounters a bulky DNA lesion, CSB forms a stable interaction with Pol II [62], [63], [64]. This stability may be due to the C-terminus of CSB latching onto Pol II or binding to DNA upstream of Pol II, mediating the initial interaction before dissociating from the ATPase domain [65]. Stalled Pol II dissociates from the lesion through degradation or backtracking [61], [66], [67]. This removal provides access to the DNA lesion for the multi-subunit transcription factor II H (TFIIH) complex [68]. TFIIH promotes the binding of XPA to ssDNA-dsDNA junctions. XPA is involved in damage verification and serves as a scaffold for NER factors. RPA binds the exposed ssDNA. The structure-specific endonuclease XPF–ERCC1 heterodimer (which cuts 50 of the lesion) and XPG (which cuts 30 of the lesion) are recruited by XPA. TFIIH binds and displaces the excised ssDNA oligonucleotide containing the damage and the ssDNA gap of 22–30 nt is then filled by DNA Pol δ or DNA Pol ε and sealed by DNA ligase 1 [69] (**Figure 4**).

1.3.2 Base excision repair (BER) pathway

The base excision repair (BER) is a highly conserved pathway responsible for addressing damage resulting from the alkylation, deamination, and oxidation of DNA bases, such as 8-oxo-G [70], [71]. Although both prokaryotes and eukaryotes employ homologous proteins with analogous functions, eukaryotes possess a range of broader enzymes in comparison [72].

In the initial step, a damage-specific DNA glycosylase recognizes the modified nucleotide, cleaving the N-glycosyl bond between the sugar and the base and forming an abasic site (AP-site). Mammalian cells possess over 11 glycosylases, categorized into mono- or bifunctional glycosylases based on their reaction mechanism [71]. Monofunctional glycosylases, like uracil-DNA glycosylase (UNG), require a partner, such as DNA-apurinic site endonuclease (APE1), for the incision step. Instead, bifunctional enzymes, such as 8-oxoguanine DNA glycosylase (OGG1) and endonuclease 8-like 1 (NEIL1), possess both glycosylation and lyase activities. The AP-site generation results in SSBs. Spontaneous formation of AP-sites can also occur after depurination or depyrimidination. The AP-site is cleaved by the AP endonuclease, marking the initiation of BER, which then can diverge into short-patch or long-patch repair subpathway. In the short-patch pathway, DNA polymerase β (Pol β) replaces the excised nucleotide, repairing the lesion. If Pol β encounters difficulty at the 5' terminus, the long-patch BER ensues, rebuilding 2-6 nt around the blocking terminus with the assistance of proliferating cell nuclear antigen (PCNA), Flap endonuclease 1 (FEN1) and DNA polymerase δ/ε (Pol δ/ε). The final step involves the ligation and removal of the remaining nick by the LIG1 and FEN1 or the Ligase III-XRCC1 complex [71], [73], [74] (**Figure 4**).

1.3.3 Mismatch repair (MMR) pathway

The Mismatch repair (MMR) pathway plays a pivotal role in maintaining DNA integrity by addressing base-base mismatches and insertion or deletion mispairs generated during DNA

replication. The MMR machinery can recognize and remove DNA lesions induced by external agents such as cisplatin [75], [76]. The MMR process involves the identification and cleavage of the lesion, followed by the re-synthesis and ligation of the DNA [77].
In eukaryotes, the MMR recognition step include the activity of the MutS heterodimer (human homologs are MSH2, MSH3, MSH6), which recognizes the lesion. MutS with the MutL heterodimer (human homologs MLH1, MLH3, PMS1, PMS2) facilitate the recruitment and binding of the exonuclease EXO1. The replication clamp, PCNA, binds to MutS and MutL, supports EXO1 in the incision and starts the re-synthesis of the DNA [78], [79]. Subsequently, RPA covers naked ssDNA stretches before the Pol δ processes them into DSBs. At the end, the remaining nick is ligated by LIG1 (**Figure 4**).

1.3.4 Double-strand break repair (DBSR) pathways

The double-strand breaks (DBSs) represent a category of lesions frequently encountered consequently to UV irradiation [80]. DSBs are not generated directly by UV-light exposure, but their formation is linked to both the photoproducts and the presence of ROS in the cells. This occurrence is often associated with impediments in transcription or replication processes. DSBs may also arise during DNA repair course, such as the BER pathway. Despite their relatively infrequent incidence, DSBs represent one of the most severe form of DNA damage that cells may confront. The homologous recombination (HR) and the non-homologous end-joining (NHEJ) repair mechanisms belong to the DSBR pathway [6], [81]. Although both the repair processes share general common steps (recognition, end processing, and ligation), the proteins participating are different. HR relies on the DNA strands homology and utilizes sister-chromatid sequences as a template and is specifically activated during the synthesis (S) and G2 phases of the cell cycle, where the condensation of the chromatin facilitates homology searching [82], [83], [84]. During HR, the MRN complex, consisting of MRE11, RAD50, and NBS1, recognizes DSBs [85]. The DNA repair protein RAD50 (RAD50) tethers the broken DNA ends, the double-strand break repair protein MRE11 (MRE11) exhibits endonuclease and exonuclease activities, and nibrin (NBS1) facilitates protein-protein interactions promoting DNA repair. The generation of ssDNA is crucial for the homology searching and is favored by the activity of MRN complex [6], [86], [87]. The resection step is regulated by CtBP-interacting protein (CtlP). EXO1, DNA replication ATP-dependent helicase/nuclease DNA2 (DNA2), Bloom syndrome protein (BLM), and Werner syndrome ATP-dependent helicase (WRN) are also participating in the resection phase of HR [6], [88]. The resulting ssDNA is coated with RPA that contributes to its stability [89], [90] and provides the platform for RAD51 that plays a crucial role in nucleofilament formation and homology searching. RAD51 works together with the E3 ubiquitin ligase breast cancer type 2 susceptibility protein (BRCA2) to facilitate strand invasion onto an undamaged DNA duplex, forming a D-loop [91], [92]. The invaded strand can be elongated by DNA polymerase and ligated to the untouched ssDNA, creating a Holliday junction (HJ). This structure can be displaced by regulator of telomere elongation helicase (RTEL1) or cleaved by MUS81-EME1 nucleases. Alternatively, if the other ssDNA undergoes invasion, a double Holliday junction (dHJ) is formed after elongation and ligation. The resolution of dHJ involves either dissolution by the BLM-TOPOIII complex or

cleavage by endonucleases GEN1, MUS81-EME1, or SLX1-SLX4, leading to crossover or non-crossover HJ, respectively [93], [94], [95] (**Figure 4**).

The NHEJ functions throughout all the cell cycle and starts with the recognition of DSBs by the Ku70-Ku80 heterodimer, which encircles the broken DNA ends. Ku70-Ku80 guides the recruitment of downstream NHEJ factors [96]. The Ku70-Ku80-DNA complex attracts 5' exonucleases ARTEMIS and APLF to the DSBs. DNA-PKcs phosphorylates ARTEMIS, activating its endo- and exonuclease activities [97]. ARTEMIS processes the DNA ends, and the XRCC4-XLF complex forms filaments, providing additional stability.

XRCC4-XLF also serves as a scaffold for downstream factors in case further end processing is required. The recruitment of APLF removes an adenylate group covalently bound to a 5' phosphate. DNA polymerase μ (Pol μ) copies the entire strand to fill the interrupted fragment and XRCC4-Ligase IV seals the DNA filaments (**Figure 4**).

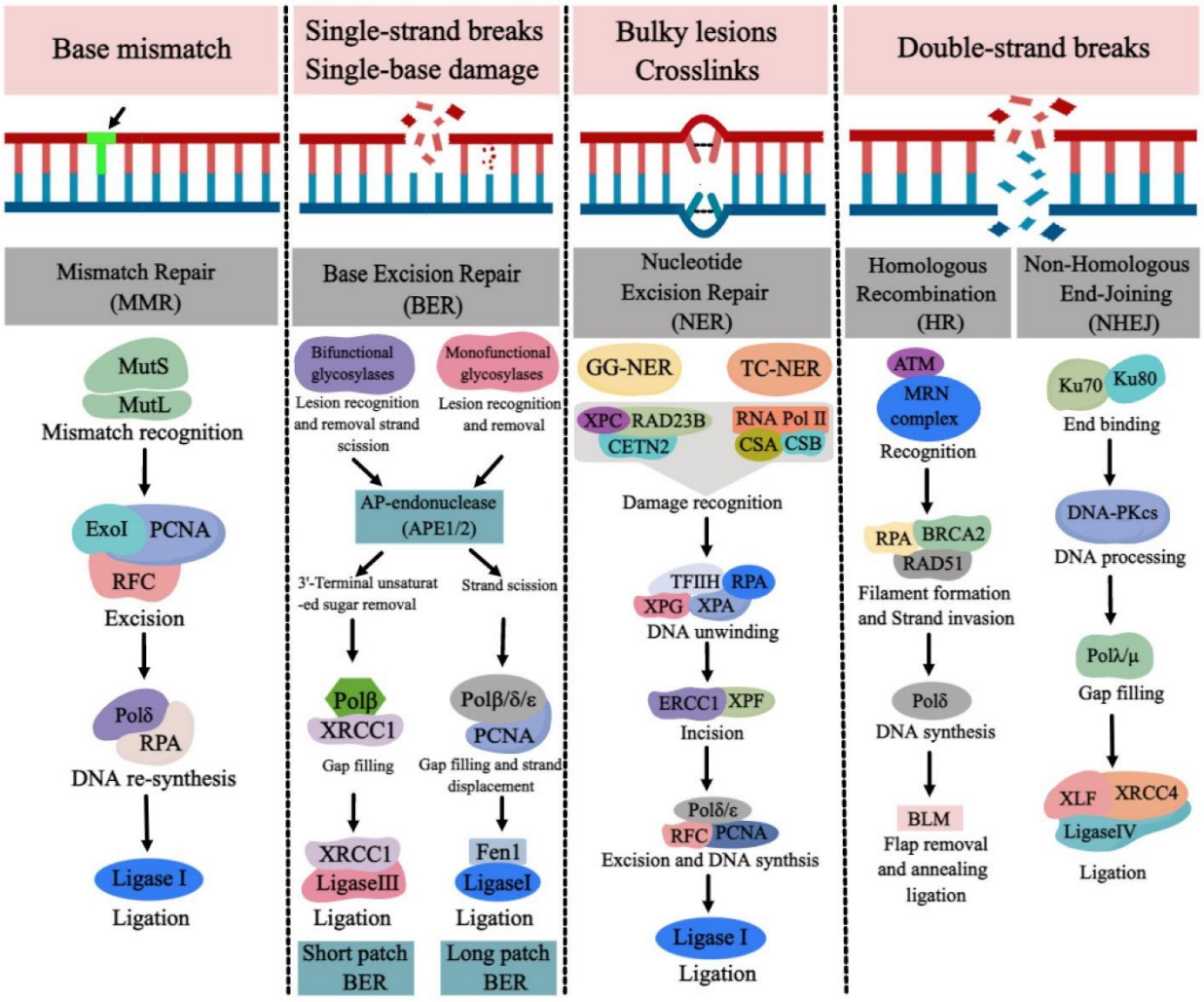

Figure 4. The main DNA repair pathways involved in the resolution of the UV-induced DNA damage
The mismatch repair (MMR), the base excision repair (BER), the nucleotide excision repair (NER), the homologous recombination repair (HR) and the non-homologous end-joining repair (NHEJ). The steps of the repair mechanisms are explained in the main text **1.3** (https://encyclopedia.pub/entry/42195).

Alternatively, poly ADP-ribose polymerase 1/2 (PARP1/2) can recognize DSBs, directing them to alternative NHEJ (alt-NHEJ). In alt-NHEJ, the MRN complex binds to PARP1/2, activating DSB signaling similar to classical NHEJ, and processes ends into short flaps (5-25 nt). CtIP and BRCA1-BARD1, together with MRN complex, execute the DSB resection. Pol δ fills the gap using ssDNA regions with microhomology, inhibiting HR events. Finally, XRCC1/Ligase III complex seals the strands [6], [98]. NHEJ predominates during the G1 phase, while HR requires a sister chromatid and prevails in late S and G2 phases [99], [100]. Alt-NHEJ can be activated in all the phases, with increased activity during S-phase accompanied by CDK activity [101].

1.3.5 Tranlesion synthesis (TLS)

Cells execute high-fidelity replication of genetic material mediated by DNA polymerases Pol δ and Pol ε, ensuring genomic stability and minimizing mutagenesis. These polymerases are integral components of repair pathways and exhibit differing fidelity and processivity. In response to UV radiation, the translesion synthesis (TLS), an unconventional repair mechanism, can be employed to avoid replication fork arrest [102]. TLS does not fully restore DNA sequence and structure, thereby increasing the chance to introduce mutations due to the persistence of lesions within the DNA strands. Eukaryotic cells employ a repertoire of TLS polymerases, including Y family (Pol η, Pol ι, Pol κ), B family (Pol ζ), X family (hPol β, λ, μ), and A family (θ and ν) [103], and the highly specialized dCMP transferase Rev1 [102]. TLS polymerases lack 3'-5' exonuclease proofreading activity, further compromising repair accuracy [102], [104]. TLS polymerases synthesize newly DNA bypassing UV-induced lesions, such as photoproducts. In particular, Pol η and Pol ζ can overcome TΛT dimers, while 6-4 TΛT dimers require REV1, thereby facilitating continuous DNA synthesis past damaged sites and preventing the formation of double-strand breaks (DSBs) [102], [103]. TLS activity is tightly regulated and ubiquitylation of PCNA appears to be crucial for lesion bypass [104], [105] even if conflicting findings exist regarding the monoubiquitylation of PCNA and its role in TLS [106].

1.3.6 Fanconi anemia (FA) repair pathway

UV irradiation can affect DNA replication by causing stalling of DNA replication forks. The Fanconi Anemia (FA) repair pathway plays a role in resolving this type of DNA damage [107]. In particular, the primary function associated with the FA pathway is the elimination of DNA interstrand crosslinks (ICLs), which are highly toxic DNA lesions that hinder replication by impeding DNA strand separation [108], [109].

The FA pathway is a complex process that is dysfunctional in a genetic disorder characterized by congenital abnormalities, bone marrow failure, and an increased predisposition to cancer. Currently, 22 FA genes have been identified and are grouped into the FA core complex (consisting of FANCA, B, C, E, F, G, L, and M subunits), the FANCI/FANCD2 (ID) complex, and downstream effector proteins. When DNA replication is obstructed by ICLs, the E3 ubiquitin ligase activity of the FA core complex monoubiquitylates the ID complex [109]. Ubiquitylated ID complex recruits downstream factors involved in transletion synthesis (TLS) and homologous recombination (HR) to initiate the removal of ICLs [110]. Recent investigations have demonstrated

that monoubiquitylation of the ID complex alters its affinity for ICLs and transforms it into a sliding DNA clamp, thereby facilitating the coordination of downstream repair reactions [111].
The process of ICLs removal is mediated by the SLX4/FANCP complex and its associated endonuclease XPF/ERCC1, which generate incisions and unhook the ICLs [112], [113]. Other nucleases, in particular MUS81/EME1 and the Fanconi-associated nuclease 1 (FAN1), have also been implicated in ICLs incision [109], [114]. The remaining ICL is bypassed by TLS polymerases REV1 and Pol ζ (a complex formed by REV3 and REV7) [115]. Finally, FANCD2 is deubiquitylated by the USP1–UAF1 complex to terminate the FA pathway [116], [117].

1.4 DNA damage response (DDR)

The DNA damage response (DDR) pathway is a complex network that aims to maintain cellular integrity by regulating key processes such as replication, transcription, RNA metabolism, repair, and protein synthesis. DDR is finely tuned by post-translational modifications (PTMs), which are covalent modifications of amino acid residues on target proteins, altering their properties and functions. PTMs like phosphorylation and ubiquitylation are crucial in DDR since they enable rapid, reversible, and dynamic responses to cellular stress [118].
Central to the DDR signaling are the serine-protein kinases ataxia telangiectasia mutated (ATM) and ataxia telangiectasia and Rad3-related protein (ATR), along with the DNA-dependent protein kinase catalytic subunit (DNA-PKcs) and poly [ADP-ribose] polymerases (PARPs). These enzymes are pivotal in initiating the DDR to various stimuli, including UV radiation [119]. ATM and DNA-PKcs primarily respond to double-strand breaks (DSBs), whereas ATR is activated by single-strand breaks (SSBs) and replication-associated damage. The modulation of chromatin structure near DNA damage sites through protein-protein interactions or PTMs facilitates an effective repair environment [6], [120]. Both ATM and ATR are initially inactive dimers that become active monomers upon activation [121], preferentially phosphorylating proteins at serine or threonine residues followed by glutamine (S/TQ motif) [122], [123].
Following DNA damage, ATM and ATR phosphorylate numerous substrates, in particular the histone H2AX at serine 139 (γH2AX) that marks the sites of damage and allows the recruitment of DNA repair proteins. γH2AX attracts chromatin-remodeling complexes, aiding in the repair process [120], [124]. The MRE11-RAD50-NBS1 (MRN) complex detects DNA damage, activating ATM, which can also be directly phosphorylated by oxidative stress. Key substrates of ATM include mediator of DNA damage checkpoint protein 1 (MDC1), nibrin (NBS1), TP53-binding protein 1 (53BP1), and breast cancer type 1 susceptibility protein (BRCA1) [125].
ATR, on the other hand, is recruited to stalled replication forks, where the ssDNA produced by the MCM2-7 complex helicase activity is coated with replication protein A (RPA). ATR recruitment and activation are triggered by interactions with ATR-interacting protein (ATRIP) and are dependent on DNA topoisomerase 2-binding protein 1 (TOPBP1) and the RAD9-RAD1-HUS1 complex [125], [126], [127].
Activation of ATM and ATR leads to the phosphorylation of downstream checkpoint kinases CHK1 and CHK2, respectively, which then inhibit cyclin-dependent kinases (CDKs), affecting the cell cycle progression. CHK1 targets CDC25 phosphatase, leading to cell cycle arrest, while CHK2

activates the tumor suppressor protein TP53, which can induce cell cycle arrest or apoptosis in response to DNA damage [128], [129]. TP53 activation is also directly influenced by ATM and ATR, which can phosphorylate TP53, leading to the release of its inhibitor, MDM2 [130].
Ubiquitylation, another critical PTM in DDR, consists on the attachment of ubiquitin to substrate proteins, affecting their function, localization, or stability. Ubiquitin is a small and highly conserved regulatory protein (8.5 kDa; 76 amino acids) [131], [132] and its carboxyl-terminal glycine residue forms an isopeptide bond with lysine residues in the substrate protein. Ubiquitin itself has seven internal lysines (K6, K11, K27, K29, K33, K48 and K63), which enable the formation of not only ubiquitylation of the substrate, but also the formation of ubiquitin chains. Ubiquitin chains exhibit diversity, with some substrates receiving a single ubiquitin molecule (monoubiquitylation), one molecule at multiple locations (multi-monoubiquitylation) or chains of multiple ubiquitin moieties (polyubiquitylation), which may be branched or folded in various conformations. The ubiquitin-proteasome system (UPS) plays a significant role in degrading damaged proteins, with ubiquitylation being a reversible process. Three enzymes drive the ubiquitylation process: E1 (ubiquitin-activating enzyme), E2 (ubiquitin-conjugating enzyme), and E3 (ubiquitin ligase). E3 ligases primarily confer substrate specificity to the ubiquitylation process [133]. In response to UV stress, E3 ligases, in particular RNF8 and RNF168, mediate the ubiquitylation of proteins like TP53BP1 and BRCA1 at damage sites, influencing the choice between HR and NHEJ repair pathways. Ubiquitylation is also crucial in the regulation of GG-NER. In fact, the UV-damaged DNA binding protein (UV-DDB) complex is involved in the recognition and ubiquitylation of the histones, XPC, and DDB2 to start the repair of the DNA lesion [134].

1.5 Transcription

1.5.1 General regulation of transcription

Transcription is an essential cellular process that takes place within the nucleus, where a strand of RNA is synthesized using a DNA strand as template. This newly created strand, known as messenger RNA (mRNA), is a product of the enzyme RNA polymerase II (Pol II). As a fundamental step in gene expression, transcription yields RNA sequences that will later be translated into proteins. The process plays a crucial role in cellular function regulation, as it allows cells to selectively produce specific genes in response to various stimuli. In the nucleus, transcription begins when general transcription factors (GTFs) identify and bind to the promoter region upstream of the transcription start site (TSS). This binding induces the assembly of the pre-initiation complex, which includes Pol II and additional factors like TFIIA, TFIIB, TFIID, TFIIE, TFIIF, and TFIIH [135]. Following this, Pol II unwinds the DNA to start the transcription of a small DNA segment, resulting in the synthesis of short RNA molecules. When the RNA transcript reaches beyond ten nucleotides, Pol II escapes the TSS and enters a phase known as promoter-proximal pausing (PPP). The transition into the elongation phase of transcription is propelled by the phosphorylation of the Pol II C-terminal domain (CTD) at serine 5. Once a transcript of 40–60 nucleotides is generated, Pol II is temporarily halted at the PPP site, where it recruits factors that aid in elongation and RNA processing, such as the capping binding complex (CBC), which protects

RNA from degradation [136]. A crucial player in Pol II pausing is the Negative Elongation Factor (NELF) complex, known to inhibit Pol II elongation activity [137]. Composed of four subunits, NELFA, NELFB, NELFC/D, and NELFE, the NELF complex interacts directly with Pol II via the polymerase association domain of NELFA and the emerging RNA strand [138], [139]. NELFB and NELFC have affinities for single-stranded oligonucleotides, while NELFE contains an RNA-binding domain [138]. PPP is recognized as a critical regulatory juncture for the expression of many genes, especially those related to development and stress responses [140]. The release of Pol II from PPP, allowing for progression into efficient elongation, is facilitated by the detachment of the NELF complex from the chromatin. Concurrently, splicing machinery components attach to Pol II, steering it into a phase of productive elongation to transcribe the gene [141]. This release from pausing is governed by the Positive Transcription Elongation Factor b (P-TEFb) kinase complex, comprising Cdk9 and Cyclin T, which phosphorylates both the Pol II CTD at serine 2 and the NELF complex, prompting the release of Pol II into the gene body for elongation [142]. The elongation phase culminates with the cleavage and the polyadenylation of pre-mRNAs at gene 3' ends, producing mature mRNA transcripts. The cleavage indicates the end of the 3' untranslated region (UTR) and is associated with transcription termination at transcription termination site (TTS) (**Figure 5**).

Errors in this process can lead to prematurely truncated gene products or transcriptional readthrough, which may have implications for the initiation of subsequent genes or generate extended 3' UTRs with potential regulatory functions [143], [144], [145]. Thus, meticulous regulation of pre-mRNA cleavage and transcription termination is essential for proper gene expression and avoiding detrimental effects.

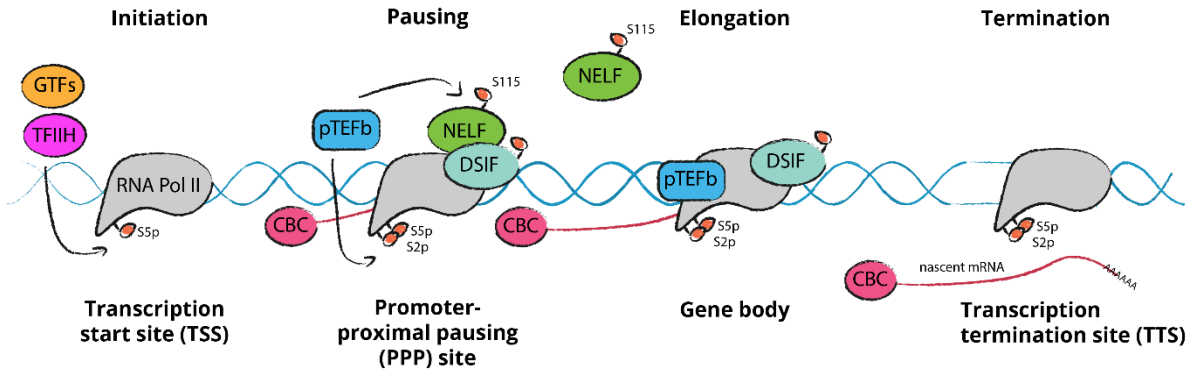

Figure 5. Schematic overview of the transcription steps
The preinitiation complex that recognizes and assembles on the upstream promoter region initiates transcription. RNA pol II (Pol II) binds to it and begins transcription with the help of the mediator complex. Shortly after the promoter (TSS), Pol II is pause d by NELF complex and the DRB sensitivity inducing factor (DSIF), which directly bind to 5' end of the nascent mRNA and regulate the recruitment of the RNA modifying proteins. The effective elongation is started by p-TEFb, which phosphorylates NELF, DSIF, and Pol II. During elongation, mRNA is processed directly by the splicing machinery and is released from Pol II as soon as it runs on PolyA signal sequence (TTS).

1.5.2 Regulation of transcription in response to UV-induced DNA damage

Following UV-light exposure, there is a rapid and widespread cessation of transcription across the genome, affecting even genes that have not been damaged. This global transcriptional shutdown is thought to be a protective strategy, allowing time for protein repair and preventing potential conflicts between the repair process and the ongoing transcription, thereby reducing the likelihood of additional damage [29], [30]. This regulation process involves the release of RNA polymerase II (Pol II) from promoter-proximal pause (PPP) site and its relocation into the gene body for accelerating the repair through the recognition of the DNA lesions [146], [147].

Despite the initial shutdown, transcription does not halt entirely [148]. In the beginning, transcription initiation resumes, albeit with a further reduction in elongation rates, affecting primarily short fragments (20–25 kb) [149], [148]. Full restoration of transcriptional elongation is observed at 48 hours after UV irradiation [148], [149]. The p38 signaling pathway is activated in response to UV light, playing a crucial role in this recovery process. Specifically, p38 phosphorylates MK2, which in turn phosphorylates p-TEFb and NELFE at S115 [150], [151]. These phosphorylation events lead to NELF complex dissociation from the chromatin through the recruitment of 14-3-3 proteins [151]. The removal of NELF allows Pol II to progress into the gene body, enhancing transcriptional elongation and thereby improving lesion recognition and repair [147], [152] (**Figure 6**).

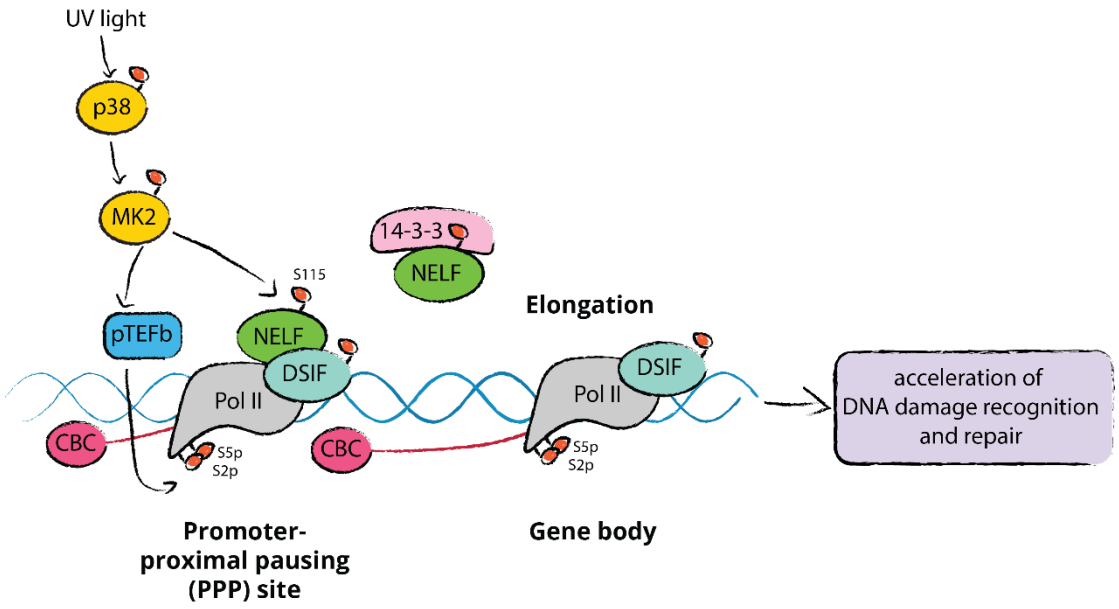

Figure 6. Regulation of Pol II at promoter-proximal pausing (PPP) site upon UV stress
Model for the NELF complex regulation by p38-MK2. Exposure of human cells to UV light leads to rapid activation of p38 and its downstream effector kinase MK2. MK2 triggers widespread phosphorylation of RNA-binding proteins, including the NELF complex subunit NELFE. Site-specific NELFE phosphorylation on S115 induces its transient interaction with 14-3-3. NELFE phosphorylation leads to dissociation of NELFE from chromatin that is accompanied by Pol II elongation and the acceleration of DNA damage recognition and repair.

As previously mentioned, DNA damage temporarily impedes transcription, with stalled Pol II prompting the recruitment of transcription-coupled nucleotide excision repair (TC-NER) factors [153]. For effective repair, stalled Pol II must be either removed or relocated from the damage site, a process regulated by PTMs. Ubiquitylation serves for Pol II dislocation, facilitating its release from DNA and subsequent degradation [146]. The residue K1268 has been identified as crucial for the ubiquitylation and degradation of RPB1, the catalytic subunit of Pol II, following UV-induced damage [154], [155]. Additionally, CSB, a factor involved in DNA damage recognition, can move Pol II either forward or backward from the lesion, as observed in both mammalian and bacterial systems [156].

The DDR-induced slowdown in transcription elongation also leads to changes in mRNA processing, such as polyadenylation and transcriptional termination. This results in alternative polyadenylation and premature termination, producing shorter RNA transcripts [157]. Several proteins play dual roles in DNA repair and transcription. For example, general transcription factors (GTFs) as TFIIH and TFIID, which include XPG and XPD, are essential for transcription initiation and are components of the NER machinery [135].

Moreover, non-coding RNAs (ncRNAs) are transcribed following double-strand breaks (DSBs) induction, potentially acting to recruit repair proteins to the damaged site [158], [159]. To increase cellular survival following UV-induced DNA damage, transcription factors are activated, among which p53 induces the transcription of p21, leading to cell cycle arrest and facilitating DNA repair [160].

1.6 Other cellular responses to UV irradiation

1.6.1 Kinase signaling pathways

Kinase signaling pathways are integral to the DNA damage response (DDR) to UV stress and play a pivotal role in determining cell fate through the regulation of processes such as replication, transcription, RNA metabolism, and protein production. DDR is modulated by post-translational modifications (PTMs), with phosphorylation and ubiquitylation being particularly significant.

Phosphorylation is mediated by protein kinases that add a phosphate group (PO_4) to the R group of amino acids. This modification transforms the nature of the protein from hydrophobic to hydrophilic, enabling conformational changes that facilitate interactions with other molecules and the dynamic assembly of protein complexes [161], [162], [163].

Upon UV exposure, cells activate signaling pathways by phosphorylating members of the mitogen-activated protein kinases (MAPKs) family that include extracellular signal-regulated kinases (ERKs), c-Jun NH2-terminal kinases (JNKs), and p38 kinases [164], [165]. These kinases phosphorylate proteins on Ser/Thr residues, and transduce extracellular stimuli from membrane receptors into cells, eliciting diverse responses [166], [167]. The MAPK pathway consists of a highly conserved signaling cascade that triggers MAPK kinase kinase (MAP3K), MAPK kinase (MAP2K) and MAPK. The cascade starts when a small GTP-binding protein of the Ras/Rho family

phosphorylates MAP3K, which activates MAP2K and, subsequently, MAPK (**Figure 7**). MAPKs are activated by dual phosphorylation within a conserved Thr-X-Tyr motif in the activation sequence. UV light, oxidative stress, hypoxia, interleukin-1 (IL-1) and TNF-α stimulate p38 MAPK signaling cascade [165], [168], [169]. p38 has four homologs (p38α, p38β, p38γ, and p38δ) activated through phosphorylation of T180-G181-Y182, the activation loop sequence. These homologs share 60% identity in the amino acid sequence and p38α is the most abundantly expressed in mammalian cells. p38 MAPK pathway initiate the phosphorylation cascade from MAP3Ks (e.g., MEKK1-3, MLK2/3, ASK1, TPL2, TAK1, TAO1/2, ZAK1) to MKK3/6 and finally p38 MAPK activation. p38 MAPK phosphorylates numerous substrates, for example MSK1/2, MNK1/2, and MK2/3, and influences transcription factors, protein synthesis, mRNA processing, and cell cycle regulation [170].

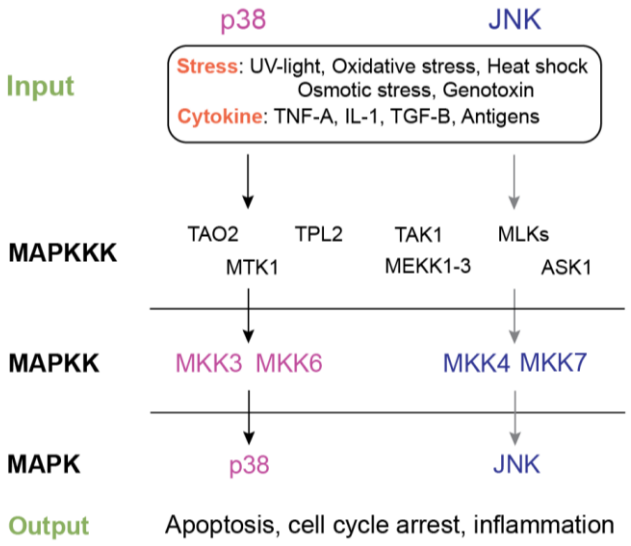

Figure 7. Regulation of cell-fate decision by stress-induced p38/JNK MAPK signaling pathways
External and internal stress, and cytokines trigger p38/JNK MAPK signaling pathways and the signaling cascade starts by activating MAPK kinase kinase (MAP3K), MAPK kinase (MAP2K), and MAPK (p38 and JNK) and induction of cellular processes as apoptosis, cell cycle arrest and inflammation.

JNK is another member of the MAPKs family and is activated by UV stress. JNK consists of three homologs (JNK1, JNK2, and JNK3) with distinct tissue expressions [167]. Upon phosphorylation of the activation loop sequence mediated by MKK4 and MKK7, activated JNK can lead to apoptosis, differentiation, or nuclear translocation, depending on the associated substrate [171] (**Figure 7**). A well-studied JNK substrate is c-Jun that, after being phosphorylated, forms the activator protein-1 (AP-1) complex with c-Fos, and modulate early gene transcription [167], [172], [173]. JNK phosphorylates various transcription factors and plays a role in repair of UV-induced DNA lesions through the phosphorylation of DGCR8, a microRNA processing protein [174]. Focusing on the role of kinase signaling pathways in response to UV stress, studies have shown that UV irradiation strongly activates both JNK and p38 [175], [176].

Furthermore, the activation of MAP3Ks, like MEKK4, by stress-inducible proteins such as GADD45 a/b/g, which bind directly to MEKK4 and induce its dimerization and

autophosphorylation, suggests a complex network of interactions leading to the activation of both p38 and JNK in response to UV stress [177], [178].

TAO family of MAP3Ks is also implicated in UV-induced response, with siRNA knockdown of TAO proteins resulting in decreased of p38 activation and reduction of UV-induced G2/M cell cycle arrest [179]. The role of ROS in the activation of p38 and JNK in response to UV irradiation has been demonstrated [180], [181]. For example, ASK1 activates p38 in response to oxidative stress [182]. In summary, kinase signaling pathways, particularly those involving MAPKs, are essential for the cellular response to UV stress, mediating a range of outcomes from cell cycle arrest to apoptosis and DNA repair [183]. These pathways are activated by a network of proteins that respond to UV-induced damage and oxidative stress, highlighting the complexity of cellular signaling in maintaining homeostasis and integrity in the face of environmental challenges.

1.6.2 Inflammatory response

As shown so far, UV irradiation is a potent environmental factor that can activate cellular signaling pathways through both direct and indirect lesions. Directly, UV exposure can lead to the production of ROS, while indirectly, it can cause DNA damage that subsequently triggers inflammatory responses. ROS are generated as natural byproducts of oxygen metabolism and are essential for a variety of physiological processes, including cellular signaling, defense against pathogens, and regulation of cell proliferation. However, when cells are exposed to UV light, there is an increased production of ROS, which can disrupt the delicate balance between ROS generation and the antioxidant defense mechanisms of the cells. This imbalance can result in oxidative stress, a state that has significant implications for cellular survival and homeostasis [184], [185].

It has been shown that UVB radiation exposure leads to a substantial increase in ROS production in human epidermal keratinocytes (HaCaT), which is accompanied by a reduction in cell viability [186]. Within the epidermis, several inflammatory signaling pathways are linked to different surface receptors, including epidermal growth factor receptors (EGFR) [187], transforming growth factor receptors (TGFR) [188], [189], toll-like receptors (TLRs) [190], IL-1 receptors, and tumor necrosis factor receptors (TNFR) [191], [192].

EGFR signaling plays a key role in regulating different aspects of keratinocyte physiology, such as proliferation, differentiation, cell adhesion, migration, and survival. The impact of EGFR on the inflammatory response following UV radiation exposure is complex. A study from El-Abaseri et al. (2013) demonstrated that UV-irradiated mice and keratinocytes treated with an EGFR inhibitor exhibited suppressed inflammatory responses, characterized by reduced immune cell infiltration and decreased levels of inflammatory cytokines, such as cyclooxygenases (COX2). This study also indicated that EGFR is partially responsible for the inflammatory response activated by the p38 mitogen-activated protein kinase (MAPK) pathway [193]. The p38 MAPK signaling pathway is known for its role in the production of pro-inflammatory cytokines and contributes to various skin pathologies, including photoaging. The UV-induced expression of COX2 is predominantly

dependent on the p38 MAPK signaling pathway [194], which regulates the secretion of prostaglandin E2 (PGE2) and contributes to immune cell infiltration, swelling, and edema.

Nuclear factor kappa B (NF-κB) is a major mediator in cellular inflammatory processes. UV stress enhances NF-κB transcriptional activity, thereby inducing chronic inflammatory signals [195]. Human keratinocytes exposed to UV light exhibit increased expression of inflammatory cytokines, including IL-1β, IL-6, IL-8, and TNF-α, through the NF-κB pathway. Members of the NF-κB family include p65 (RelA), p50, RelB, cRel, and p52. These transcription factors are initially sequestered in the cytoplasm, forming complexes with inhibitory proteins of the inhibitory κB (IκB) family, which includes IκBα, IκBβ, Iκβε, NF-κB1, and NF-κB2. Activation of the NF-κB pathway typically involves the phosphorylation of an IκB member, primarily by the IκB kinase (IKK) complex. The phosphorylated IκB then undergoes ubiquitylation and subsequent proteolysis, leading to the translocation of NF-κB into the nucleus to modulate gene transcription [195]. IκBα plays a pivotal role in the early activation of NF-κB following ligand stimulation [196]. NF-κB1 is a substrate for GRK5, and GRK5-mediated phosphorylation of NF-κB1 regulates TLR4-induced NF-κB1 phosphorylation in macrophages [197].

G protein-coupled receptor kinases (GRKs) are serine/threonine kinases initially recognized for their role in the phosphorylation of G protein-coupled receptors (GPCRs) [198]. Studies have shown that GRKs phosphorylate a range of cytoplasmic and nuclear proteins, as well as other classes of membrane-localized receptors [199], [200]. The seven GRKs are highly conserved and divided into three subfamilies based on sequence and functional similarities: the rhodopsin kinase subfamily (GRK1 and GRK7); the GRK2 subfamily (GRK2 and GRK3); and the GRK4 subfamily (GRK4, GRK5, and GRK6). GRKs share a similar structural organization, with N-terminal, catalytic, and C-terminal domains [198].

TLRs transduce signals leading to NF-κB activation, which stimulates the expression of pro-inflammatory cytokines and chemokines in epidermal keratinocytes and Langerhans cells, playing a crucial role in UV-mediated inflammation [201]. In human Langerhans cells, TLR4 is more activated in response to UV stress, regulating UV-induced cutaneous immunosuppression [202]. UV-damaged keratinocytes release noncoding RNA that activates TLR3, triggering downstream inflammatory responses involving IL-6 and TNF-α [203]. TNF Receptor (TNFR) responds to UV irradiation by significantly increasing both soluble and full-length TNF-α. TNF-α, in turn, can induce keratinocyte apoptosis through the UV-induced TNFR-1 or p55 receptor pathway.

TGF-β signaling plays a critical role in various physiological and pathological events [204]. TGF-β acts as a growth inhibitor for keratinocytes and a growth stimulator for dermal fibroblasts [205]. Its growth-inhibitory effect positions TGF-β as a potent tumor-suppressive factor at the early stage of cancer. During photoaging, TGF-β is upregulated and activated, inducing excessive matrix metalloproteinases (MMPs), leading to progressive collagen degradation and aberrant elastic fibers [206], and pro-inflammatory cytokines. Furthermore, UV-irradiation induces loss-of-function mutations/deletions in TGF-β signaling components, including TGF-β type I (TGFβRI) and TGF-

β type II (TGFβRII) receptors, and Smad4, acting as genetic drivers for the initiation and progression of cutaneous squamous cell carcinoma [207], [208], [209], [210], [211]. TGF-β is mainly expressed in basal layers and contributes to epithelial homeostasis, wound healing, and anti-inflammatory responses. It has been shown that chronic UV irradiation reduces TGF-β2 synthesis by diminishing TGFβRII mRNA expression [208], [212].

1.6.3 Cell cycle regulation in response to UV-induced DNA damage

The cell cycle encompasses a sequence of events during which cellular components undergo duplication and are accurately distributed into daughter cells. In eukaryotes, DNA replication specifically occurs in the Synthesis (S)-phase, while chromosome segregation takes place during Mitosis (M)-phase. The S- and M-phases are interspersed by two Gap phases, G1 and G2, which are not periods of cellular inactivity. Instead, they serve as stages where cells accumulate mass, integrate growth signals, organize a replicated genome, and prepare for chromosome segregation. Cells can also exit from the cell cycle to enter the G0 phase, in which cells are in a state of quiescence [213], [214].

The regulation of the cell cycle plays a crucial role in maintaining genome integrity. Cyclin-dependent kinases (CDKs) drive the progression of the cell cycle, which are serine/threonine protein kinases responsible for phosphorylating key substrates to facilitate DNA synthesis and mitotic progression. The catalytic subunits of CDKs remain inactive until bound by their corresponding cyclin subunits. The synthesis and ubiquitin-dependent proteolysis of cyclins tightly regulate their availability. Additionally, CDK activity is subject to negative regulation through the binding of small inhibitory proteins (CKIs) or inhibitory tyrosine phosphorylation, which hinders phosphate transfer to substrates [215]. Moreover, growth factors also contribute significantly to cell cycle regulation, representing a group of proteins that stimulate tissue growth in a controlled manner [213], [216].

1.6.3.1 G1 and G2 checkpoints: cell size control

To guarantee cell size and the equal distribution of genetic and biosynthetic material to daughter cells, cells must precisely double their contents before division. The regulation of cell size is crucial for managing nutrient allocation within the cell and for governing organ size and function in multicellular organisms. The checkpoints in G1 and G2 play a role in coordinating cell size with cell cycle progression. Early evidence suggests that the size of newly formed daughter cells post-mitosis influences cell cycle dynamics, with larger daughter cells expediting progression through G1 and/or G2, while smaller daughter cells impede exit from these growth phases [217], [218].

An example of the mechanism for size control involves monitoring protein translation. Ribosomal mass, indicative of translational activity, is thought to correlate with cell size [219]. Translational sizers, such as Cln3 and Cdc25, are proposed as products of translation that accumulate with cell size, exerting control over the cell cycle after reaching a certain threshold. This mechanism also explains how cell size and the cell cycle respond to nutritional status, as signaling pathways like

PKA and TOR regulate ribosome biogenesis, making translational activity a cellular indicator of nutritional status [220].

1.6.3.2 DNA damage checkpoint

As explained so far, DNA damage induces cell cycle arrest allowing repair pathways to act before proceeding with the later phases of the cell cycle. Although DNA repair mechanisms exhibit lesion-specific responses, common checkpoints are activated in response to different DNA lesions. First, CDKs need to be in the inactive form until the DNA lesion is removed. Previous study has demonstrated that UV irradiation induces both G1 and G2 cell cycle arrests, with a p53-dependent or independent pathway, respectively [221]. The G1-S and intra-S checkpoints prevent the replication of damaged DNA, while the G2-M checkpoint safeguards against the segregation of damaged DNA to daughter cells [130].

CHK1 pathway is evolutionarily conserved from yeast to humans [222], [223], [224]. CHK1 activation occurs in response to various forms of DNA damage, with higher efficiency during S- and G2-phases compared to G1, and is specifically limited to post-replicative lesions [225], [226], [227]. The event triggering the DNA damage checkpoint is the formation of the ssDNA covered by RPA [228], [229]. The recruitment of phosphorylated and active CHK1, substrate of ATR, aims to maintain the mitotic CDK Cdc2 in its Y15 phosphorylated and inactive form. Eventually, CHK1 undergoes dephosphorylation by type 1 phosphatases, allowing cells to resume cycling into mitosis [230], [231].

p53 plays a crucial role in DNA damage checkpoints, particularly during the G1 phase [232]. p53 undergoes regulation through a myriad of posttranslational modifications, including N-terminal phosphorylation on S15 catalyzed by ATR, ATM and DNA-PKcs. Activated p53 triggers the expression of numerous genes, including p21. Through this mechanism, CDKs involve in G1 are inhibited, allowing the repair of the DNA damage before restarting DNA replication. However, p53 can also repress gene expression and is essential for prolonged G2 arrest in the presence of persistent DNA damage [233], [234]. Additionally, p53 can dictate alternative cell fates such as apoptosis or senescence [235]. The function of p53 in cell cycle arrest appears to be a later-acquired role, as Drosophila p53 primarily regulates apoptosis rather than cell cycle progression [236].

In addition, ATR plays a pivotal role in initiating subsequent events, such as the phosphorylation of p53 or CHK1 [130]. Moreover, some proteins involved in DNA repair pathways, such as XPA and XPD, could also play a role in regulating cell cycle upon UV stress. For example, XPA is responsible for damage verification in NER system and can affect cell cycle checkpoint signaling too [237], [238]. Mutations in XPA have profound effects on cellular physiology, participating in both GG-NER and TC-NER, and are associated with Xeroderma pigmentosum (XP), characterized by extreme UV radiation sensitivity and increased cancer predisposition [239]. Conversely, it has been demonstrated that the overexpression of XPD induces G1 phase cell cycle arrest [238].

In addition, the DNA replication factor Cdt1 (CDT1) is involved in the formation of the pre-replication complex through replication licensing in the late M-phase or early G1-phase. In fact,

upon UV irradiation, CDT1 degradation in the M-phase leads to the blockage of the "license" after the cell enters the G1 phase, resulting in G1 arrest [240]. In summary, defects in components of the DNA damage response may compromise cell-cycle checkpoints and amplify genomic instability in defective cells [17].

1.6.3.3 Mitotic spindle checkpoint

The separation of sister chromatids during anaphase is intricately regulated by the mitotic spindle, a structure composed of microtubules and motor proteins located at both the centrosome and kinetochore ends. Additional motors facilitate force generation between overlapping microtubules that do not attach to kinetochores [241].

Proper spindle attachment occurs in a bi-oriented manner, ensuring tension on sister chromatids at metaphase, where they are connected to both poles of the spindle. Once all kinetochores are appropriately attached and aligned at the metaphase plate, the progression to anaphase is facilitated by the Anaphase-Promoting Complex (APC), a large E3 ubiquitin ligase. APC targets crucial proteins, including mitotic cyclins and securin. The degradation of mitotic cyclins terminates CDK activity, while the degradation of securin releases separase, allowing it to cleave cohesin complexes at the kinetochores. APC activity is regulated by two accessory proteins: cell division cycle protein 20 homolog (Cdc20), which operates up to metaphase-anaphase, and fizzy-related protein homolog (CDH1), which continues to facilitate APC-mediated ubiquitination once cyclin and separase degradation has commenced [242]. Upon the release of sister chromatid cohesion, spindle tension, and associated motor proteins enable the separation of sister chromatids, leading to the formation of identical daughter nuclei. The mitotic spindle checkpoint serves to prevent the activation of APC/Cdc20 in situations where kinetochores lack spindle microtubule occupancy or are attached but not under tension. Under these circumstances, the spindle checkpoint protein MAD2 inhibits Cdc20 activity, forming a mitotic checkpoint complex at unattached kinetochores. Additionally, MAD2 inhibits APC-bound molecules. The mitotic spindle checkpoint involves various proteins, with its complexity increasing across evolutionary scales. The Polo, Aurora, and NIMA-related (Nek) kinases regulate spindle formation and the detection and correction of spindle defects [243], [244]. In summary, the mitotic spindle checkpoint prevents cell cycle transitions while effectors correct genome-altering defects. However, the mitotic spindle checkpoint uniquely aims to maintain CDK activity, distinguishing it from those acting in interphase, which aim to sustain CDK inactivity.

1.6.3.4 Intra-S-phase checkpoint: regulation of DNA replication

During S-phase, cells face heightened susceptibility to DNA damage. Cells need to repair these lesions as occurring in G1- and G2-phases, but these lesions also physically obstruct the replicative polymerases. DNA replication starts at specific loci known as replication origins, which are epigenetically defined by various proteins to ensure their activation occurs precisely once per cell cycle. The initiation of replication is regulated by the phosphorylation of two key proteins, Cdt1 and Cdc6, which is catalyzed both CDKs and the Dbf4-dependent protein kinase (DDK) Cdc7. The replication origin cannot undergo additional rounds of firing [245].

When the DNA polymerase and its associated proteins (the replisome) encounters an obstacle hindering its progression, it is crucial to maintain stable association with the replicating chromatid. This ensures that replication can resume once the obstacle is removed. Such obstacles may include modified deoxyribonucleotide triphosphates (dNTPs), abasic sites (AP-sites), protein-DNA complexes, or depletion of dNTPs. The function of stabilizing the replisome in response to such impediments is carried out by the intra-S-phase checkpoint.

The effector kinase of the intra-S-phase checkpoint is CHK2. When replication stalls, the replisome component mediator of the replication checkpoint (MRC1) is phosphorylated by ATR. This phosphorylation event creates a binding site for CDS1/CHK2, which is subsequently phosphorylated by ATR and fully activated through autophosphorylation [246]. Activated CDS1/CHK2 then stabilizes the stalled replisome by phosphorylating several subunits, such as the minichromosome maintenance (MCM) complex [247], [248].

1.6.3.5 S-M phases dependency

After encountering a DNA lesion, the replisome stops until it is resolved. Alternatively, cells can utilize post-replication repair pathways to circumvent the lesion. This can involve recruiting mutagenic bypass polymerases or switching templates through recombination, using the complementary nascent strand as a template [249]. Regardless of the approach, checkpoints are essential to prevent entry into mitosis until replication is completed, as premature mitosis can result in decreased ploidy. Mitotic entry is inhibited through the phosphorylation of tyrosine 15 (Y15) on Cdc2, a crucial step mediated by upstream checkpoint components. If the obstruction arises from DNA damage, the CHK1 pathway is activated. Some investigations suggest that CDS1 also influences cell cycle progression [250], [251]. However, in the absence of CDS1, the stalled replisome dissociates from its template, a phenomenon known as fork collapse, which triggers DNA damage activation of CHK1.

To maintain ploidy, it is equally crucial to ensure one round of replication per cell cycle. This dependency can be disrupted when the degradation of CDT1 and Cdc6 is impaired, leading to constitutive replication origin firing [252]. Similarly, cells lacking mitotic cyclins bypass mitosis, indicating their role in signaling the G2 state [253].

1.7 Zebrafish as model organism for genotoxic studies

In the recent years, zebrafish have become a valuable system employed across scientific research fields [254], [255]. Zebrafish development has been broadly explored [256], [257]. One of the primary advantages of using this model is the transparency of zebrafish embryos during early developmental stages, enabling the comprehensive monitoring of this entire phase and the detection of any developmental changes [255], [257]. Zebrafish exhibit rapid development, with embryos hatching within 48–72 hours post-fertilization (hpf), significant organ development occurring by 120 hpf, and reaching adulthood within 3 months [256]. The rapid development provides the efficient tracking of the toxic effects within a relatively short timeframe [258]. Around 70% of

zebrafish genes have human orthologs and its genome has been sequenced even if there is still a limitation in gene and protein annotation.
Moreover, the recent improvement in our understanding of signaling pathways induced by DNA damage and the genes involved in repair mechanisms, further encourages using zebrafish as replacement for mammalian model [259], [260], [261]. In fact, zebrafish possess nearly all the genes associated with DNA repair mechanisms, including BER, MMR and NER from eukaryotic pathways.

1.7.1 UV-induced DNA repair pathways in zebrafish

UV-B can penetrate clear water and fish have developed mechanisms as protection against UV-light [1]. As mentioned previously, zebrafish emerge as promising model system for studying DNA damage and repair mechanisms [262], [263] (**Figure 8**).
Zebrafish possess orthologs for nearly all mammalian repair pathways. Genes that are involved in the p53-mediated damage recognition pathway exhibit functional and structural similarities to mammalian p53 and are highly effective in repairing UV-induced DNA damage [264].
As for mammals, BER operates across all cell cycle stages and is vital for cell viability, addressing frequent damages like oxidation, deamination, and spontaneous hydrolysis [72]. BER is particularly relevant for non-bulky damage in bases and AP-sites, with DNA glycosylase acting as the primary enzyme in SSBs repair [265]. The main proteins taking part in BER pathway are apex1, pol β, creb1, ogg1, and p53 [261]. BER initiates with lesion recognition and excision by the DNA glycosylase enzyme [266]. Subsequent hydrolysis of the N-glycosidic bond generates a toxic AP site, cleaved by apurine/apyrimidine endonuclease 1 (apex1). Pol β replaces the missing nucleotide, and the XRCC1- LIG3α complex seals the resulting nick [261], [266].
Importantly, evidence suggests distinct execution of the BER pathway in zebrafish embryos compared to adults, with differences in the expression of key proteins [267] Zebrafish embryos lack pol β, leading to a prevalence of replicative polymerases and Mg^{2+}-dependent endonuclease activity [267]. Apex1 and apex2 are significantly expressed in embryos compared to adult zebrafish, and apex1 is involved in repairing oxidative damage during early developmental stages [268] The enzyme 8-Oxoguanine DNA Glycosylase 1 (ogg1) is essential in embryo development, contributing to DNA repair in BER pathway and maintaining the function of cardiac progenitor cells during cardiogenesis [269].
The conserved non-homologous end joining (NHEJ) pathway repairs double-strand breaks (DSBs) arise from exposure to UV irradiation. DNA ends are recognized by Ku70 and Ku80 that recruit the proteins for performing end joining without requiring a homologous template [270], [271]. It has been showed that Ku80 promoted survival of irradiated cells during embryogenesis and that apoptosis resulting from loss of Ku80 is p53 dependent [271]. Ku70 protein is involved in protecting the developing nervous system from radiation-induced DNA damage during embryogenesis [271].
Homologous recombination (HR) repairs DSBs in the late S-G2 phase of the cell cycle. First, a single-stranded region of DNA for strand invasion is generated, then a Holliday junction is formed and finally DNA synthesis is initiated using the intact strand as the template. HR has been reported

in intact zebrafish embryos at early developmental stages [272] and in zebrafish cell cultures [273]. Findings demonstrated conserved function of Brca2 [274].

As mentioned previously, NER pathway is highly conserved and repairs CPD and 6-4PP induced by UV light [275]. It consists of two subpathways: GG-NER and TC-NER [266]. Key genes involved in the NER pathway include xpc, xpd, xpa, xpf, p53, p21, ddb2, gadd45a, cyclinG1, and vitellogenin [261]. Studies conducted in vivo highlight differences in factors between adults and embryos, along with variations in gene expression during zebrafish development [276].

In addition to NER, zebrafish possess an alternative mechanism to remove photoproducts that is the photoenzymatic repair (PER) system. PER removes the photoproducts via the deoxyribodipyrimidine photolyase enzyme, encoded by phr. It is more direct and energy-efficient process, less prone to errors when reversing pyrimidine dimers to their monomeric form [277]. Operating at a faster pace than NER, PER depends on both UV-A and blue light (400–500 nm) for the reversal of pyrimidine dimers [266], [277], [278], [279].

The photolyase enzyme is also involved in the direct reversal (DR) repair system, addressing damage caused by UV radiation to pyrimidine dimers and alkylated bases [280]. DR repair pathway include the methyl guanine methyl transferase (mgmt) and (phr), as key genes [261]. DR specifically reverses certain damage without disrupting the DNA phosphodiester skeleton, exemplified by the repair of O6-methylguanine lesions by mgmt [266].

Mismatch Repair (MMR) is a highly conserved pathway in zebrafish responsible for recognizing and repairing mismatched bases, as well as the insertion and erroneous deletion of nucleotides, thereby maintaining genomic stability and suppressing homologous recombination [261].

1.8 Other features developed by the organisms as UV-light protection

During evolution, organisms have developed some features as protection against UV radiation. A relevant example is the migration of hematopoietic stem and progenitor cells (HSPCs) in organisms during transition from aquatic to terrestrial environment. In adult mammals, the niche of HSPCs is located in the bone marrow, whereas in other organisms, as in teleost fish, it is located in the kidney marrow. Recent studies demonstrated that a melanocytes umbrella is present on the kidney marrow of zebrafish, contributing to protect HSPCs against UV light. The same feature exists also in aquatic tetrapod larvae, such as amphibians *Xenopus leavis*, that is moving to the bone marrow in the development to terrestrial amphibians. In particular, the transition from the melanocyte-cover niche to the bone marrow occurred over the course of the development of legs still in aquatic habitat and cortical bone around the bone marrow works as shield against UV light in terrestrial environment [281]. Since UVB passes through clear water [1], fish have also a sunscreen compound called gaudosol [282].

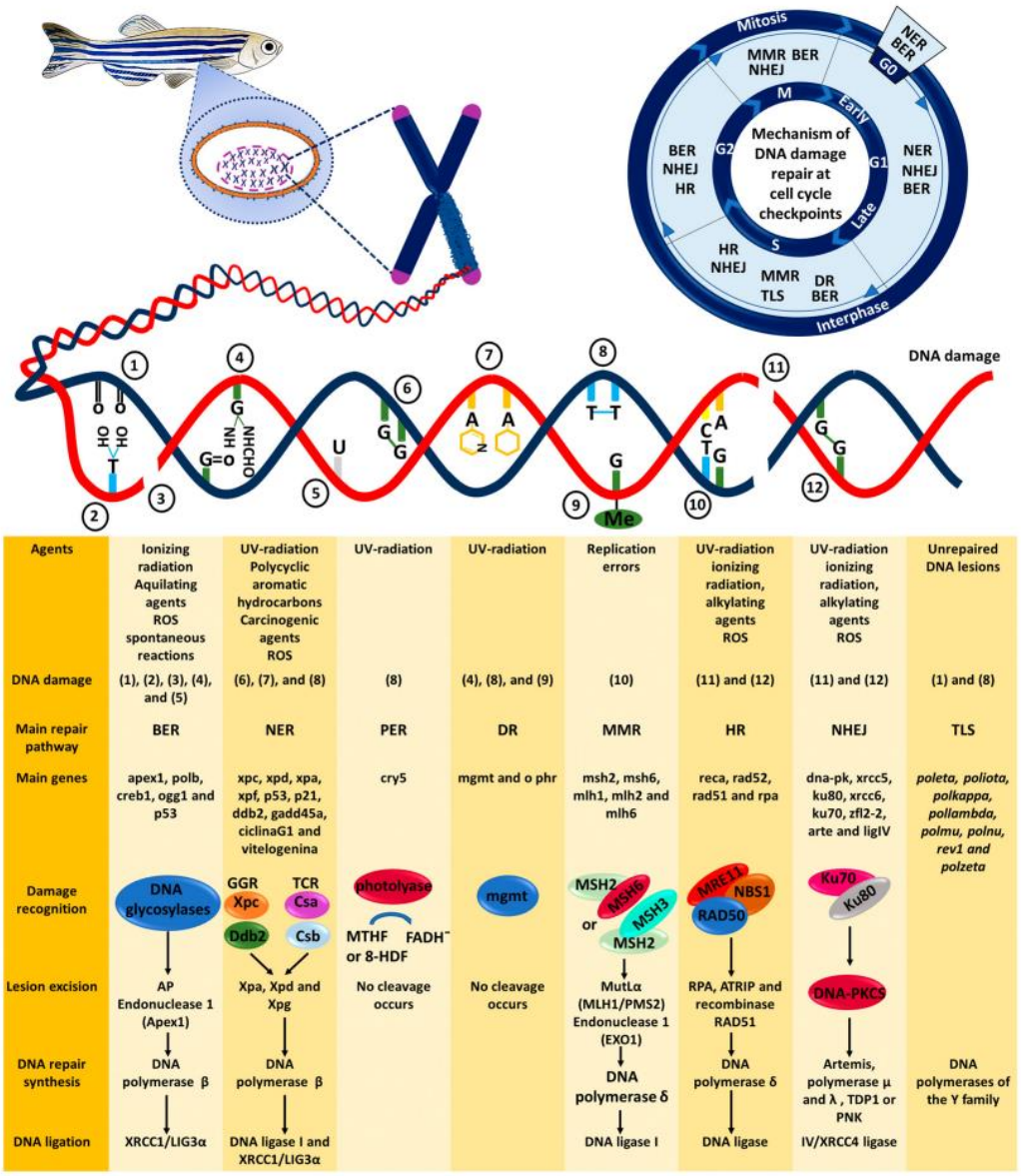

Figure 8. DNA repair pathways in zebrafish

(1) Abasic sites; (2) thymidine glycol; (3) single-strand break; (4) oxidation at guanosine site; (5) uracil; (6) intra-strand crosslink; (7) base adducts; (8) pyrimidine dimerization; (9) alkylated bases; (10) mismatch; (11) double-strand break; (12) inter-strand crosslink (from [399]).

1.9 Aims of the study

UV-C irradiation represents the most dangerous wavelength of UV-light. UV-C induces the formation of DNA adducts, in particular, cyclobutane pyrimidine dimers (CPDs) and 6-4 photoproducts (6-4PPs) [22]. Upon their generation, these DNA lesions induce distortions within the DNA double helix [283]. The presence of these bulky lesions can interfere with important cellular processes like transcription and replication, which can compromise genome stability and cell viability [284]. In fact, DNA adducts can obstruct the progression of the transcribing RNA polymerase II (Pol II) and thus result in the inhibition of transcription and initiation of transcription-coupled nucleotide excision repair (NER) for removing the DNA lesions [64]. If not resolved, their accumulation can lead to the rise of cancer, such as cutaneous squamous cell carcinoma, basal cell carcinoma and cutaneous melanoma [285].

Moreover, our recent publication [23] showed that UV-C and formaldehyde (FA) produce RNA-protein crosslinks (RPCs) and their resolution is regulated by K6-ubiquitylation together with an evolutionary conserved ubiquitin E3 ligase, RNF14.

In the recent years, zebrafish has become a valuable system employed across various research fields [254], [255]. Around 70% of zebrafish genes have human orthologs [286]. Recent improvement in the understanding of signaling pathways following DNA damage and the genes involved in repair mechanisms further support the use of zebrafish to complement studies performed in mammalian cells [259], [260], [261]. In fact, zebrafish have nearly all the genes associated with DNA repair mechanisms, including NER, from mammalian pathways [261]. Moreover, zebrafish possess a competent p53-dependent NER pathway for repairing UV-induced DNA damage leading to the phosphorylation of histone H2AX, like in human. Furthermore, zebrafish develop cancers, like melanoma, that resemble human tumors both at molecular and histopathological levels [2], [287]. In addition, from an experimental point of view, the extra utero development provide easier exposure to UV radiation [2].

The current study has the aim to enhance the comprehension of the intricate cellular response to UV-C irradiation in whole organisms. Using zebrafish embryos, we will explore the changes in gene expression and underlying protein-based molecular mechanisms and cell signaling pathways induced by UV-C damage in a whole organism. In particular, we will investigate the changes in protein levels (total proteome), protein phosphorylation (phosphoproteome), mRNA levels (transcriptome) and protein ubiquitylation (ubiquitylome). Finally, we will compare our results with studies performed in human cells [3].

2 Results

2.1 Characterization of UV-C-induced DNA damage in human cells

2.1.1 HaCaT and RPE-1 cells are sensitive to UV-C irradiation

To study the sensitivity of human cells to UV-C irradiation, we performed clonogenic assay in HaCaT and RPE-1 cells. These cells were selected since they are in physiological conditions exposed to UV light and are not of tumor origin. HaCaT cells are TERT-immortalized human keratinocytes and the RPE-1 are (TERT-immortalized) human retinal epithelial cells. We treated them with different doses of UV-C (5, 10, 20, 40, 80 J/m^2) and determined the lethal dose for 50% of the total cells (LD_{50}), which occurs at 15 J/m^2 and 12 J/m^2 in HaCaT and in RPE-1 cells, respectively (**Figure 9**). Both cell lines show similar sensitivity to UV-C irradiation, even if HaCaT cells appeared to be slightly more sensitive to 5 J/m^2 compared to RPE-1 cells.

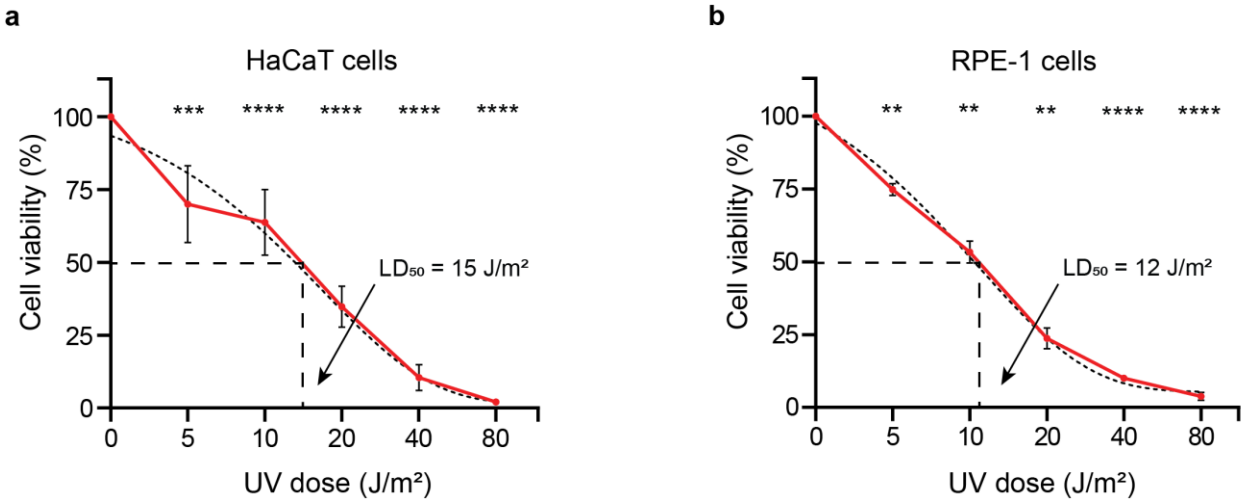

Figure 9. Sensitivity of HaCaT and RPE-1 cells to UV-C radiation
a) HaCaT and **b**) RPE-1 cells were treated with different doses of UV-C (X-axis) and left growing for at least 10 days. After crystal violet staining, colonies were counted using the Leica M80 stereomicroscope. The error bars show the standard deviation (SD) of the results obtained in three independent experiments performed in three technical replicates. The dotted line indicates the fitting of the curve. Two-sided Student's T-test was used to assess the significance (**p-value ≤0.001, ***p-value ≤0.005, ****p-value ≤0.0001).

2.1.2 UV-C light induces the formation of bulky adducts in human cells

Exposition to UV-C light leads to the formation of bulky adducts, inducing distortion of the DNA helix that can be dangerous for the organism if they are accumulated. CPDs and 6-4PPs are the most common adducts formed and their accumulation can result in severe consequences, such as cancer. We investigated the formation and resolution of those two photoproducts by performing immunofluorescence (IF) assays in both HaCaT and RPE-1 cells. We analyzed recovery times from 1 h up to 48 h post-UV-C irradiation. At 1 h, which is also the shortest time point examined the highest amount of CPDs and 6-4PPs occur in both cell lines. CPD resolution occurs slower in RPE-1 than in HaCaT cells (**Figures 10a** and **10b**). In RPE-1 cells, CPDs are removed slower compared to HaCaT cells and in both cell lines the DNA damage appears to be resolved at around 48 h. It has

been shown that UV-C irradiation produces less of 6-4PPs compared to CPDs [288], but they are also produced immediately after UV-C irradiation, as shown at 1h. The resolution of 6-4PPs is faster [289], with the majority of the lesions be removed in the first hours after the damage induction (**Figures 9c** and **9d**).

2.1.3 Activation of DDR and transcription shutdown induced by UV-C light

Upon exposure to genotoxic stress, cells activate the DNA damage response (DDR) to activate cell cycle checkpoint and repair the lesions. The phosphorylated form of the histone H2AX (γH2AX) is accumulated at double strand breaks (DSBs) and at the ssDNA stretches, the last ones are formed during the removal of the lesions through NER pathway. H2AX is a variant of the H2A protein family, which is a component of the histone octamer in nucleosome [290]. ATM and ATR can phosphorylate it and this event represents the first step for recruiting and localizing DNA repair proteins at the DNA damage site. It appears to be slowly activated reaching its peak around 3 h post-UV, and it takes longer to be resolved, especially in RPE-1 cells (**Figures 10e** and **10f**).

During transcription, elongating Pol II stalls at bulky adducts since it is not able to overcome them. To detect the effect of UV-C radiation on general transcription, HaCaT and RPE-1 cells were incubated with 5-Ethynyl-Uridin (EU), a modified nucleotide incorporated by nascent RNA.

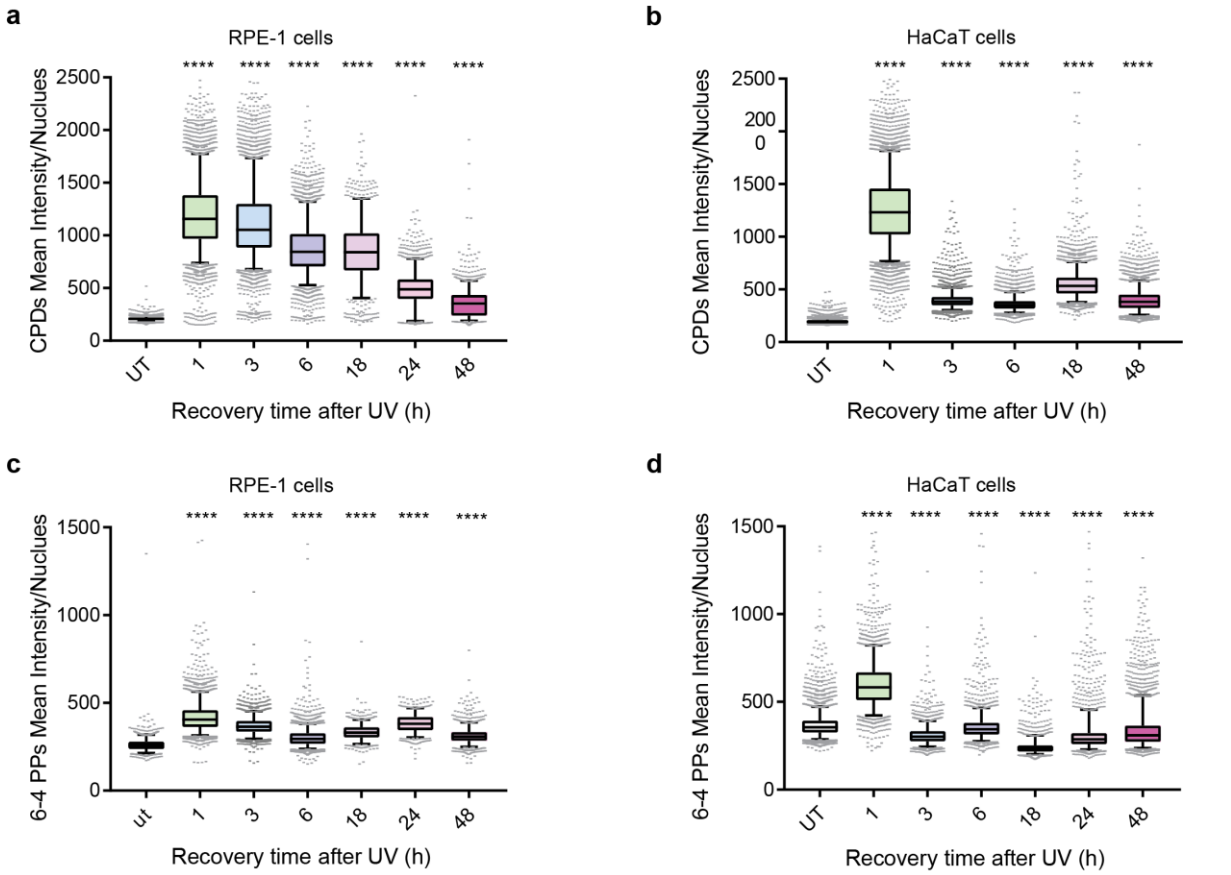

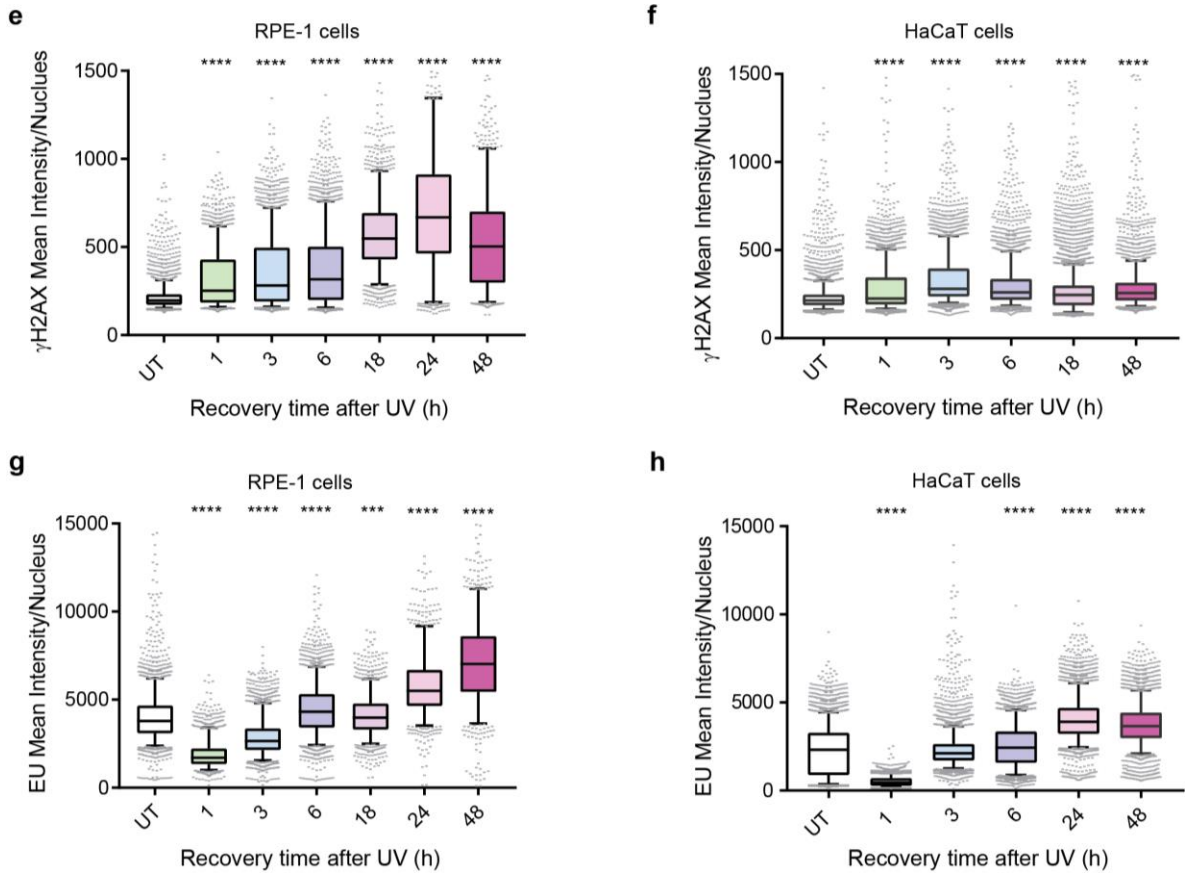

Figure 10. Formation of photoproducts, shutdown of transcription and activation of UV-C-induced DDR
HaCaT and RPE-1 cells, upon UV-C treatment (15 J/m^2 and 12 J/m^2, respectively) were incubated with EU (250 μM) for 30 min before harvesting at different time points (indicated on X-axis). Then cells were fixed with paraformaldehyde to perform IF. To detect the UV-induced DNA damage, CPDs and 6-4PPs were revealed using α-CPDs antibody (**a** and **c**) and α-6-4PPs antibody respectively (**d** and **c**) and as secondary antibody, α-mouse 488 was used. To reveal DNA damage induction, α-γ-H2AX antibody and α-mouse 488 were used (**e** and **f**). In addition, to detect EU incorporation, click reaction and staining with a-streptavidin 647 were carried out (**g** and **h**). For the acquisition of the images, Opera Phenix was employed. The experiment was performed once and the intensity was acquired on at least 500 cells/condition. Anova test was performed for statistical analysis (***p-value≤0.001, ****p-value≤0.0001).

It is evident that 1 h after UV-C exposure, decreased levels of EU intensity are observed corresponding to a general shutdown of transcription in cells. Subsequently, a restoration of the normal level of transcription occurs at around 6 h post-UV in both cell lines (**Figures 10g** and **10h**).

2.2 Characterization of UV-C-induced DNA damage in zebrafish embryos

2.2.1 UV-C affects zebrafish embryos development and generates malformations

To study the response triggered by UV-C irradiation in a whole organism, we investigated the changes in protein levels (total proteome), protein phosphorylation (phosphoproteome) and mRNA levels (transcriptome). We performed whole proteome and phosphoproteome analysis, and

transcriptomic analysis in 24 hours post fecundation (hpf) zebrafish embryos. We considered an early and a late recovery time post-UV-C. Thus, we irradiated zebrafish embryos with UV-C (254 nm, 24 J/m^2) and harvested them at 0.5 h post-UV (early response) and at 4 h post-UV (late response). As a control, zebrafish embryos harvested together with the ones from the early response (24 hpf + 30 min untreated (UT)). After extraction and digestion of proteins, we performed TMT-labeling, and then phosphorylated peptides were enriched over titanium dioxide (TiO_2) beads. We worked with three independent biological replicates to gain a robust relative quantification of protein levels and phosphorylation sites, and to allow statistical evaluation of the proteomics data. Instead, for transcriptomic analysis, upon RNA extraction, we enriched the samples with pull downs using poly-A, and then fragmented the mRNA, followed by reverse transcription, library generation and RNA sequencing on Illumina NextSeq500 instrument. After obtaining the raw data, proteome and phosphoproteome data were analyzed with MaxQuant, and transcriptome data were analyzed with STAR (**Figure 11a**).

As first, to choose the suitable UV-C dose for the experiments, we performed the viability assay upon UV-C on zebrafish embryos [291]. We irradiated 24 hpf-zebrafish embryos with 0, 12, 24, 48 and 120 J/m^2 and monitored them up to 72 h. The lowest dose, 12 J/m^2, did not affect the viability of the embryos. The dose of 24 J/m^2 kept alive around 80% of the embryos. 48 J/m^2 induced the loss of approximately 50 % of the embryos and 120 J/m^2, the highest UV-C dose, resulted to be lethal for all the zebrafish embryos at 48 h post-UV (**Figures 11b**). In addition, UV-C leads to the rise of malformations in zebrafish embryos (**Figure 11c**).

The development of zebrafish embryos is faster compared to human and few hours during the development can result in relevant changes. In order to understand the developmental difference before and after UV-C irradiation, we investigated the protein changes in zebrafish embryos at 24.5h and 28h post UV-C irradiation, corresponding to the untreated early and late response, respectively. We carried out another total proteome analysis with label-free quantitative (LFQ) analysis (**Figure 12a**). In total, we quantified 1579 proteins. By applying the cutoff of the p-value of less than 0.05 and the Fold Change (FC) of at least 1.5, 76 proteins increased in their levels and 81 decreased in their levels at the late development stage (28 hpf), comparing with the early one (24.5 hpf) (**Figure 12b**). Moreover, we were interested in understanding the differential singling pathways activation between the two different developmental stages. After performing Gene Ontology (GO)-term analysis, at early development, the most enriched terms are the ones involved in the egg coat and protein localization to the lysosome. The egg coat provides structural support and can play an essential role in oogenesis, fertilization and early development (**Figure 12c**). Instead, at the 28hpf-stage, the GO-term analysis shows enrichment of terms involved in muscle contraction and formation (**Figure 12d**). In fact, at this stage it is known that muscles are forming, including the heart [256].

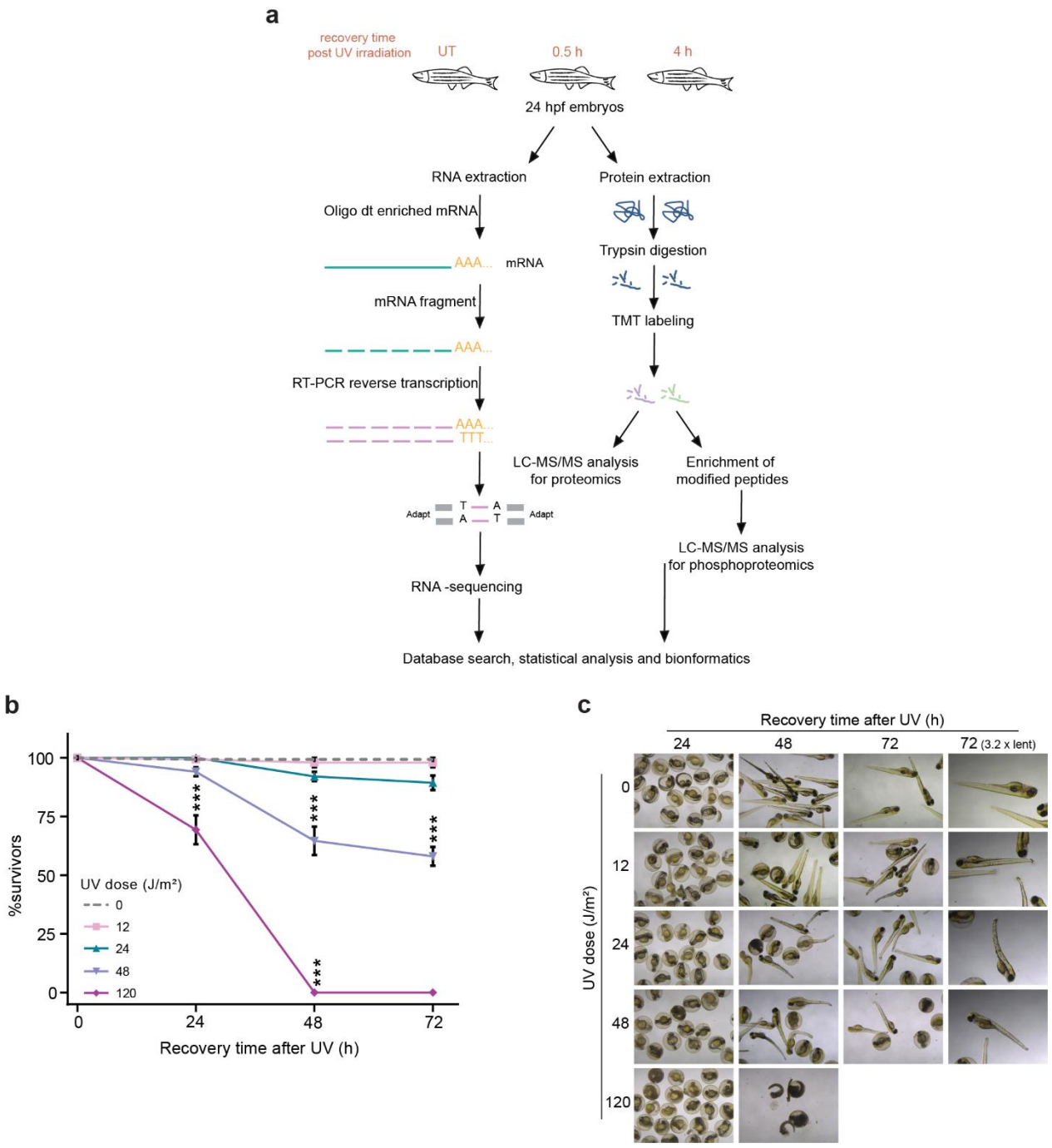

Figure 11. Schematic approach and sensitivity of zebrafish embryo to UV-C radiation

a) Scheme of transcriptomic, proteomic and phosphoproteomic experiments. 24.5hpf-zebrafish embryos were used for each condition in three technical replicates (UT, 0.5h post UV (early response) and 4h post UV (late response)). TMT-labeling was performed for proteomic and phosphoproteomic analysis. The same conditions, in four replicate each, were used for RNA sequencing. Bioinformatics analysis was performed with R studio. **b**) Sensitivity of zebrafish embryos to UV-C doses. 24hpf -zebrafish embryos were treated with the following UV-C doses 0, 12, 24, 48, 120 J/m^2, and recovered at different time points (indicated on X-axis) and the survivors were counted. The error bars show the SD of results obtained from three replicates. Two-sided Student's T-test was used to assess the significance (***p-value ≤0.005). **c**) Pictures of the malformations generated in zebrafish embryos upon UV-C irradiation (the conditions are the same described in **b**).

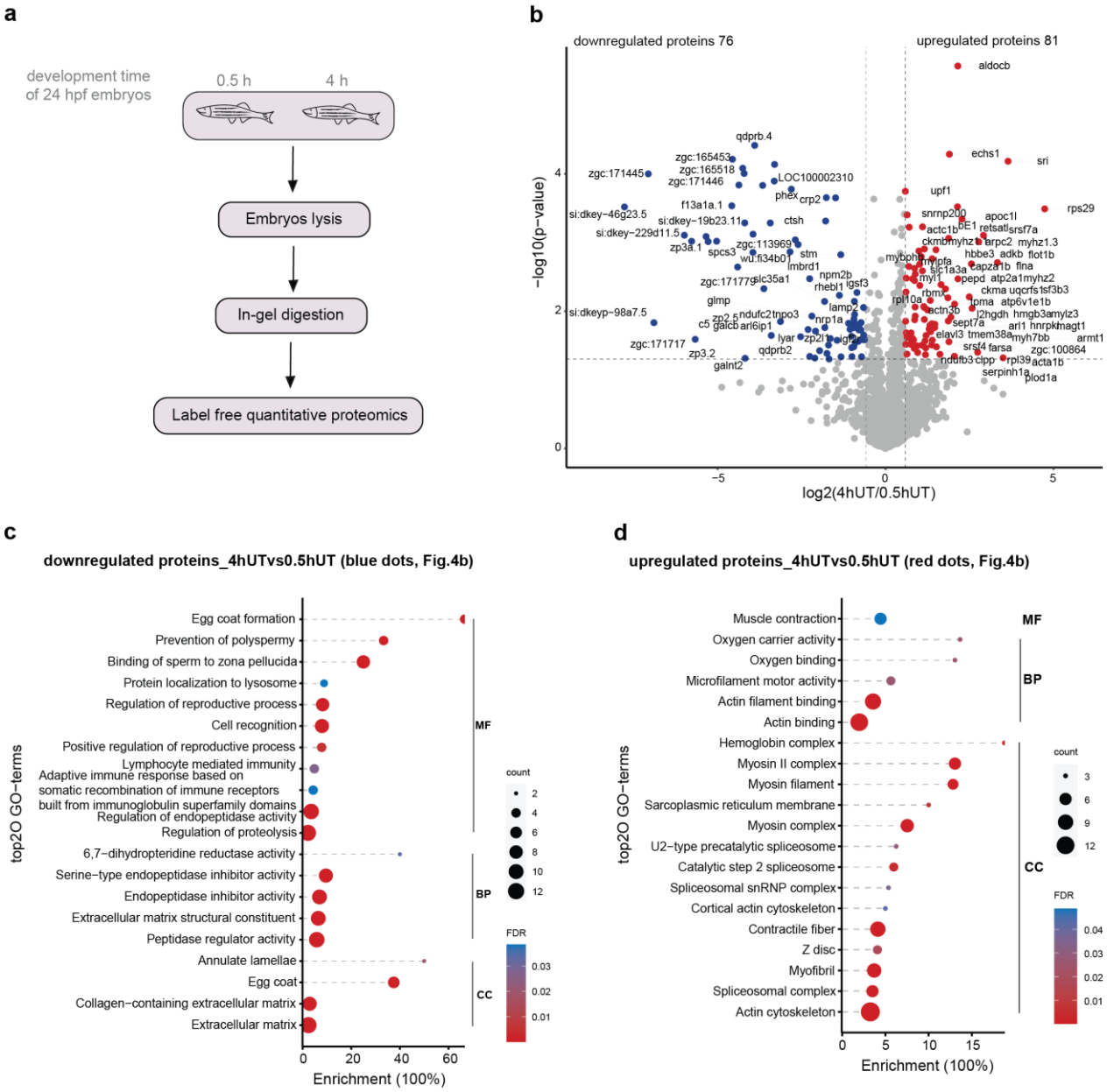

Figure 12. Developmental stages of zebrafish embryos and changes in proteome

a) Schematic approach of the proteomic experiment using LFQ LC-MS/MS of zebrafish embryos at the 24.5 hpf and 28hpf. For each condition was used three replicates. **b**) The volcano plot shows the significant upregulated (red dots) and downregulated (blue dots) proteins at 4h vs 0.5h in 24hpf-zebrafish embryos. P-value≤ 0.05 and FC≤ or ≥1.5 were considered. The dot plots show the enrichment of the GO-term analysis of **c**) downregulated and **d**) upregulated proteins shown in **b**. String database was used for the analysis and "ggplot2" package from R studio to generate the plots. MF= Molecular Function; BP= Biological Process; CC= Cellular Component.

2.2.2 UV-C decreases the levels of proteins involved in DNA replication, ATP production and tRNA transport

To study how the levels of proteins change upon UV-C irradiation at early and late response, we performed the total proteome analysis using TMT labeling as described in **Figure 11a**. Principal Component Analysis (PCA) was employed to validate the similarity between biological replicates and demonstrated a high level of reproducibility (**Figure 13a**). Further analysis showed a quantitative correlation with the Pearson coefficient among biological replicates (**Figure 13b**). Corrected p-value (q-value), calculated using the Benjamini and Hochberg False Discovery Rate (FDR), of less than 0.05, and the FC of at least 1.5, was considered for the analysis. We found that 12 proteins increased their total level and 45 decreased their protein levels at early response. Instead, 109 proteins increased and 96 decreased their levels at late response. The comparison between late and early responses shows 14 proteins that are increased in their total levels that are mainly involved in muscle contraction, such as myhz2, mylpfb and tnnt3a, and others belonging to the hemoglobin complex, such as hbbe3, hbbe1.3 and hbae1.3 (**Figure 13b**). This is due to the different developmental stages according to our previous results (**Figure 12d**). To expand our view on the changes induced by UV-C irradiation, we performed the clustering profile for all the identified proteins (without setting any FDR and FC cut-off) and we obtained 10 clusters (**Figure 14a**). The proteins that are downregulated upon UV-C exposure are represented in clusters 2 and 3. GO-term analysis of those proteins highlights the enrichment of the proteins involved in tRNA transport from the nucleus, DNA replication and ATP production, shown from the Reactome (RCT) terms (**Figure 14b**). Afterwards, we focused on the upregulated proteins upon UV-C stress, represented in clusters 4 and 7 (**Figure 14c**). Among the Cellular Component (CC)-terms, the majority belongs to the spliceosome and the proteins we found are sf3a2, rbmx, rbmx2, snrpf, snrpb2, hnrnpub, lsm8. The most enriched Biological Process (BP)-term is "RNA polymerase II C-terminal domain binding", which includes leo1, hnrnpub, scaf4a and scaf4b. In particular, scaf4a and scaf4b have the RNA binding function and Pol II C-terminal domain phosphoserine binding function, involved in negative regulation of termination of Pol II transcription, poly(A)-coupled. This potentially indicates that transcription block may induced the accumulation of interrupted mRNAs that are tagged for degradation. In addition, the most enriched CC-term is "Paraspeckles". Paraspeackles are non-membrane organelles in the nucleus generated by protein liquid-liquid phase separation (LLPS) using RNAs as an anchor during stress conditions, including UV radiation [292]. The proteins we found belonging to this term are nono, sfpq, cpsf6 and hnrnpm, and are significantly increased in their total level upon UV-C radiation (**Figure 14d**).

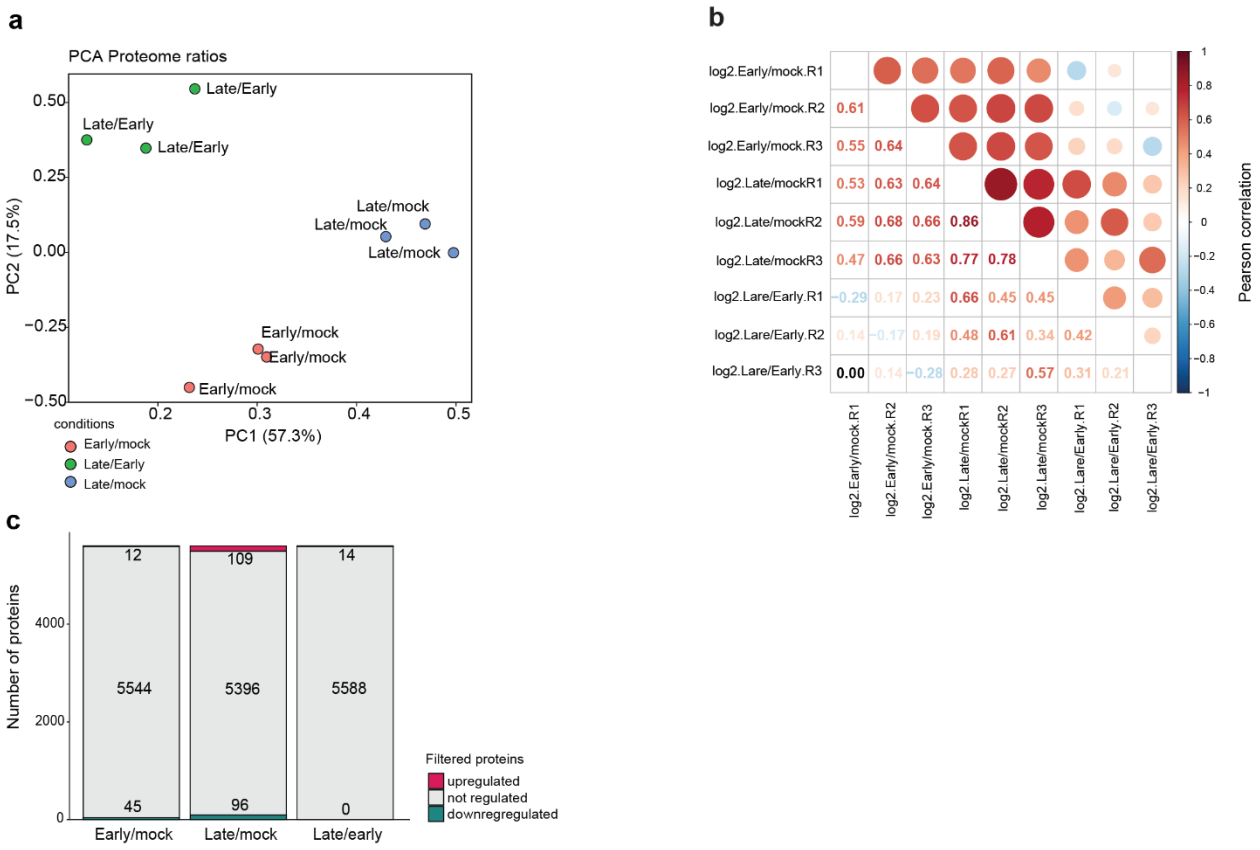

Figure 13. Differential regulation of the proteome in zebrafish upon UV-C radiation

a) The scatterplot shows the PCA of proteomic samples. In particular, the distribution of the ratio of the intensity of each sample. **b**) Correlation between the ration of the samples. **c)** The bar plot shows the upregulated (pink) and the downregulated (green) proteins in different conditions. FDR≤0.01, FC≤ or ≥1.5.

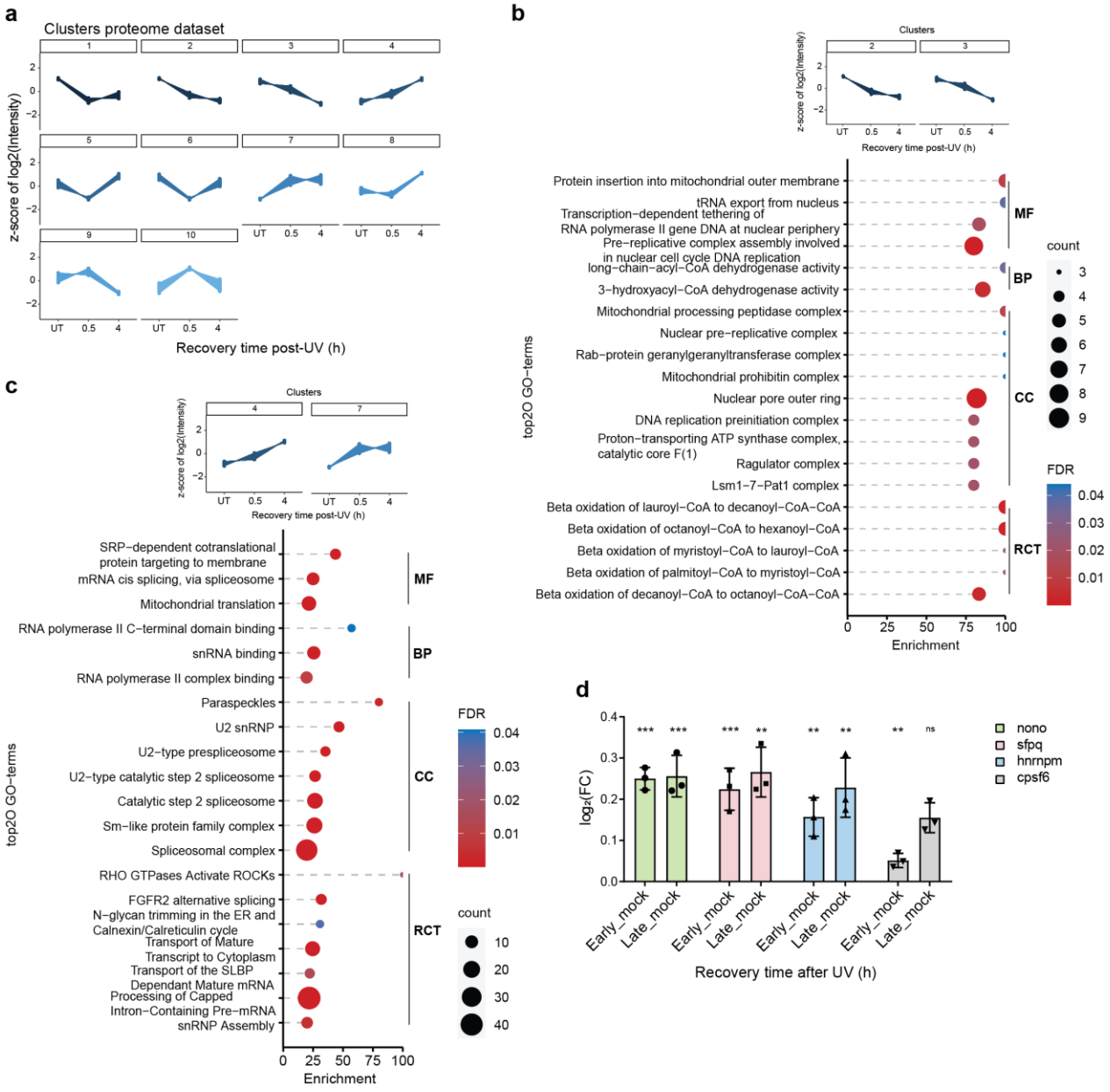

Figure 14. Clustering profile of the zebrafish proteome upon UV stress

a) The graph represents the 10 clusters of the proteomic dataset detected using NbClust, package from R. The dotplots show the enrichment of the top 20 terms of the GO-terms and RCT pathways of the **b**) downregulated and **c**) upregulated proteins (MF: Molecular Function, BP: Biological Process, CC: Cellular Component, RCT: Reactome). **d**) The barplot shows the FC of the regulation of proteins belonging to the paraspeckles core upon UV irradiation (**p-value≤0.01; ***p-value≤0.001; ns= not significant).

2.2.3 Activation of ATR, GRKs and MAPKs is triggered by UV-C radiation

To identify the cell signaling pathways triggered by UV-C, we irradiated zebrafish embryos with UV-C (245 nm, 24 J/m^2) and harvested them at 0.5 h post-UV (early response) and at 4 h post-UV (late response). As control, we used zebrafish embryos harvested together with the ones from the early response (24 hpf + 0.5 h untreated (UT)). After extraction and digestion of proteins, we performed TMT-labeling, and the phosphorylated peptides were enriched over titanium dioxide (TiO_2) beads. We worked with three independent biological replicates to gain a robust relative quantification of protein levels and phosphorylation sites and to allow statistical evaluation of the proteomics data (**Figure 11a**). PCA and Pearson correlation was utilized to assess the similarity and difference among biological replicates, revealing a robust level of reproducibility (**Figure 15a, 15b**). In the phosphoproteomic analysis, we identified 4439 phosphorylation sites, corresponding to 2158 proteins (**Figure 15c**). With the cutoff of FDR≤ 0.01 and FC ≤ or ≥1, we found 103 upregulated and 86 downregulated phosphorylation sites at early response. At late response, we identified 220 upregulated and 176 downregulated phosphorylation sites (**Figures 15d**). The GO-term analysis of the proteins with upregulated phosphorylation sites at the early response reveals that the most enriched terms are involved in translation, splicing and DNA damage. Considering the MF-terms, the most enriched term is "Eukaryotic initiation factor 4E binding". Interestingly, some phosphorylation sites, for example eif4ebp1 Tyr-67 and eif4ebp2 Tyr-66, have been demonstrated to affect the translation process by regulating eif4e [293], [294] (**Figure 15e**). At both early and late response, "Sites of the DNA damage" is one of the enriched CC-terms and includes vcp, xpc, timeless and rif1 (**Figures 15e** and **15f**). On the other hand, at late response, the most enriched CC-term is the "ATAC complex", in which we found pole3 and yeats2 being phosphorylated in conserved sites (yeats2-S373, pole3-S122). This complex has a histone acetyltransferase activity that is involved in cell cycle progression and precaution of apoptosis in embryogenesis by coordinating MAP kinase to regulate JNK target genes [292].

To look into the phosphorylated sequences after UV-C stress, we performed the analysis of the amino acid sequence surrounding UV-C upregulated phosphorylation sites. It revealed an overrepresentation of the glutamine (Q) in the +1 position at both early and late response. This motif, known as the S/TQ motif, is recognized by ATM/ATR/DNA-PKcs [123], [295] (**Figures 16a** and **16c**). To reveal which kinases are activated upon UV-C-induced DNA damage, we conducted the kinase prediction analysis using the kinase library (https://kinase-library.phosphosite.org/ea) (**Figures 16b** and **16d**). This library is based on human kinases and we made our analysis based on the homology between human and zebrafish kinases [296] since a kinase library for zebrafish is not available yet. As expected and predicted by the overrepresentation of the S/TQ motif, the increased activity of ATR occurs and is higher at the early response compared to the late response. Interestingly, at both early and late response, there is an overrepresentation of the members of the GRKs family. The GRKs regulate the activity of the GPCRs by desensitization upon stimulation of different agents [198], [297]. In particular, overexpression of GRK2 or GRK5 enhances TNFα-induced NF-kB activity [199]. GRK1 and

GRK7 are photoreceptors and have been shown to participate in cone opsin desensitization upon light stimulation [298].

Another group of proteins, appearing among the top ones, is involved in the Bone Morphogenetic Proteins (BMP) signaling pathway. Those proteins are BMPR1B, BMPR1A, ACVR2A, ACVR2B and ALK2 which are respectively type I (the first two) and type II (the last three) receptors that form the heterotetrameric complex interacting with the BMPs and starting the signaling cascade (**Figures 16d** and **16e**) [299]. BMPs belong to the TGF-β superfamily and are important in embryogenesis and development, such as cell growth, apoptosis and differentiation [300], [301], [302]. In addition, it has been demonstrated that BMPs are also involved in regulation and maintenance of adult homeostasis, for example, maintenance of the integrity, initiation of fracture repair and vascular remodeling [303], [304].

PLK3 and PLK2 are also activated upon UV-C stress. PLK3 is known to induce phosphorylation of TP53 and PLK2 can be activated by p53/TP53 [305], [306] (**Figure 16b**). At late response, we identified other kinases such as COT (also known as MAP3K8) that is presumably involved in the transduction of the TNF signal that activates JNK and NF-kB in some cell types, and MOS that is a positive regulator of the MAPK cascade (**Figure 16d**).

Among the kinases that are less activated at the early response, various members of p21-activated kinases (PAKs) are evident. PAKs play pivotal roles, serving as converging junctions for distinct signals originating from the cell surface and orchestrating multiple intracellular signaling cascades [307]. Cellular stress, including UV-C irradiation, induce the cleavage of PAK2 through a caspase-dependent mechanism triggering apoptosis [308] (**Figure 16b**). However, at late response, the less activated kinases are mainly involved in cell cycle progression and cell growth, such as PKACA and AURA (**Figure 16d**).

To compare our results with the UV-C response triggered in human cells, we used the dataset previously published by our laboratory [3] and generated the kinase prediction analysis in human cells upon UV-C stress (**Figure 16e**). In this study, U2OS cells were UV-C irradiated and harvested upon 1 h of recovery. The top kinases identified are the isoforms of JNK and p38, which are known to be phosphorylated upon UV stress and start their signaling cascade leading to cell arrest, apoptosis, repair and inflammation [309], [310]. On the other hand, the kinases less activated in human cells are mainly CDKs and ERKs, indicative of the arrest of cell cycle and cell growth (**Figure 16e**).

The prominent difference between the prediction kinases in human cells and zebrafish embryos upon UV-C stress appears to be the stimulation of the kinase receptors such as GRKs and TGFBR (**Figures 16d**, **16d** and **16e**). To have the clearer overview of the regulation of kinases activated by UV-C irradiation in cells and in a whole organism, we plotted all the kinases identified in both human and zebrafish datasets (**Figure 17**). ATM, ATR and DNA-PK are activated in both models. The GRK1, GRK2 and GRK6 are significantly activated in embryos. Interestingly, among the significant overrepresented kinases in embryos, there is FAM20C that is involved in the post-translational response to maintain endoplasmic reticulum (ER) proteostasis and plays an important

role in protecting from ER-stress-induced death [311]. We found also IRE1 that is an ER transmembrane sensor [312]. It has been shown that IRE1 hyperactivation under prolonger ER stress can trigger apoptosis through the TRAF2-ASK1-JNK pathway [313], [314].

To narrow down our focus, we highlighted 17 proteins with a pS/TQ motif upon UV-C irradiation that potentially are substrates of ATM/R in zebrafish embryos (**Figure 18a**). Some of these phosphorylation sites are conserved and phosphorylated in humans upon UV stress as well. We listed them in the table in **Figure 18b**, and among them we find nuck1a (S54), epb41l3b (S44), vcp (S784), srsf4 (S299), smc3 (S1067) and tp53bp1 (S492).

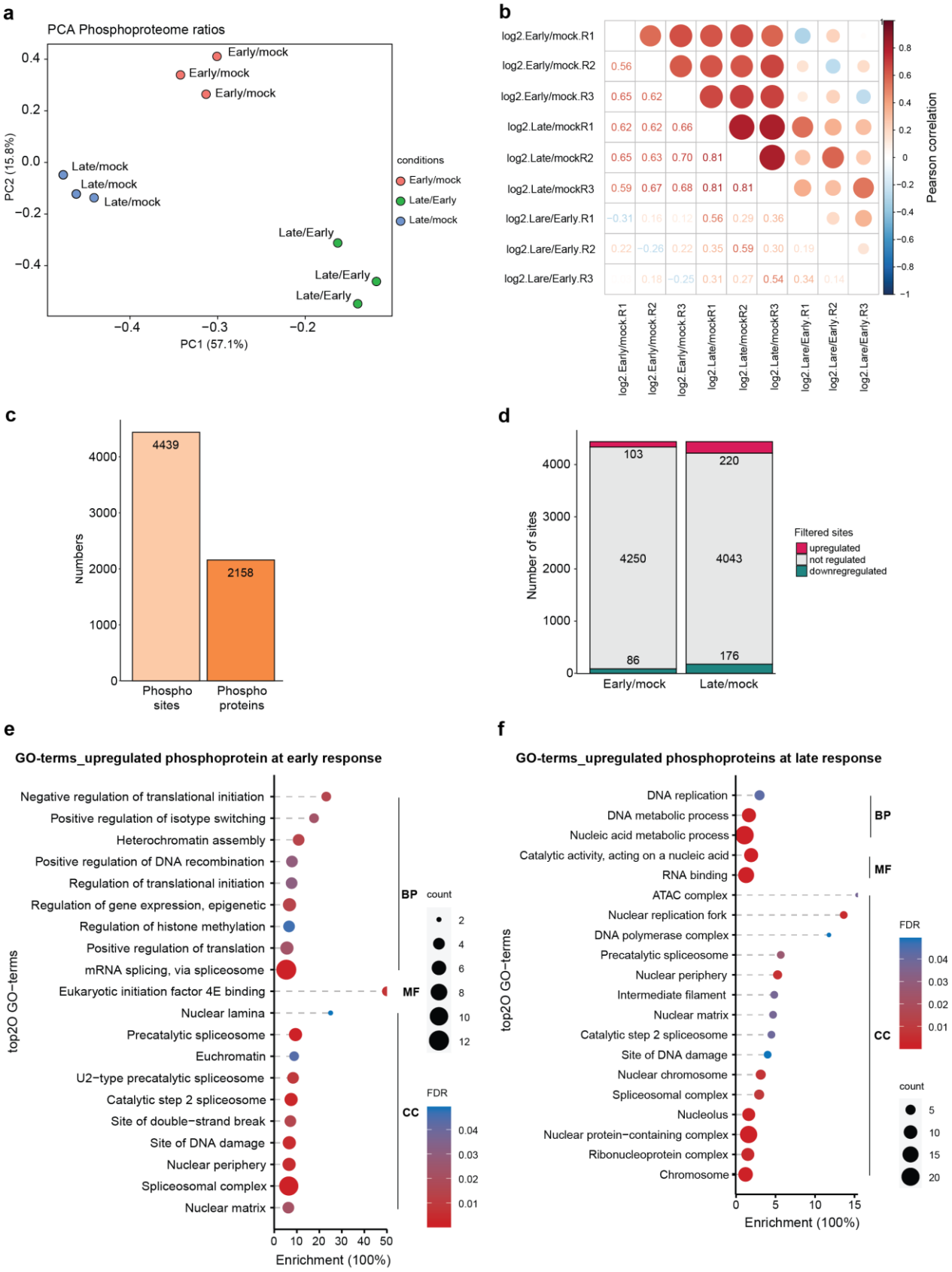

Figure 15. (Legend in the next page)

Figure 15. Variation of cell signaling in zebrafish embryos at early and late UV-C response
a) The scatterplot shows the PCA of the ratio of zebrafish samples of the phosphoproteome (early/mock, late/mock, late/early). **b)** The graph shows the Pearson correlation among the ratio of the single replicate. **c)** The barplot shows the identified phosphoproteins (light orange) and phosphosites (dark orange) upon UV stress. **d**) The barplot shows the upregulated (pink) and the downregulated (green) proteins in different conditions. FDR≤0.05, FC≤ or ≥1.5. The dotplots show the GO-terms analysis of upregulated phosphoproteins at **e**) early and **f**) late response (BP: Biological Process; MF: Molecular Function; CC: Cellular Component).

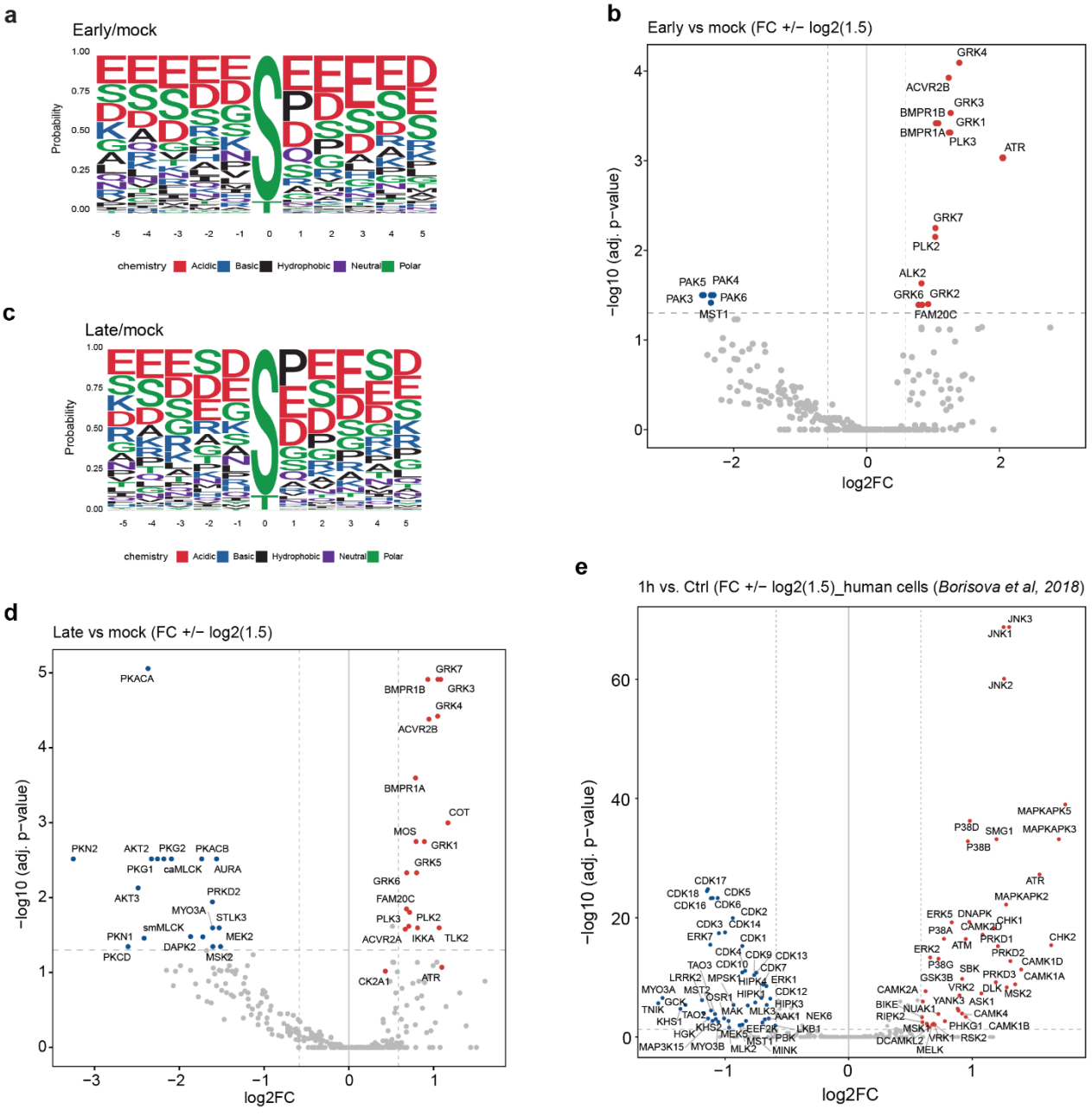

Figure 16. (Legend in the next page)

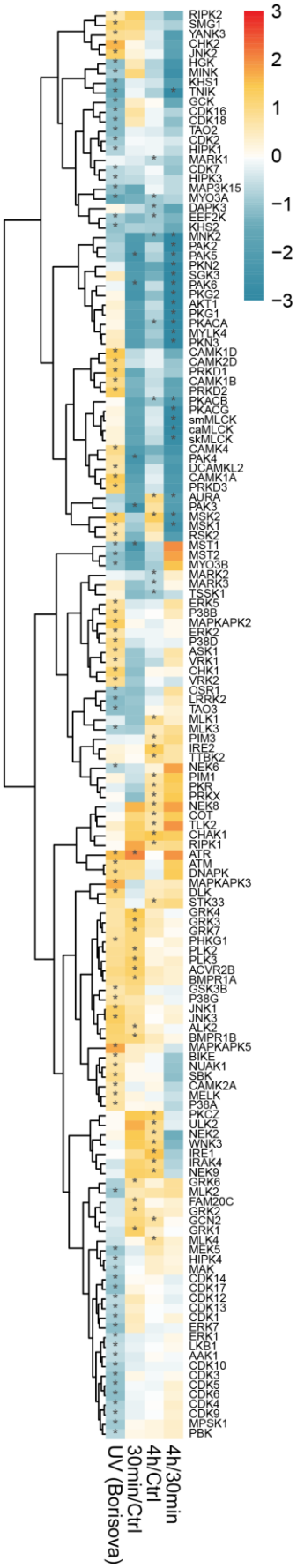

Figure 16. Phosphorylation of cellular signaling pathways in zebrafish embryos and human cells upon UV stress

a) The amino acid sequence analysis (-/+ 5aa) of the upregulated phosphosites at early response. Amino acids probabilities are plotted using R. **b**) The volcano plot represents the kinases that are upregulated (red dots) and downregulated (blue dots) at early response using FDR≤0.01 and FC≤ or ≥1.5. **c**) The amino acid sequence analysis (-/+ 5aa) of the upregulated phosphosites at late response. Amino acids probabilities are plotted using R. **d**) The volcano plot represents the kinases that are overrepresented (red dots) and underrepresented (blue dots) at late response using FDR≤0.01 and FC≤ or ≥1.5. **e**) The volcano plot shows the kinases that are overrepresented (red dots) and underrepresented (blue dots) at 1h post-UVR in human cells (from [3]). The kinase prediction was generated using the kinase library (https://kinase-library.phosphosite.org/ea).

Figure 17. Differential regulation of the kinases between human cells and zebrafish embryos

Heatmap shows the kinases identified in the kinase prediction in figures 15b, 15d and 15e. *FDR≤0.01.

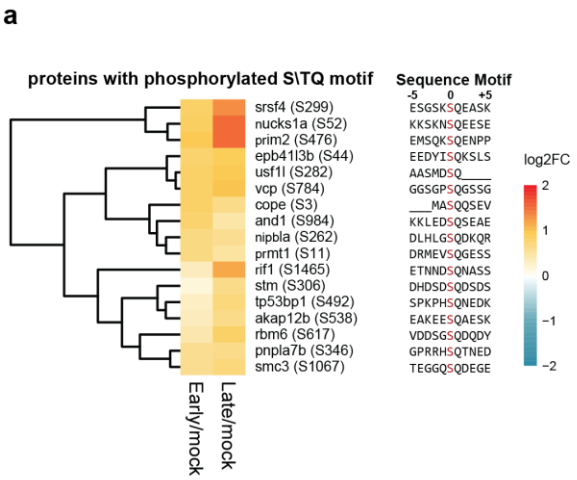

b

Sites phosphorylated by ATM/R

Gene	Zebrafish phosphosite	Human phosphosite
and1	S984	–
nipbla	S262	–
prmt1	S11	–
cope	S3	–
nucks1a	S52	S54
epb41l3b	S44	S88
usf1l	S282	–
prim2	S476	–
vcp	S784	S784
srsf4	S299	S304
smc3	S1067	S1067
rif1	S1465	–
akap12b	S538	–
stm	S306	–
tp53bp1	S492	S580
pnpla7b	S346	–
rbm6	S617	–

Figure 18. Novel S/TQ sites identified in response to UV stress in zebrafish
a) The heatmap shows the differential regulation of the pSQ motif upon UV stress in zebrafish. **b**) The table shows the conservation of the pSQ motif upon UV stress in human. The alignment analysis for checking the conservation of each specific serine (S) in human was performed using Clustal Omega (https://www.ebi.ac.uk/Tools/msa/clustalo/).

2.2.4 MAPK pathways and conservation of NELFE phosphorylation at S115 upon UV-C

UV exposure induces the activation of the DNA damage response (DDR) for inducing cell cycle arrest and allowing the repair of the DNA lesions. Cell cycle is regulated by ERK3/MAPK6 and its phosphorylation at S189 promotes the entry in the cell cycle. We identified the significant hypo-phosphorylation of the S189 of MAPK6 upon UV stress in zebrafish, confirming a general shut down of cell cycle progression and the development, with a stronger effect at early response compared to the late response (**Figure 19a**).

As mentioned previously, to compare the cell signaling pathways triggered in cells (human) and in whole organism (zebrafish embryo), we used the dataset published by Borisova et al. to perform kinase prediction analysis. The kinases activated in human cells are the isoforms of JNK and p38, known to be triggered by external stimuli and stress [315]. In our phosphoproteome in zebrafish embryos, we identified their activation sites (p38-T181, Y183; JNK-T183) (**Figure 19a**). To have a complete overview of the behavior of these kinases, we checked also their total protein level that appears to be significantly upregulated upon UV-C stress (**Figure 19b**).

Previous study from our laboratory demonstrated that NELFE is phosphorylated at S115 and released from Pol II, allowing the release of paused Pol II upon UV stress [3] (**Figure 19c**). Interestingly, we also showed that the phosphorylation of NELFE on S115 is significant upregulated at both early and late response in zebrafish embryos (**Figure 19d**). The alignment of the amino acid sequence proves the conservation of this site across the different species (**Figure 19e**). This finding suggests that, upon UV-C radiation, the mechanism that allows the removal of NELFE and release of Pol II into elongation for accelerating the repair is conserved in zebrafish.

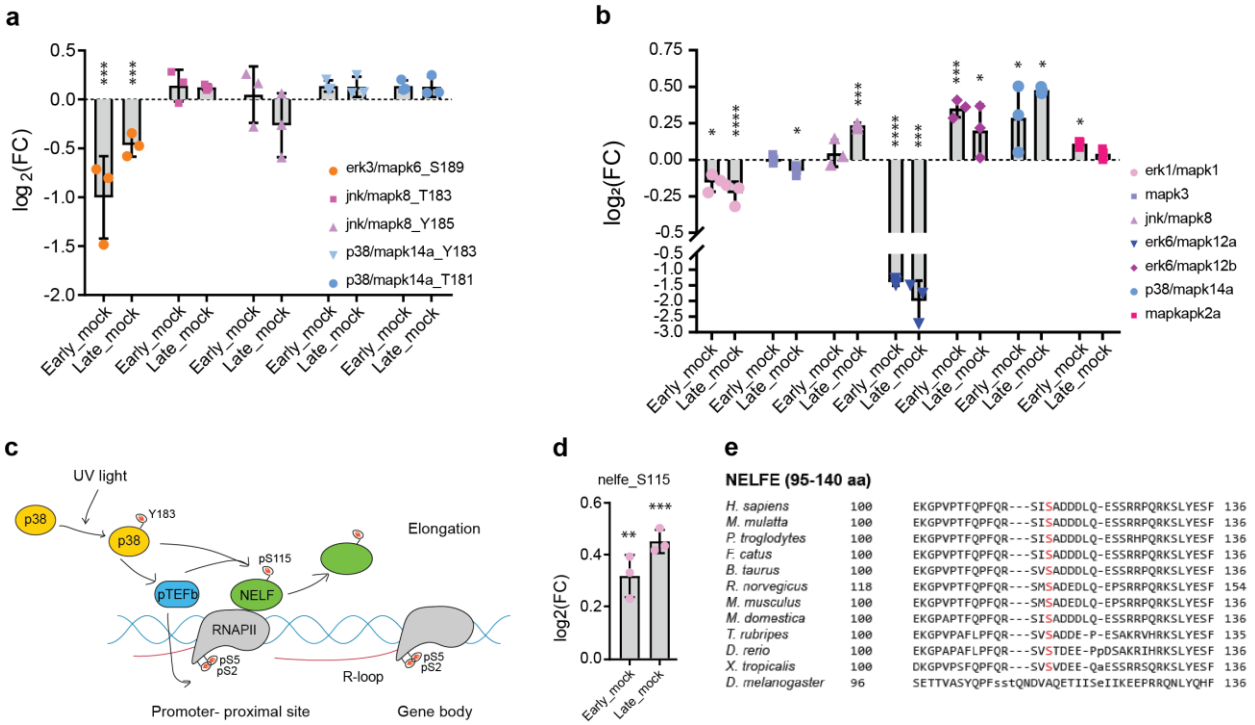

Figure 19. Identification of canonical sites of JNK and p38 and conservation of NELFE S115
a) The barplot shows the regulation of phosphorylation of the canonical sites of the MAPK family kinases. **b**) The barplot shows the differential variation of MAPKS total protein upon UV stress. plotting the mean of the FC of the triplicates of each condition. **c**) Schematic model of NELFE action upon UV-C exposure. **d**) The barplot shows the increased phosphorylation of NELFE at S115 upon UV stress. **e**) Alignment of amino acid sequence of NELFE of different organisms including the S115. Alignment performed using Clustal Omega. T-Student test was performed for statistical analysis (*p-value≤0.05, ***p-value≤0.001, ****p-value ≤0.0001).

2.2.5 Differential regulation of genes involved in cell cycle and development upon UV-C

To investigate the variation in gene regulation induced by UV-C irradiation, we performed transcriptomic analysis as described in **Figure 11a**. PCA and Pearson correlation was utilized to assess the similarity and difference among biological replicates, revealing a robust level of reproducibility (**Figure 20a**). With the cut-off of FDR≤ 0.01 and FC≤ or ≥1, we found 514 upregulated and 1009 downregulated genes at early response (**Figure 20b**). At late response, 3318 upregulated and 3545 downregulated genes were identified. Among the most upregulated genes, there are genes involved in cell cycle arrest upon DNA damage (gadd45aa, cdkn1a and nupr1a), but we also find polr2a (**Figures 20b** and **20c**). The GO-term analysis (Biological Process (BP)) of the upregulated genes at early response showed the enrichment of terms such as "Ribonucleoprotein complex biogenesis", "mRNA processing" and "cellular response to xenobiotic stimulus" (**Figure 20e**). On the other hand, the downregulated genes are mainly involved in the development process, such as "Muscle structure development", "epidermis development" (**Figure 20d**). At late response, the upregulated genes showed the enrichment of terms such as "muscle cell development", "muscle tissue development", "muscle contraction" and genes involved in "response to hypoxia" (**Figure 20f**). Interestingly, at late response, the

downregulated genes are enriched in terms, such as “ribosome biogenesis”, “rRNA processing”, “glycoprotein metabolic process”, showing the change in the regulation of the ribosome genes between the early and late response.

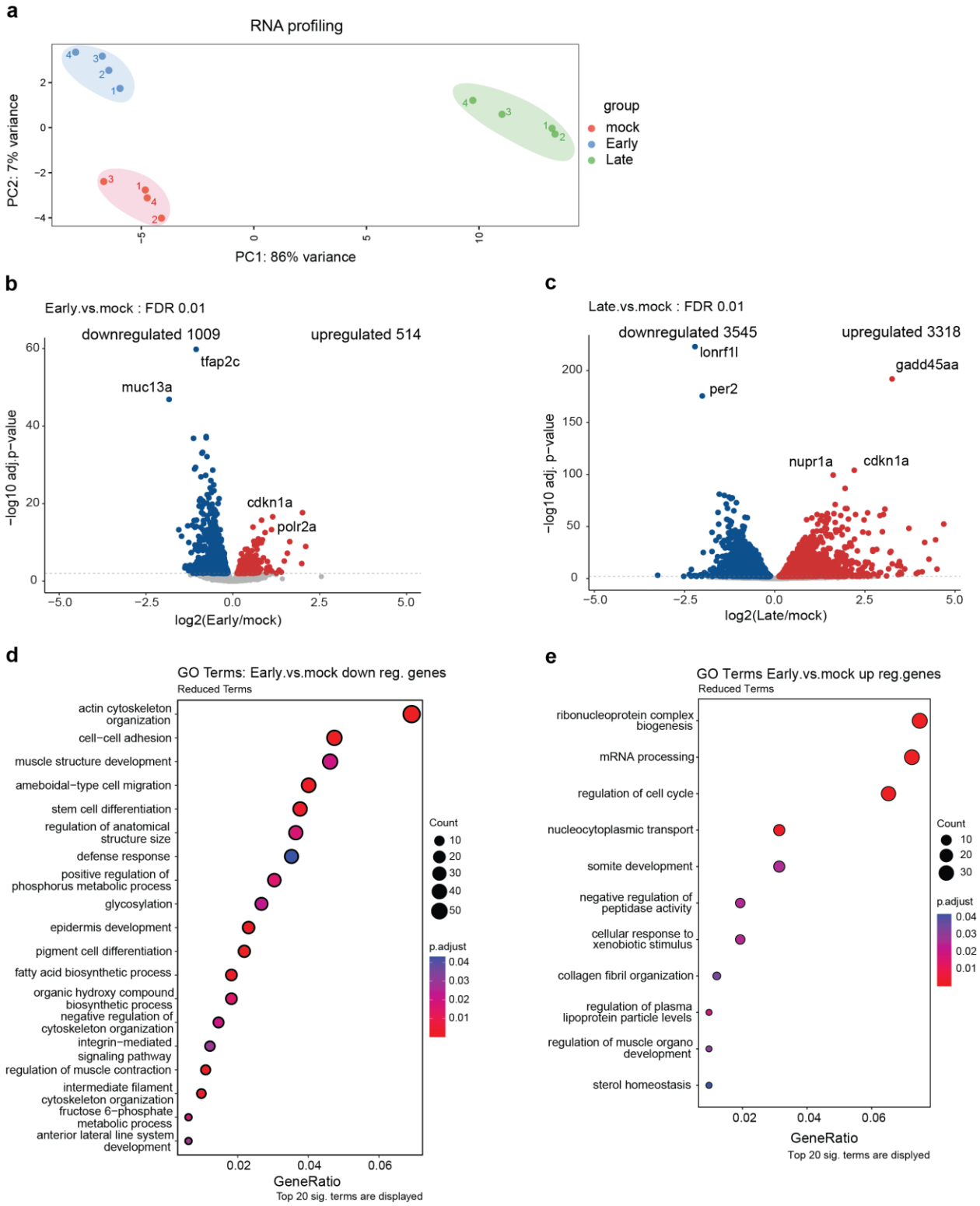

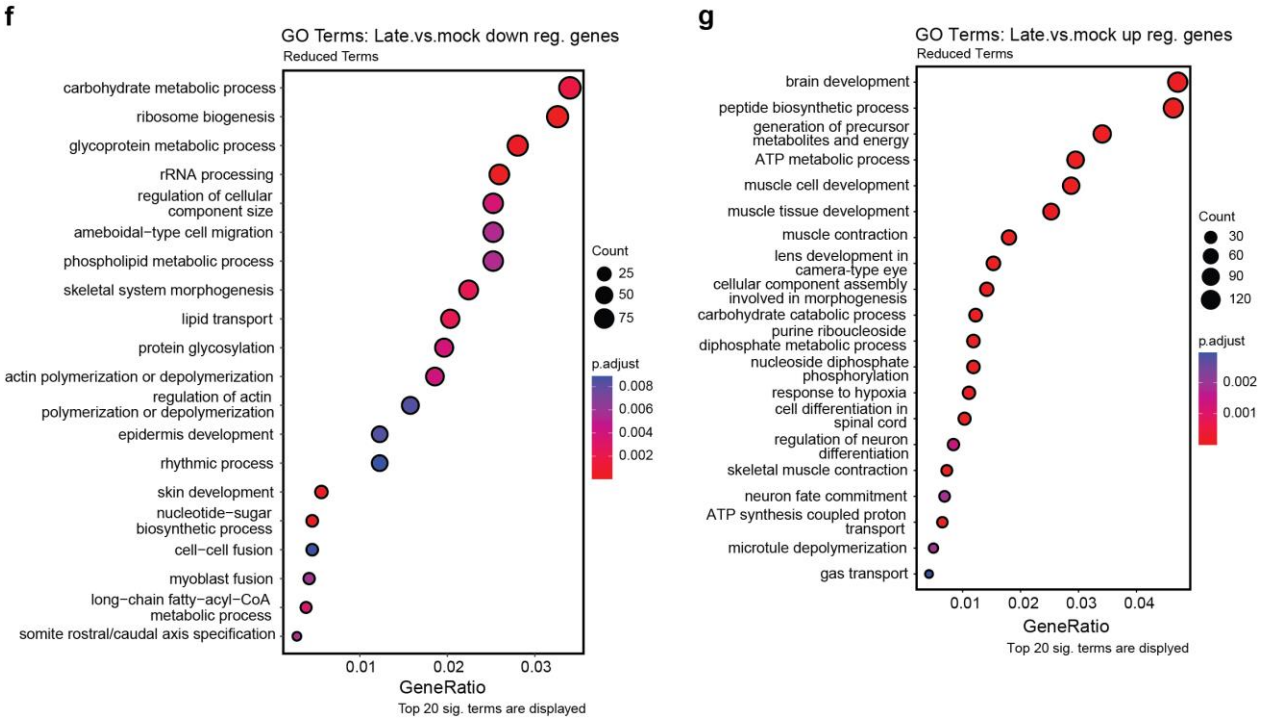

Figure 20. Transcriptomic analysis shows the downregulation of genes involved in development after UV-C
a) Quantitative PCA scatterplot of zebrafish samples at the transcriptomic level. **b)** The volcano plot shows the differential regulation of gene expression at early response compared to mock. The upregulated (red dots) and downregulated (blue dots) genesFDR≤0.01. **c)** The volcano plot shows the differential regulation of gene expression at late response compared to the mock. The upregulated (red dots) and downregulated (blue dots) genes.FDR≤0.01. **d)** The dotplot shows the reduced top 20-BP terms of upregulated genes at early response. **e)** The dotplot shows the reduced top 20-BP terms of upregulated genes at late response. **f)** The dotplot shows the reduced top-20 BP terms of downregulated genes at early response. **g)** The dotplot shows the reduced top-20 BP terms of downregulated genes at early response. The analysis was performed using the enrichment from STRING database.

2.2.6 Differential regulation of the ubiquitylome induced by UV-C

Another relevant post-translational modification (PTM) in DDR and cell signaling pathways is the ubiquitylation. Depending on the ubiquitylation-chain tagging a protein, the fate of the protein can change. To investigate how the ubiquitylation profiling is affected by UV-C irradiation, we combined a pulldown using OtUBD, a high-affinity ubiquitin-binding domain (UBD) derived from an Orientia tsutsugamushi deubiquitylase (DUB) able to purified ubiquitylated proteins [4], with quantitative proteomics in zebrafish embryos. We conducted the experiment in technical triplicates and used the same conditions employed to proteomic and transcriptomic experiments (early and late response), adding the 28 hpf untreated (UT) zebrafish embryos, as control for the late response embryos (**Figure 21a**). We performed the OtUBD pulldown and measured the proteome through LC-MS/MS (**Figure 21a**). We identified 964 ubiquitylated proteins. For the analysis, we applied the cut-off of FDR≤0.05 and FC≤ or ≥1.5. At early response, 9 proteins are enriched and 5 proteins are less enriched with OtUBD upon UV-C irradiation (**Figure 21b**). At late response, we detected more proteins (29) with increased ubiquitylation, and 9 proteins with decreased ubiquitylation upon UV-C irradiation (**Figure 21d**). To have a broader overview, we performed GO-term analysis just applying the cutoff of the FC= 1.5. Among the proteins with increased ubiquitylation, we identified

PCNA, FANCI and FANCD2. It has been shown that ubiquitylation of PCNA at K164 is important in the response to UV-C irradiation in human cells [316], [317]. We identified increased ubiquitylation of Pol II (polr2a/RPB1). Indeed, K1268 has been identified to be the main residue involved in RPB1 (the catalytic subunit of Pol II) ubiquitylation and degradation upon UV-C stress [154], [155]. Nccrp1 shows an increased ubiquitylation and is involved in SCF-dependent proteasomal ubiquitin-dependent protein catabolic process.

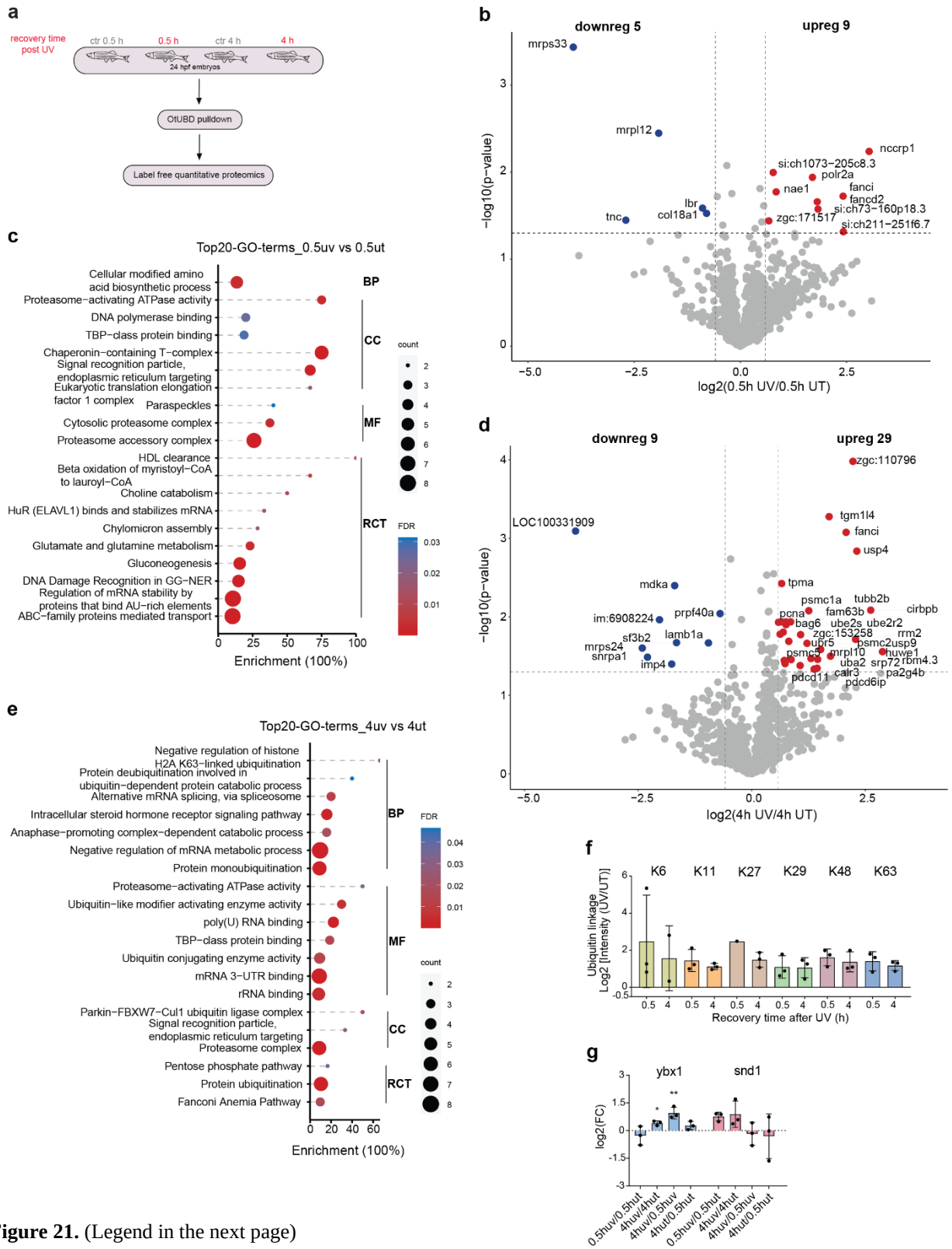

Figure 21. (Legend in the next page)

.

Figure 21. UV-C-induced regulation of ubiquitylation in zebrafish embryos
a) Workflow of the OtUBD pulldown-proteomics performed using zebrafish embryos lysates. For each condition three technical re-plicate was used. The volcano plots represent the proteins with increased (red dots) and decreased (blue dots) ubiquitylation at **b**) early and **d**) late UV response (FDR≤ 0.05 and FC ≤ or ≥1.5). The dotblots show the enrichment of the top20 GO-terms of the proteins with increased ubiquitylation at **c**) early and **e**) late UV-C response. **f**) The barplot represents the variation of the identified ubiquitin chains at early and late UV-C response (on x-axis). **g**) The barplot shows the FC of the ubiquitylation of ybx1 and snd1 (K6-ubiquitylated proteins from Suryo Rahmanto et al., [23]). The statistical analysis was performed with T-Student test. * p-value≤0.05, ** p-value≤0.001.

2.3 UV-C induces RNA-protein crosslinks (RPCs)

A recent study from our laboratory [23] showed that UV-C and formaldehyde (FA) induce RNA-protein crosslinks (RPCs) (**Figure 22a**) and inhibit translation in human cells. Their resolution is regulated by K6-linked ubiquitylation. In this study, we used an artificial way to induce RPCs consisting of labelling nascent RNA with 4-thiouridine (4SU, 5µm) for 45 min and subsequently exposure to UV-A (345nm, 0.5 J/m^2). This allowed us to identify the proteins that crosslink to the mRNA and, subsequently, that are K6-ubiquitylated, including YBX1, YBX3, SND1 and SERBP1 (**Figures 22b** and **22c**). Those are proteins located mainly in the cytoplasm as shown by the IF of endogenous proteins (**Figure 22d**). We hypothesized that these proteins form covalent crosslinks with RNA (forming RPCs) that are marked by K6-ubiquitin chain upon UV-C stress and FA treatment.

To explore the pool of proteins interacting with the RPC-proteins, we performed pulldowns using transiently overexpressed proteins tagged with GFP and performed the interactome analysis by LC-MS/MS (**Figure 23a**). Upon RPCs induction, analysis of the interaction profile of the YBX1, YBX3 and SND1shows the significant enrichment of 144, 360 and 144 proteins (**Figures 23b**, **23d** and **23e**). Their GO-term analysis highlights the association with cytoplasmic factors, ribosomes and translation (**Figures 23c**, **23e** and **23g**). This supported their involvement in translation shutdown upon RPCs induction.

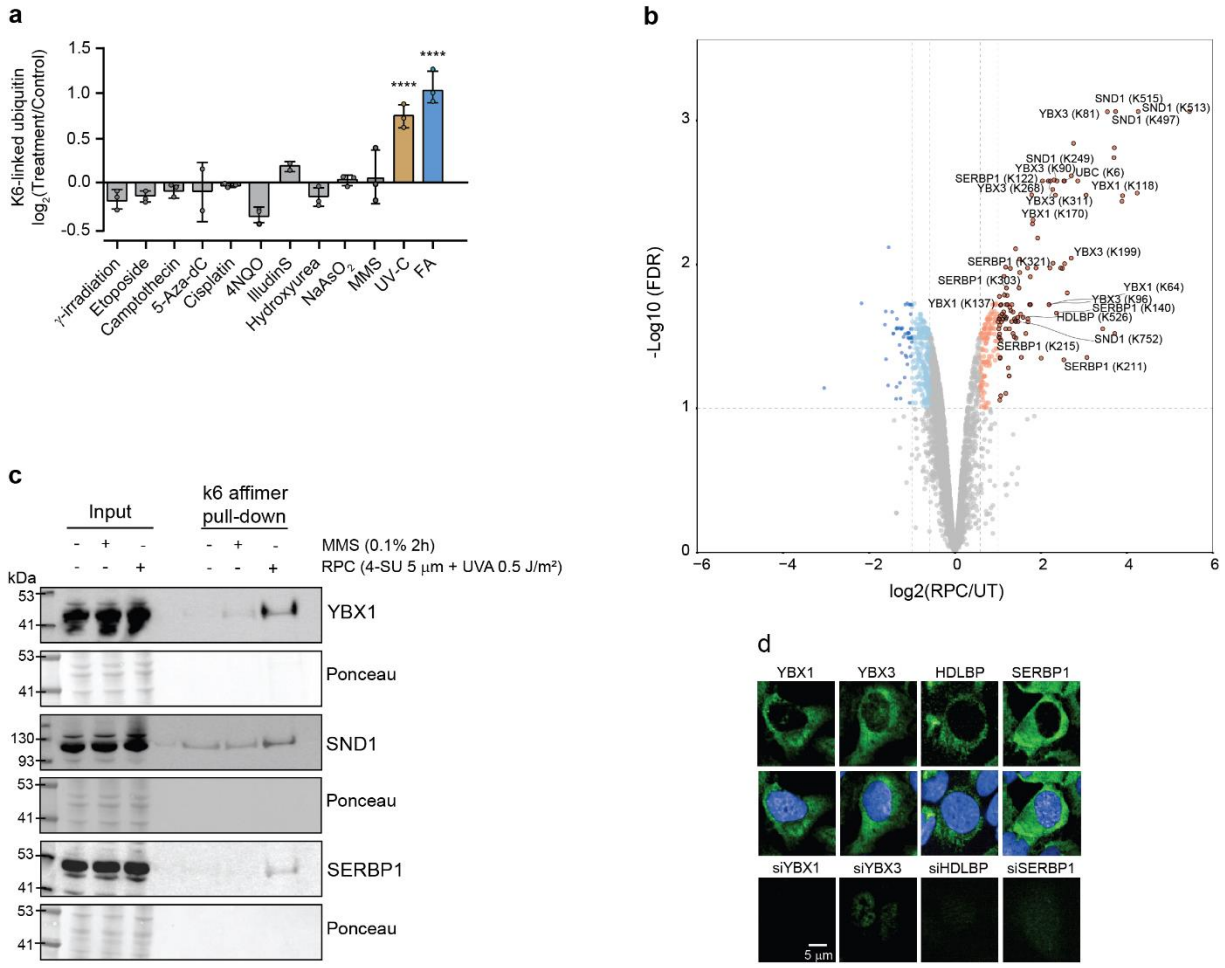

Figure 22. Induction of K6-ubiquitin chain after UV-C irradiation and ubiquitylation of proteins forming RPCs

a) Quantification of K6-linked ubiquitin specific peptide in U2OS cells. The bar plot shows the mean FC in log2-transformed SILAC ratios. The error bars represent the standard deviation. ****p≤0.0001; two-way Anova with Bonferroni correction (Suryo Rahmanto et al., 2023). **b**) Volcano plot of ubiquitylation sites quantified by ubiquitin remnant profiling with three biological replicates. The mean of log2-transformed SILCA ratios (RPC/control) of all replicates is plotted against –log10-tranformed q value. The q value and enrichment were calculated using limma (Suryo Rahmanto et al., 2023). **c**) Representative blots of the pulldown with K6 ubiquitin affimer after RPC induction in U2OS cells. **d**) Immunofluorescence analysis of RPC-forming proteins in U2OS cells. Scale bar 5 µm.

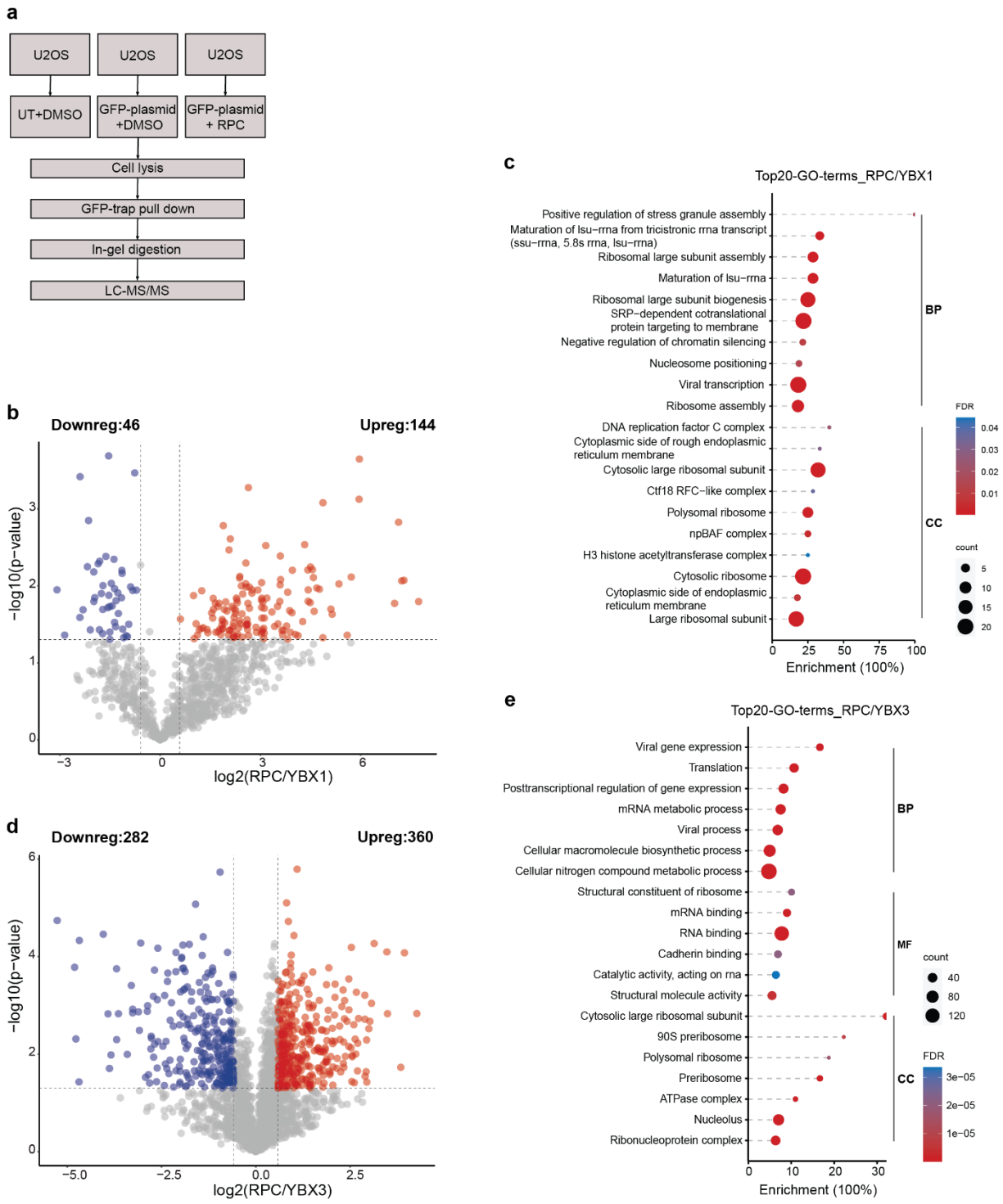

Figure 23. (Continue to the next page)

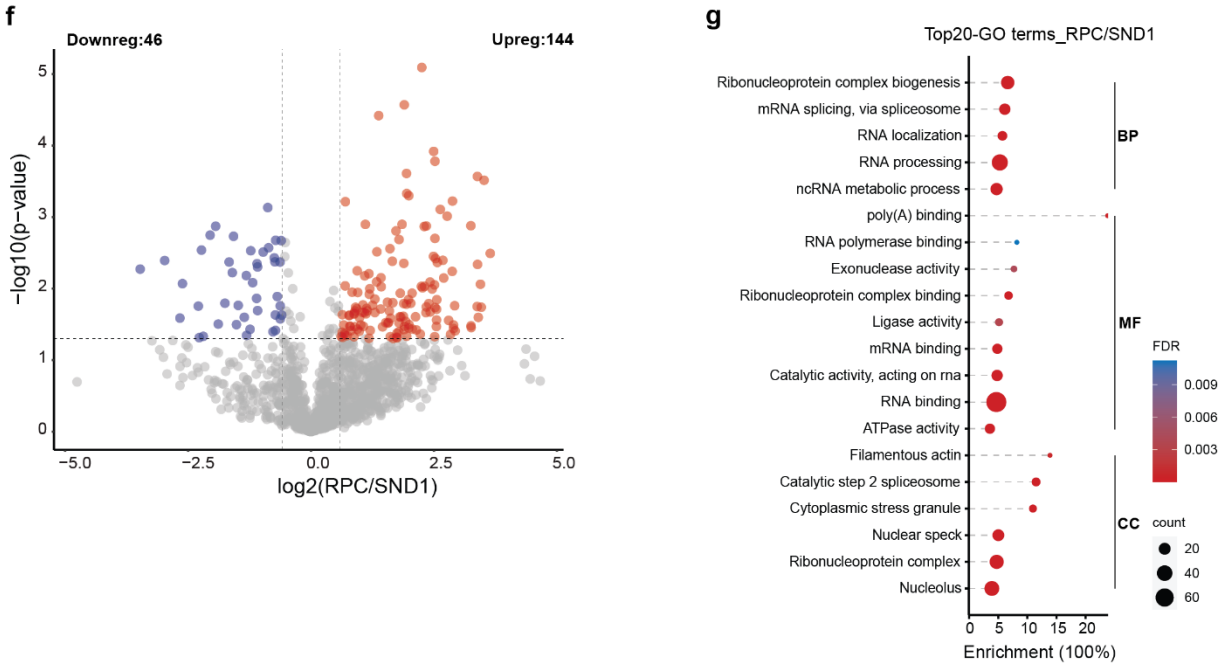

Figure 23. Analysis of the interaction profiling of RPC-proteins

a) Schematic approach for studying the protein interaction profile of RPC- proteins (YBX1, YBX3, SND1). U2OS cells were transfected with GFP-plasmid and treated with DMSO or for RPC-induction (as described in the text). Proteins were digested with trypsin and peptides were analyzed by LC-MS/MS. Volcano plots of interacting proteins of RPC-proteins upon RPC-induction **b**) RPC/exogenous YBX1, **d**) RPC/exogenous YBX3, **f**) RPC/exogenous SND1. The mean of the log_2-transformed LFQ intensities of all replicates is plotted against the -log_{10}-transformed p value. The p value was calculated using Perseus, the Benjamini-Hochberg method. The GO-term analysis of the increased proteins of the following conditions: **c**) RPC/exogenous YBX1 **e**) RPC/exogenous YBX3 **g**) RPC/exogenous SND1. Enrichment analysis performed using String database.

3 Discussion

The current study has the aim to enhance the comprehension of the intricate cellular response to UV-C irradiation in whole organisms. Using zebrafish embryos, we investigated the changes in gene expression and underlying protein-based molecular mechanisms and cell signaling pathways induced by UV-C irradiation in a whole organism and compared the results to the knowledge we have in human cells [3].

We started characterizing the kinetics of the UV-C-induced DNA lesions and the responses in HaCaT and RPE-1 cells, human cells that in physiological conditions are exposed to UV-light and are not of the tumor origin. Afterwards, we used zebrafish embryos as a model organism to have the overview of the UV-C-induced DNA damage response (DDR) in whole organisms. In particular, we investigated the changes of the total protein levels (proteome) at the early and the late UV-C response. In addition, we monitored the cell signaling pathways triggered by UV-C response (phosphoproteome). Subsequently, upon UV-C irradiation, we investigated the alterations of the ubiquitylated proteins by performing OtUBD affinity purification with quantitative proteomics (ubiquitylome). To complete the overall picture, we investigated the changes in gene expression resulting by UV-C induced DNA damage (transcriptome). At the end, we compared our study in zebrafish embryos to studies performed in human cells [3]. We highlighted the conservation of selected ATM/ATR phosphorylation sites and the cell signaling pathways activated by UV-C irradiation in zebrafish embryos.

UV-light is divided into three different categories depending on the wavelength: UV-A (320-400 nm), UV-B (280-320 nm) and UV-C (100-280 nm). UV-C irradiation represents the most dangerous wavelength range of UV light since it induces the formation of DNA adducts, in particular cyclobutane pyrimidine dimers (CPDs) and 6-4 photoproducts (6-4PPs) [22], and RNA-protein crosslinks (RPCs) [23]. Upon their generation, CPDs and 6-4PPs induce distortions within the DNA double helix [283]. The presence of these bulky lesions can interfere with important cellular processes like transcription and replication, which can compromise genome stability and cell viability [284]. DNA adducts can obstruct the progression of the transcribing RNA polymerase II (Pol II), inhibiting transcription and initiating the transcription-coupled nucleotide excision repair (TC-NER) [64]. The resolution of the CPDs takes longer compared to the resolution of 6-4 PPs [289] and this is supported also from our IF data (**Figures 10a**, **10b**, **10c** and **10d**). If not resolved, the accumulation of DNA damage and mutations can lead to the development of cancers, such as cutaneous squamous cell carcinoma, basal cell carcinoma and cutaneous melanoma [285]. Our recent publication [23] showed that UV-C irradiation and formaldehyde (FA) produce RNA-protein crosslinks (RPCs) and their resolution is regulated by K6-ubiquitylation together with an evolutionarily conserved ubiquitin E3 ligase, RNF14.

In the recent years, zebrafish became a valuable model system employed across various research fields [254], [255]. Around 70% of zebrafish genes have human orthologs [286] and the improved knowledge of both the UV-induced DDR and the genes involved in repair mechanisms, including NER, further supports the use of zebrafish as complementary mammalian models [259], [260],

[261]. In particular, zebrafish have a competent p53-dependent NER pathway for repairing UV-induced DNA damage leading to the phosphorylation of histone H2AX. In addition, zebrafish develop cancers, like melanoma, that resemble human tumors both at molecular and histopathological levels [2], [287]. From the experimental point of view, the extra utero development of zebrafish provides easier exposure to UV radiation [2].

3.1 UV-C induced DNA damage response

In human cells, UV-C irradiation induces the formation of photoproducts that impede DNA replication and transcription [64]. To preserve genome stability, cells evolved the DDR for synchronizing DNA repair with cell cycle progression, DNA replication and RNA metabolism. ATM and ATR are the primarily kinases that are activated upon DNA damage. ATM regulates the repair of double-stranded breaks (DSBs) [121]. Instead, ATR responds to different types of DNA damage that have in common the presence of single-stranded breaks (SSBs), that are generated as intermediates of DNA repair pathways (for example NER), and stalled replication forks [6].

Although ATM and ATR are activated by different stimuli, their substrates significantly overlap [318]. Once the activated ATM/ATR kinase is at the damage site, it phosphorylates a variety of targets facilitating cellular responses to the damage. One important ATM/ATR target is the histone H2AX [319], [320]. The phosphorylated form of H2AX (γH2AX) serves as a platform for recruitment of additional DDR factors and enhancement of signaling pathways [6]. Previous studies have revealed the phosphorylation of H2AX at the damaged sites upon UV exposure [320], as shown also from our IF data (**Figures 10e** and **10f**).

ATR-CHK1 pathway is recognized as the principal coordinator of the cellular response to UV-C irradiation [321]. CHK1 is the most relevant downstream target of ATR which induces cycle arrest in the S and G2/M phases in response to DNA damage [6] [318]. Both PI-3Ks, ATM, and ATR have been demonstrated to phosphorylate proteins on with serines or threonines located within the S/TQ motif in response to stress [123], [295], [322]. The S/TQ motif is indeed overrepresented in our sequence analysis in zebrafish embryos upon UV-C irradiation (**Figures 16a** and **16c**).

Spatiotemporal protein reorganization at DNA damage sites induced by genotoxic chemotherapies is crucial for DDR, which influences response by directing cancer cell fate. This process is orchestrated by valosin-containing protein (VCP), an AAA+ ATPase that extracts polyubiquitylated chromatin proteins and facilitates their turnover. The phosphorylation of VCP at S784 is important for DNA damage response [323]. Upon UV irradiation, VCP undergoes phosphorylation at S784 in its C-terminal domain [119], [322], [324] and this modification selectively enhances chromatin-associated protein degradation and is required for DNA repair, signaling, and cell survival [325]. This site is phosphorylated by ATM, ATR, or DNA-PKcs [326]. Phosphorylation of VCP at S784 dependent on ATM/ATR upon UV-C irradiation is supported by our analysis in zebrafish embryos (**Figures 18a** and **18b**).

The conserved chromatin-associated protein NUCKS1 has a role in the DNA damage response. It has been showed that the phosphorylation of nucks1a at S54 (in zebrafish S52) depends on ATM and is involved in HR pathway [122], [327].

DSBs repair is crucial to preserve genomic integrity and maintain cellular homeostasis. TP53-binding protein 1 (TP53BP1) is an important and conserved regulator of the cellular response to DSBs that promotes NHEJ. The phosphorylation of five serine residues shows strong upregulation induced by ATM/ATR kinases (S398, S580, S831, T855, S1068) [3], [29], [328], [329]. It has been demonstrated that the function of TP53BP1 in promoting NHEJ crucially depends on RIF1 [330].

The above-mentioned phosphosites we found to be conserved and phosphorylated in response to UV-C irradiation in zebrafish embryos. In particular, we identified VCP S784, NUCKS1 S54 (S52 in human) and TP53BP1 S492 (S580 in human) upon UV-C irradiation. We identified increased phosphorylation of RIF1 at S1465 and this site appears not conserved in humans (**Figure 18**).

After UV-C irradiation, ATM/ATR activation induces cell cycle arrest through p53/p21 pathway [331], [332]. In addition, it is also showed that, indirectly, p38 MAPK affects the cell cycle through the activation of the tumor suppressor p53, which induces the transcription of a number of genes regulating cell cycle, in particular p21 and Gadd45 [333], [334]. p21 and Gadd45 are the most upregulated genes in our zebrafish transcriptomic analysis after UV-C irradiation, confirming the activation of p53 signaling pathway and the resulting cell cycle arrest (**Figures 20b** and **20c**).

Stress conditions, including UV irradiation, induce the formation of paraspeckles. These are non-membrane organelles in the nucleus generated by protein liquid-liquid phase separation (LLPS) [335]. Their formation requires a specific long noncoding RNA (lncRNA), nuclear paraspeckle assembly transcript 1 (NEAT1) [336], [337], [338]. Paraspeckles are enriched with other types of RNAs [339], [340] and paraspeckels proteins (PSPs) [341]. The PSPs, such as PSP1, NONO [342], SFPQ [343] belong to the Drosophila behavior human splicing (DBHS) family. There are also other proteins involved in paraspeckles, as HNRNPM and CPSF6 [344]. In line with that, in zebrafish proteomic analysis, the total protein level of the paraspeckles proteins NONO, SFPQ, CPSF6 and HNRNPM increases upon UV-C radiation.

3.2 Signaling pathways induced by UV-C in zebrafish embryos

The effects of UV light go beyond activation of DNA damage response pathways, and include inflammatory signaling, systemic immune response and general stress responses [203]. Cells constantly communicate through a myriad of signaling pathways, the activation of which depends on parameters such as dose, time of exposure and wavelength of UV light [164]. Both ROS and pro-inflammatory cytokines, resulting from UV exposure, can function as activators of the signaling transduction pathways [165], [345]. The generation of ROS can cause several types of DNA lesions, for example DNA-protein crosslinks, strand breaks and AP-sites, and changes in protein structure and function that result in alteration in the collagen fibers and dermis conformation [20]. In fact, in our study we found a set of genes (col5a3a, col2a1a, loxl1, col11a2, spint1a) involved in collagen fibril organization (GO-BP terms) transcriptionally elevated at early

response (**Figure 20e**). This could mean that organisms compensate for ROS-induced collagen damage by upregulating collagen production.

TGF-β signaling pathway plays an important role in regulation of different processes including cell growth, differentiation, immune and inflammatory responses, and angiogenesis [204]. The latent form of TFG-β is activated upon the interaction with factors, such as ROS and cytokines, which allow the release of the mature TGF-β [346]. Mature TGF-β interacts with a couple of serine/threonine kinase receptors, TGFβII and TGFβI, triggering the intracellular signaling cascade [205]. Our kinase prediction analysis based on zebrafish phosphoproteome shows the TGFβII and TGFβI receptors as ones of the most activated kinases appearing upon UV-C irradiation and indicating that this pathway is highly activated in a whole organism and is employed for counteracting the UV induced stress response.

A subgroup of proteins belonging to the TGF-β family includes the bone morphogenetic proteins (BMPs) [347]. The TGF-β/BMPs signaling pathway is mainly involved in the regulation of early development and homeostasis of various adult tissues [301], [348], [349]. Recent studies have demonstrated the implication of the BMP signaling in modulating various post-injury processes, in particular endogenous cell replacement, cell death and damage response [301], [350], [351], [352], [353]. Interestingly, in our zebrafish kinase prediction analysis, we found several BMPs receptors (such as BMPR1B, ACVR2B, BMPR1A and ACVR2A), activity of which increases upon UV-C irradiation. In this case, we could exclude their participation in developmental processes considering the normalization performed over the corresponding untreated embryos (early response) and link the activation to the UV-C response for repairing the lesions.

UV-C radiation triggers MAPK signaling pathways [354]. The activation of the conserved MAPK pathways occurs with the phosphorylation of the sites belonging to the consensus sequence that consists of a dual-phosphorylation domain (Thr-Xxx-Thyr) [355], [356], [357], [358]. Depending on the subfamily of MAPKs, this sequence can slightly change. In fact, ERKs have the TEY sequence, JNKs have the TPY sequence and p38 MAPKs have the TGY sequence [172], [359], [360]. Upon stimulation, phosphorylation of Y180 plays a crucial role in p38 activation, whereas phosphorylation on Y182 is crucial for stabilization with substrates and p38 autophosphorylation [167]. In line with this, in our zebrafish phosphoproteome analysis, we identified the conserved sites belonging to the consensus sequence of p38 (T181-Y183) and JNK (T183-Y185) (**Figure 19a**). A downstream target of p38 MAPK signaling cascade is NELFE, the smallest subunit of the NELF complex that blocks Pol II at promoter proximal pausing (PPP) site. In particular, phosphorylation of NELFE at S115 triggers the detachment of the NELF complex from the chromatin [3] and release of Pol II from the PPP. S115 of NELFE is conserved in different organisms and we found its phosphorylation significantly increasing upon UV-C exposure in zebrafish embryos, suggesting the conservation of the mechanism regulating Pol II in response to UV-C irradiation in zebrafish (**Figures 19d** and **19e**).

ERK3/MAPK6 is considered as an atypical MAPK since its consensus sequence contains a Ser-Glu-Gly (SEG) motif compared to the typical TXY [361]. ERK3/MAPK6 is phosphorylated by the

group I p21-activated protein kinases (PAK1/2/3) [362], [363]. Phosphorylation of ERK3/MAPK6 at S189 plays an important role in invasiveness-promoting ability in lung cancer cells [364] in cell cycle arrest and in response to UV-C [3], [29], [365]. Downstream target of ERK3/MAPK6 cascade is the MAP kinase-activated protein kinase 5 (MK5). MK5 mediates phosphorylation of HSP27/HSPB1 in response to p38-regulated/activated kinase (PRAK /PKA/PRKACA) stimulation, inducing F-actin rearrangement [366], [367]. Dephosphorylation of S189 ERK3/MAPK6 by DUSP2 negatively regulates ERK3/MK5 pathway [368] (**Figure 19a**). As mentioned previously, PAKs phosphorylate ERK3/MAPK6 [362]. In accordance with the dephosphorylation of ERK3/MAPK6 at S189, our kinase prediction analysis in zebrafish embryos shows less activation of PAKs (**Figure 16b**).

The GRKs are protein kinases that function together with arrestins to regulate a variety of GPCRs. The GPCRs function in a variety of signaling pathways and their persistent stimulation may alter physiological properties of the normal cells. Their regulation through GRKs represent a mechanism for preventing their dysfunction and limit their hyperactivation. In fact, GRKs trigger the kinase-dependent homologous desensitization of GPCRs by phosphorylating the receptor and allowing the recruitment of arrestin in a canonical pathway, preventing excessive stimulation of the cascade. GRKs can also activate a non-canonical signals interacting with other proteins [198]. Their function depends on the GRKs isoform and the location of the body in which it is expressed. GRK1 and GRK7 are photoreceptors that can be activated by photons. Studies performed in mammals demonstrated that after light stimulus, when Ca^{2+}-concentration decreases, recoverins (Rec) dissociate from GRKs. Rec specifically regulates GRKs activity in a Ca^{2+}-dependent manner and then controls phosphorylation of photoexcited opsin [369], [370], [371]. In most mammals, both GRK1 and GRK7 have been identified, which are expressed in rods (GRK1) and cones (GRK1 and GRK7) in a species-specific manner [298]. Instead, in zebrafish four different isoforms of GRKs corresponding to GRK1 and GRK7 are found (zGRK1a, zGRK1b, zGRK7a and zGRK7b) and are present in the retina ([372], [373], [374]. In zebrafish kinase prediction, GRK1 is significantly activated compared to human, in which its activity appears to decrease. On the other hand, the activity of GRK7 increases in both models upon UV-C stress (**Figures 16b**, **16d** and **17**).

Recent studies have demonstrated a link between the DDR and the unfolded protein response (UPR) [375], [376], [377]. The UPR is the primary mechanism through which cells attempt to resolve endoplasmic reticulum (ER) stress caused by misfolded proteins in the ER. Among the UPR regulators, IRE1a is an ER transmembrane sensor that functions as a dual protein kinase and endoribonuclease [312]. A recent study showed that IRE1a is required for the proper function of the UV DDR, influencing checkpoint activation and repair of CPDs [378], and its hyperactivation under prolonged ER stress can trigger apoptosis through the TRAF2-ASK1-JNK pathway [313], [314]. In line with this, we found the increased activity of IRE1a in our kinase prediction analysis in zebrafish embryos. In addition, it is known that Fam20C phosphorylates protein disulfide isomerase (PDI) as a rapid post-translational mechanism for integrating ER proteostasis sensing and cell fate control. Phosphorylated PDI induces the attenuation of IRE1a activity in prolonged ER-stress, which is critical for protecting against ER stress-induced liver damage [311]. In

zebrafish embryos, among the kinases we found the significant increased activity of FAM20C (**Figures 16b**, **16d** and **17**).

UV-C irradiation leads to the activation of PLK3 that phosphorylates CHEK2, promoting the G2/M transition checkpoint, and CDC25A, p53/TP53 and p73/TP73 by promoting G1/S transition checkpoint [379], [380], [381], [382]. This is confirmed by our kinase prediction analysis in zebrafish embryos.

Furthermore, COT is a kinase required for TLR4-mediated activation of the MAPK/ERK pathway in macrophages, thus being critical for production of TNF-α during immune responses. It may also play a role in the transduction of TNF signals that activate JNK and NF-kB in some cell types.

Recently, study from our laboratory demonstrated that UV-C irradiation induces the formation of RPCs and their resolution depends on K6-ubiquitylation [23]. We identified some RPC proteins, in particular YBX1 and SND1. In zebrafish ubiquitylome analysis, we confirmed the increased K6-linked ubiquitylation, and ubiquitylation of YBX1 and SND1, upon UV-C irradiation (**Figures 21f** and **21g**), suggesting the conservation of K6-ubiquitin linkage function in zebrafish embryos and as a relevant response in a whole organism in response to UV-C.

Upon UV-induced DNA damage, Pol II degradation is thought to occur in order to expose the lesion, only when backtracking is not possible [66]. More recently, it has been demonstrated that Pol II stalling induces ubiquitylation of the catalytic subunit of Pol II, RPB1, at K1268, with implications in lesion repair, RPB1 degradation and gene expression [154], [155]. The increased Pol II ubiquitylation has been confirmed also from our ubiquitylome analysis in zebrafish embryos (**Figure 21b**).

It has been reported that UV radiation induces monoubiquitylation of the FANCI/FANCD2 (ID) complex that promotes DNA repair through the Fanconi anemia (FA) pathway [107], [383]. ATR-mediated phosphorylation of FANCI acts as major molecular switch to activate the FA pathway upon replication stress [384]. It has been demonstrated that monoubiquitylated PCNA stimulates FANCD2 and FANCI monoubiquitylation and is their important regulator [111], [385], [386]. Ubiquitylation of PCNA and ID complex increases significantly in zebrafish embryos upon UV-C stress indicating a possible activation of the FA pathway in a whole organism (**Figures 21b** and **21d**).

3.3 Comparison of UV-C induced response from cells to a whole organism

Taking into account the study performed by Borisova et al., we were able to highlight the main differences and similarities between the kinases regulation in human cells and in zebrafish embryos upon UV-induced DNA damage. We leverage the kinase library based on human (https://kinase-library.phosphosite.org/ea), as a zebrafish-specific resource is yet to be available and we relied on the high homology between human and zebrafish kinases [296].

In human cells, it has been observed that MAPKs, in particular the isoforms of JNK1s and p38, emerge as prominently activated kinases in response to UV-C irradiation [3]. Intriguingly, our predictive kinase analysis in zebrafish embryos reveals a distinctive pattern, with members of the GRKs family, particularly GRK6 and the photoreceptor GRK1, exhibiting significant activation compared to human cells. Additionally, another notable group of kinases showing significant activation in zebrafish embryos, in contrast to human cells, comprises the BMP receptors, such as BMPR1A, BMPR1B, ACVR2B, and ALK2.

Of particular interest is that our analysis performed in zebrafish embryos underscores the significant activation of FAMC20 and IRE1a kinases, implicated in ER-stress response. Remarkably, from our analysis this pathway is not stimulated in human cells.

Expectedly, key DNA damage response kinases such as ATM, ATR, and DNA-PK exhibit activation in both cellular and embryonic models upon UV-C exposure.

Furthermore, our findings reveal the phosphorylation of NELFE at S115 following UV-C irradiation, indicating the conservation of its functional role in regulating Pol II in zebrafish embryos. Additionally, we observed ubiquitylation events involving K6-linkage and RPC proteins, alongside the ubiquitylation of PCNA, FANCI, and FANCD2, components of the FA repair pathway.

In conclusion, our study provides a comprehensive overview of the UV-C induced response in a whole organism, offering a valuable resource for the scientific community. Through the demonstration of conserved and activated pathways in zebrafish embryos compared to human cells, we shed light on both similarities and differences. Notably, the activation of ER-stress response and the resolution of RPCs emerge as intriguing pathways for further investigation and clarification of the UV-induced response.

4 Materials and Methods

4.1 List of all consumables, software and equipment

Table 1: Buffers/Solutions/Consumables

Cell culture	**Composition / vendor**
4-thiouridine (4SU)	Jena Bioscience
5-Ethynyl-2-deoxyuridine (EdU)	Jena Bioscience
5-Ethynyl uridine (EU)	Jena Bioscience
Bafilomycin A (BafA)	Sigma Aldrich
Biotin-phenol	Iris Biochem
Bortezomib	Selleckchem
Cyclohexamide (CHX)	Merck
Dialyzed FBS (10,000 molecular weight cut-off)	Thermo Fisher Scientific
Dimethyl sulfoxide (DMSO)	Sigma Aldrich
D-MEM for SILAC without lysine and arginine	Sigma Aldrich
Dulbecco's Modified Eagle Medium (D-MEM)	Gibco
Dulbecco's Phosphate-Buffered Saline (D-PBS)	Gibco
Fetal bovine serum (FBS)	Gibco
Human bone osteosarcoma epithelial cells (U2OS)	ATCC
Human colorectal carcinoma epithelial cells (HCT116)	ATCC
Human embryonic kidney cells (HEK293T)	ATCC
Human hTERT-immortalized retinal pigment epithelial cells (RPE-1)	ATCC
Hydrogen Peroxide	Sigma Aldrich
L-arginine (Arg0)	Cambridge Isotope Laboratories
L-lysine (Lys0)	Cambridge Isotope Laboratories
L-arginine-U-13C6 99% (Arg6)	Cambridge Isotope Laboratories
L-lysine-4,4,5,5,-D4 96–98% (Lys4)	Cambridge Isotope Laboratories
L-arginine-U-13C6-15N4 99% (Arg10)	Cambridge Isotope Laboratories
L-lysine-U-13C6-15N2 99% (Lys8)	Cambridge Isotope Laboratories
L-glutamine	Gibco
MG132	Sigma Aldrich
Penicillin/Streptomycin	Gibco
Pladienolide B (PladB)	Santa Cruz Biotechnologies
Puromycin	InvivoGen
Quenching solution	1 mM Sodium azide, 10mM Sodium ascorbate and 5mM Trolox in D-PBS
Roswell Park Memorial Institute 1640 Medium (RPMI)	Gibco
Trypsin-EDTA (0.05%)	Gibco
Transfection	
Lipofectamine RNAiMAX	Life Technologies
Opti-MEM with GlutaMAX	Gibco
Cell lysis	
Complete protease inhibitor cocktail tablets	Roche Diagnostics
Modified RIPA buffer	50 mM Tris-HCl pH 7.5, 150 mM NaCl, 1 mM EDTA, 1% NP-40, 0.1% Sodium-deoxycholate
No-salt modified RIPA buffer	50 mM Tris-HCl pH 7.5, 1 mM EDTA, 1% NP-40, 0.1% Sodium-deoxycholate
N-ethylmaleimide (NEM)	Sigma Aldrich
NuPAGE LDS Sample Buffer (4×) (LDS SB)	Thermo Fisher Scientific
Magnesium Chloride ($MgCl_2$)	
Phosphatase inhibitors:	
1 mM sodium orthovanadate	Sigma Aldrich
5 mM β-glycerophosphate	Sigma Aldrich
5 mM sodium fluoride	Sigma Aldrich

QuickStart Bradford 1x Dye Protein Reagent	BioRad
RIPA buffer	50 mM Tris-HCl, pH 7.4, 1% Triton X-100, 0.5% Sodium Deoxycholate, 0.1% SDS, 150mM NaCl
Sm Nuclease	IMB PPCF

Pull-downs

ANTI-FLAG M2 Affinity Gel	Merck Millipore
Biotin-conjugated diK6 affimer	Inhouse
Dynabeads Protein G beads	Thermo Fisher Scientific
GFP-conjugated diK6 affimer	Millipore
Neutravidin beads	Thermo Fisher Scientific
Urea	Sigma

SDS-PAGE and Western blotting

0.45 µm nitrocellulose	Sigma Aldrich
Blocking buffer	10% skimmed milk solution in PBS-T or 5% BSA in PBS-T or 3% BSA in PBS-T
Bovine serum albumin (BSA)	Sigma Aldrich
Dithiothreitol (DTT)	Sigma Aldrich
NuPAG MOPS SDS Running Buffer (20X)	Thermo Fisher Scientific
NuPAGE Bis-Tris gels 4-12%	Thermo Fisher Scientific
PBS-T	1x PBS, 0.1% Tween-20
Ponceau S	Sigma Aldrich
Ponceau S solution	0.1% (w/v) Ponceau S, 5% acetic acid
SuperSignal West Pico Chemiluminescent Substrate	Thermo Fisher Scientific
Transfer buffer	25 mM Tris, 192 mM Glycine, 20% (v/v) ethanol, pH 8.3

Microscopy and flow cytometry

4% paraformaldehyde (PFA) in PBS	Affymetrix
Alexa Fluor 647 azide	Thermo Fisher Scientific
Copper (II) sulfate pentahydrate in PBS	Sigma Aldrich
Blocking buffer	5% BSA in PBS-T
Hoechst 33342	Thermo Fisher Scientific
Permeabilization buffer	0.3% Triton X-100 in PBS
Sodium L-ascorbate	Sigma Aldrich

Mass spectrometry

In-gel digestion

Buffer B	80% ACN, 0.5% acetic acid
Chloroacetamide (CAA)	Sigma Aldrich
Colloidal Blue Staining Kit	Life Technologies
Destaining solution	50% Ethanol, 50 mM ABC buffer pH 8.0
Digestion buffer	25 mM ABC buffer pH 8.0
Peptide extraction buffer	30% ACN, 3% TFA
Sequencing grade Trypsin (0.5 µg/µl in 50 mM acetic acid)	Serva

In-solution digestion

Denaturation buffer	6 M urea, 2 M thiourea in 10 mM HEPES-NaOH pH 8.0
SepPAK C18 cartridges	Waters

Stage tipping

Buffer A	0.1% formic acid
Buffer B	80% ACN, 0.1% formic acid
C18 elution buffer	50% ACN, 0.1% formic acid
C18 Empore 47 mm extraction disks	CDS Analytical

Micro-SCX fractionation

SCX elution buffers	40 mM acetic acid, 40 mM boric acid, 40 mM phosphoric acid. (Adjust pH to the indicated pH values with sodium hydroxide. Add 40% ACN before use)
SCX Empore Cation 47 mm extraction disks	CDS Analytical
SCX wash buffer	40% ACN, 0.1% TFA

mRNA sequencing

DNase	New England Bioloabs
Direct-zol™ RNA MiniPrep Plus	Zymo research
RNeasy Plus Mini Kit	Qiagen
RNase-free water	Sigma Aldrich
RNAaseZAP	Sigma Aldrich
TRIzol	Invitrogen
TruSeq Stranded mRNA LT Sample Prep Kit	Illumina

Critical commercial assays	**Source**	**Identifier**
Gateway LR clonase II enzyme mix	Thermo Fisher Scientific	Cat# 11791020
Invitrogen Qubit RNA High Sensitivity	Thermo Fisher Scientific	Cat# Q32852
TMTpro 11plex Label Reagent Set	Thermo Fisher Scientific	Cat# A37724

Table 2: List of primary antibodies used in this study. Unless otherwise stated, indicated dilutions refer to western blotting.

Antibody	**Product number**	**Manufacturer**	**Dilution**	**Origin**
CPD	CAC-NM-DND-001	Hölzel Diagnostika Handels GmbH	IF 1:500	mouse
6,4-PP	NMDND002	Hölzel Diagnostika Handels GmbH	IF 1:500	mouse
FLAG M2	F1804	Sigma-Aldrich	1:1000	mouse
GFP	sc-9996	Santa Cruz Biotechnology	1:500	mouse
γH2AX (S139)	05-636	Millipore	1:1000 1:500 (IF)	mouse
HDLBP	ab109324	Abcam	1:500 1:1000 (IF)	rabbit
SND1	HPA002632	Sigma-Aldrich	1:1000	rabbit
PAI-RBP1(F-8)	sc-376832	Santa Cruz Biotechnology	1:1000 1:1000 (IF)	mouse
YB1	4202	Cell Signaling Technology	1:1000 (IF)	rabbit
YBX3	HPA034838	Sigma-Aldrich	1:1000	rabbit
Ubiquitin	sc-8017	Santa Cruz Biotechnology	1:1000	mouse

Table 3: List of secondary antibodies used in this study. Indicated dilutions refer to western blotting, unless otherwise stated.

Antibody	**Product number**	**Manufacturer**	**Dilution**	**Origin**
Alexa Fluor 488, 568	A11001, A11004	Life Technologies	1:1000 (IF)	mouse
Alexa Fluor 488, 568	A1108, A11011	Life Technologies	1:1000 (IF)	rabbit
Alexa Fluor 488 Azide	A10266	Life Technologies		
Streptavidin-HRP	21130	Thermo Scientific	1:5000	

Table 4: List of siRNAs used in this study.

Oligonucleotides	**Source**	**Identifier**
ON-TARGETplus non-targeting	Horizon Discovery	Cat# D-001810-10

siRNA pool ON-TARGETplus Human YBX1 siRNA pool	Horizon Discovery	Cat# L-010213-00
ON-TARGETplus Human YBX3 siRNA pool	Horizon Discovery	Cat# L-010213-00
ON-TARGETplus Human HDLBP siRNA pool	Horizon Discovery	Cat# L-019956-00
ON-TARGETplus Human SERBP1 siRNA pool	Horizon Discovery	Cat# L-020528-01

Recombinant DNA	**Source**
Invitrogen Gateway pDEST53-GFP-HDLBP	Surymo Rahmanto et al., 2023
Invitrogen Gateway pDEST53-GFP-SND1	Surymo Rahmanto et al., 2023
Invitrogen Gateway pDEST53-GFP-YBX3	Surymo Rahmanto et al., 2023
Invitrogen Gateway pDEST53-GFP-YBX1	Surymo Rahmanto et al., 2023
Invitrogen Gateway pDEST53-GFP-SERBP1	Surymo Rahmanto et al., 2023

Table 5. List of software used in this study.

Software
Adobe Illustrator CC2021
Blc2fastq (version 1.19)
BWA (version 0.7.17-r1188)
Cytoscape (version 3.8.2)
DESeq2 (version 1.34)
featureCounts (version 2.0.0)
GraphPad Prism (version 7.04)
Harmony High-Content Imaging and Analysis Software (PerkinElmer) (version 4.4)
Integrated Genome Browser (version 2.12.3)
MaxQuant v (Cox lab)
Perseus (version 1.6.15.0)
R studio ("Cherry Blossom" Release (3c53477a, 2023-03-09) / R (version 4.2.3)
STAR (version 2.7.10)
Thermo Xcalibur (Thermo Fisher Scientific)

Table 6. Machines

Machines	**Vendor**
3311 Forma Steri-Cult CO_2Incubator	Eppendorf
Bioruptor NGS	Diagenode
ChemiDoc imaging system	BioRad
CL-1000 Ultraviolet Crosslinker	UVP
Easy-LC-1000	ThermoFisher Scientific
Easy-LC-1200	ThermoFisher Scientific
M80 Microscope	Leica
NanoDrop 2000	ThermoFisher Scientific

NextSeq550	Illumina
NuPage Novex Gel System	ThermoFisher Scientific
Opera Phenix High Content Screening System	PerkinElmer
Orbitrap Exploris 480 masss pectrometer	ThermoFisher Scientific
Q Exactive Plus	ThermoFisher Scientific
Qubit 2.0 Fluorometer	Life Technologies
Sonifier 450	Branson
Thermoshaker	Eppendorf
UV-C irradiator (human cells)	In-house built
UV-A irradiator	peQlab
Vacufuge Plus	Eppendorf
Xcell II Blot-Modul	ThermoFisher Scientific

4.2 Experiments performed in human cells

4.2.1 Human cells

ATCC provided human osteosarcoma cells (U2OS), human epidermal keratinocyte cells (HaCaT) and human retinal pigment epithelial-1 (RPE-1). U2OS and HaCaT cells were cultured in D-MEM medium and RPE-1cells were cultured in RPMI medium, supplemented with 10% fetal bovine serum (FBS), 2 mM L-glutamine, and 100 U/ml Penicillin/Streptomycin. Puromycin was also added to stable cell lines at a concentration of 1 g/l. Cells were washed in PBS, detached with 0.05% trypsin, and resuspended in complete D-MEM/RPMI medium to stop the enzymatic activity. This was followed by spinning down at 250x g for 5 minutes and re-plated to the desired confluence. Cells were grown in a humidified incubator with 5% CO2 at 37 °C. Cells were irradiated using an in-house built UV chamber.

4.2.2 Transfection of cells

For siRNA transfection of cells in a 10cm dish, cells were grown to 60% confluence in 10 ml complete D-MEM before being transfected. Following that, 8 µl of siRNA (10 µM) and 10 µl siRNA Max were diluted in 500 µL Opti-MEM. For DNA transfection, 5 µg of plasmid DNA and 15 µL polyethylenimine (PEI) was diluted in 500 µL Opti-MEM. The mixtures were combined into a master mix and incubated for 15 minutes at RT, and then added to the cells for 6 hours before the medium was changed to fresh D-MEM. Cells were used for experiments 48 to 72 hours after being transfected with DNA or siRNA. Transfection volumes in different culture dish sizes were scaled based on surface area depending on the experimental demand.

4.2.3 UV-C treatment

An in-house built UV-C machine has been used for the UV-C treatment in HaCaT and RPE-1 cells (245 nm). For the IF assay, HaCaT and RPE-1 cells were irradiated with 15 J/m^2 and 12 J/m^2, respectively. For the viability assay, both cell lines were UV-C irradiated using different doses: 5, 10, 20, 40, 80 J/m^2.

4.2.4 EU treatment

To examine changes in RNA synthesis upon treatment, nascent RNAs were labeled by incubating the cells with 100 mM EU (Jena Bioscience) for 30 minutes.

4.2.5 RPC treatment

Cells were treated with 4-Thiouridine (4SU) (Jena Bioscience) overnight and irradiated using UV-A irradiation (345 nm, 0.5 J/m^2) (peQlab) and harvested after 45 minutes.

4.2.6 Colony-forming assay

Cells were plated at a density of 2000 cells per plate in 6-well plates. Cells were UV-C irradiated (5, 10, 20, 40, 80 J/m^2) and let grow in the incubator at 37 °C for 10 days. Colonies were stained with 0.5% crystal violet solution in 25% methanol and counted 12-14 days after the irradiation using the microscope Leica M80.

4.2.7 Immunofluorescence assay

Cells were fixed with 4%paraformaldehyde and permeabilized with 0.3% Triton X-100 in PBS and stained with designated primary antibodies (1:1000) in 5% (w/v) BSA/PBS overnight at 4°C. Cells were incubated with the secondary antibodies (1:1000) in 5% (w/v) BSA/PBS for 2 h in a humidified dark chamber at RT. Nuclei were counterstained with 1 mg/ml Hoechst 33342. Cells were washed twice with PBS and kept at 4 °C in PBS until imaging. Imaging was performed with an Opera Phenix (PerkinElmer) microscope using a 4031.1NA water objective. Image analysis was performed by using Harmony High-Content Imaging and Analysis Software (version 4.4, PerkinElmer). Standard building blocks allowed for nuclei segmentation based on the Hoechst 33342 signal and cells at the edges of the field were excluded.

4.2.8 Gateway cloning

The GFP-expression vectors were generated from Destination vectors and Entry / DONR vectors using the Gateway LR Clonase II Enzyme Mix, as directed by the manufacturer. The vectors used in this work are listed in 4.1 (Table 4).

4.2.9 Pull-downs with K6-ubiquitin affimer

Following cell lysis in modified RIPA buffer, pre-cleared protein lysate was incubated with 1 mM GFP or biotin-tagged reagent with affinity toward K6-ubiquitin (GFP- or biotin-conjugated K6-ubiquitin affimer) for 1 h at 4 C. M-280 Streptavidin Dynabeads (15 ml per sample) or Chromotek GFP-Trap (4 mg of protein lysate per condition) were added and incubated for 1 h at 4°C on a rotating wheel to precipitate biotin- or GFP-conjugated probes, respectively. Beads were washed four times with modified RIPA buffer supplemented with protease inhibitors and 10mMN-ethylmaleimide to remove nonspecific binders prior to elution in NuPAGE LDS 23 Sample Buffer (Life Technologies).

4.2.10 Pull-downs with GFP-tagged proteins

Cells were transiently transfected with a GFP-tagged construct for 48 h prior to RPC induction (5 mM 4-SU, 0.5 J/cm2 UV-A). Cells were lysed in modified RIPA buffer. MgCl2 (2.5 mM) and 1:1000 Sm Nuclease (IMB Core Facilities) were added to the lysates, which were then incubated at 4°C for 30 min. NaCl was added at a final concentration of 450 mM and the mixture was incubated for 15 min on ice. Protein concentration was measured using the Bradford method, and an equal volume of dilution buffer (10 mM Tris-HCl, pH 7.5, 150 mM NaCl, 0.5 mM EDTA) was added to the lysate. GFP-Trap agarose (10 ml per sample) was added to the cleared lysate, followed by incubation for 1 h at 4°C on a rotation wheel. The beads were washed three times with modified RIPA buffer supplemented with protease and phosphatase inhibitors and then twice with phosphate-buffered saline (PBS). Bound proteins were eluted in NuPAGE LDS 23 Sample Buffer (Life Technologies) supplemented with 1 mM DTT, heated at 95 °C for 10 min, alkylated by the addition of 5.5 mM chloroacetamide for 30 min, and loaded onto 4%–12% gradient SDS-PAGE gels. Proteins were stained using the Colloidal Blue Staining Kit (Life Technologies) and digested in-gel using trypsin. Peptides were extracted from the gels and desalted on reverse-phase C18 StageTips.

4.2.11 SDS-PAGE and Western blotting

Proteins were resolved on 4%–12% gradient SDS-PAGE gels (NuPAGE Bis-Tris Precast Gels, Life Technologies) and transferred onto PVDF membranes. Membranes were blocked using 5% (w/v) skim milk solution in PBS supplemented with 0.1% Tween-20. Secondary antibodies coupled to horseradish peroxidase (Jackson ImmunoResearch Laboratories) were used for immunodetection. Detection was performed with the SuperSignal West Pico Chemiluminescent Substrate (Thermo Scientific).

4.3 Experiments performed in zebrafish embryos

4.3.1 Zebrafish embryos

Wild-type zebrafish embryos (*Danio rerio* AB-strain) were provided by the Ketting's laboratory at IMB institute (Mainz, Germany). Animals were maintained under a 14 h light/10 h dark cycle at 28 °C. Developmental stages are provided as hour post fertilization (hpf) based on standard developmental stages.

4.3.2 Zebrafish embryos viability assay

Zebrafish embryos (50 per replicate) were plated into each well of a 6-well plate and UV-C irradiated using the CL-1000 Ultraviolet crosslinker (UVP) (245 nm, 12, 24, 48, 120 J/m^2) [291]. Following UV-C irradiation, E3 medium was added and the embryos were maintained at 28°C. Triplicate petri dishes were irradiated for each dose and monitored over time. Embryos were maintained for up to 120 hours and surviving embryos were counted.

4.3.3 UV-C treatment

Excluding the viability assay, all the experiments were performed treating zebrafish embryos with UV-C (245 nm, 24 J/m^2) using the CL-1000 Ultraviolet crosslinker (UVP) in E3 medium and kept in the incubator at 28 °C for the needed recovery time

4.3.4 TMT-11plex labeling

A minimum of 150 µg of peptide was subjected to TMT labeling at 1.5:1 for 1 hour in 150 mM HEPES buffer (pH 8.5). TMT labeling was terminated with the addition of a 0.4% hydroxylamine solution, and excess labels were removed using reverse-phase Sep-Pak C18 cartridges. The TMT-labeled samples were pooled and desalted as previously described.

4.3.5 OtuBD pulldown

For identify the ubiquitylated proteins induced by UV-C irradiation in 24hpf- zebrafish embryos, we performed ubiquitylome analysis using OtUBD, a high-affinity ubiquitin-binding domain (UBD) derived from an Orientia tsutsugamushi deubiquitylase (DUB), as described from Zhang et al., [4].

4.3.6 Phosphoproteomic and proteomic analysis

For the analysis of proteomes and phosphoproteomes, 50 UV irradiated and untreated 24 hpf-zebrafish embryos/per condition were collected in lysis buffer (25 mM Tris pH 7.5, 150 mM NaCl, 1.5 mM $MgCl_2$, 0.5 % Triton-X-100, 0.5 % NP40, 1Mm DTT, cOmplete™ Mini EDTA-free Protease Inhibitor Cocktail (11836170001, Roche), phosphatase inhibitors (5mM β-glycerophosphate, 5 mM NaF, 5 mM $NaVo_3$). Zebrafish embryos were incubated for 30 minutes and 5x syringing for 3x in total in intervals of 10 minutes each using Omnifi-F® tuberculin 0.01-1ml (B/BRAUN). The lysate were centrifuged for 10 min at 20,000xg at 4 °C and the supernatant were transferred to new tubes, and the pellet were discarded. Total protein concentrations were estimated using the QuickStart Bradford Protein assay (Bio-Rad) from the pre-cleared lysates and the amount of protein from each TMT-labeled protein lysate was calculated and combined at a 1:1:1 ratio. Combined protein lysates were precipitated in a fourfold excess of ice-cold acetone and subsequently re-solubilized in 6 M urea/2 M thiourea buffered in 10 mM HEPES (pH 8.0). Cysteine residues were alkylated with 5.5 mM chloroacetamide in the presence of 1 mM dithiothreitol (DTT) prior to digestion with sequencing-grade modified trypsin (Serva). Trypsin digestion was performed at a 1:150 ratio at room temperature for 18 hours and terminated by acidification using 0.5% trifluoroacetic acid (TFA). Digested peptides were purified using reverse-phase Sep-Pak C18 cartridges (Waters) and eluted in 50% aqueous acetonitrile. Ubiquitin remnant peptides were enriched on 80 µl of diglycine-lysine antibody resin (Cell Signaling Technology) for 4 hours at 4°C on a rotation wheel. The beads were washed three times in IAP buffer and then washed three times in water. The enriched peptides were eluted with 0.15% aqueous TFA, separated into six fractions using microcolumn-based strong-cation-exchange chromatography (SCX), and desalted on reverse-phase C18 StageTips. For phosphoproteome analysis, phosphorylated peptides were enriched from 5 mg of trypsin-digested peptide over 10 mg of TiO_2 spherical beads in the acetonitrile/TFA buffer (50% acetonitrile and 6% TFA) for 1 hour. Unbound peptides were washed

away with the ACN/TFA buffer and the enriched phosphopeptides were eluted in a mixture of 10% NH_4OH and 25% acetonitrile. Next, the eluted phosphopeptides were concentrated and acidified using a SpeedVac prior to SCX fractionation and C18 desalting of the eluted phosphopeptides. For whole proteome analysis, 50 µg of trypsin-digested peptides were fractionated using SCX microcolumns into eight fractions and desalted on reverse-phase C18 StageTips prior to MS analysis.

4.3.7 Peptide identification

Raw data were analyzed using MaxQuant (development version 1.5.2.8) [387]. Parent ion and MS^2 spectra were searched against a database containing ~ 48.000 (reviewed and unreviewed) protein sequences for Danio rerio (Zebrafish) obtained from UniProtKB (June 2023 release) using the Andromeda search engine[388]. Spectra were searched with a mass tolerance of 6 ppm in MS mode, 20 ppm in HCD MS^2 mode and strict trypsin specificity, allowing up to three miscleavages. Cysteine carbamidomethylation was searched as a fixed modification, whereas protein N-terminal acetylation and methionine oxidation were searched as variable modifications. The dataset was filtered based on posterior error probability (PEP) to arrive at a false discovery rate (FDR) of less than 1% estimated using a target-decoy approach [389].

4.3.8 Computational analysis

MaxQuant-derived protein groups as well as phosphorylation sites were further processed in the R software environment (V. 4.2.1). First, the intensity distributions of all TMT11plex samples were inspected and samples 4 and 9 were subsequently removed from the downstream analysis for proteome and phosphoproteome due to inconsistent intensity distribution and possible experimental issues. Then, all proteins and phosphorylation sites with missing quantification across all samples, potential contaminants and reverse reads were removed. Additionally, phosphorylation sites with localization probability of <0.75 were removed from the phosphoproteome analysis. The raw intensity values of the remaining proteins and phosphorylation sites were quantile normalized using the limma R package (10.1093/NAR/GKV007). For proteins and phosphorylation sites, differential abundance between all experimental conditions was tested using limma (10.1093/NAR/GKV007) and P-values calculated using a moderated t-test with a minimum quantification count of 2 out of the 3 replicates. P-values were adjusted for multiple testing using FDR correction. Sequence motif graphs were generated using the ggseqlogo R package (10.1093/BIOINFORMATICS/BTX469). To identify possible kinases that are affected by the treatments, we used the enrichment analysis tool of the human kinase library (10.1038/s41586-022-05575-3). As foreground test sets, we used the amino acid sequences (+/- 7 AA) of upregulated or downregulated phosphorylation sites and the sites that were not upregulated or downregulated as the respective background sets. The estimated FCs and the FDR adjusted p-values by the enrichment analysis tool were used in downstream analysis. Clustering profile analysis was done using the NbClust package in R. GO-enrichment analysis was done using the String enrichment and plots were performed using the ggplot package in R.

4.4 RNA Sequencing and Data Analysis

4.4.1 RNA extraction

RNA from zebrafish embryos untreated or treated with UV-C (245 nm, 24 J/m^2) and harvested after 0.5h or 4h post-UV, was isolated and used for sequencing. In brief, TRIzol (Invitrogen) was added to the embryos and they were dissolved by pipetting. After adding the GlycoBlue (Invitrogen), the lysates was added to the Phase Lock Gel-Heavy tubes (Quantabio) and incubated for 5 min at RT. Chloroform was added and samples were shortly shacked and centrifuged at 12,000 g for 10 min at 4°C. The aqueous phase containing the RNA was transferred into a new tube. Isopropyl alcohol was added and samples were mixed and incubated for 10 min at RT. After 10 min of centrifugation, the visible RNA was purified using the Direc-zol RNA Miniprep Plus kit (Zymo research). NGS library prep was performed with Illumina's TruSeq stranded mRNA LT Sample Prep Kit following TruSeqStrandedmRNAReferenceGuide (Oct.2017) (Document # 1000000040498v00). Libraries were prepared with a starting amount of 1000 ng and amplified in 10 PCR cycles.Libraries were profiled in a High Sensitivity DNA on a 2100 Bioanalyzer (Agilent technologies) and quantified using the Qubit dsDNA HS Assay Kit, in a Qubit 2.0 Fluorometer (Life technologies). All 12 samples were pooled in equimolar ratio and sequenced on 1 NextSeq 500 Highoutput FC, SR for 1x 84 cycles plus 7 cycles for the index read.

4.4.2 mRNA analysis

The libraries for the mRNA sequencing were sequenced on an Illumina NextSeq500 instrument. The sequencing was run with a readlength of 84. Demultiplexing was carried out using bcl2fastq v1.19. The read data was mapped against Grz11 ([390], release 109) using STAR ([391], v2.7). Reads per gene were quantified using featureCounts ([392], v 2.0.0). Diff. expression analysis was performed using the DESeq2 ([393], 1.34.0) package from R/Bioconductor ([394], 2.54.0) genes with and FDR < 1% were considered significant. GO Term and pathway analysis was performed using clusterProfiler ([395], 4.2.0), ReactomePA ([396], 1.38.0) and rrvgo ([397], 1.6.0).

5 List of abbreviations

Abbreviations	Full form
6-4PPs	6’-4’ photoproducts
8oxo-G	8oxo-2’-deoxyguanosine
ABC	Ammonium bicarbonate
ACN	Acetonitril
ACVR1/2	Activin receptor type-1/2
aEJ	Alternative end-joining
AID	Activation-Induced Cytidine Deaminase
alt-NHEJ	Alternative NHEJ
APC	Anaphase-promoting complex
APE1	DNA-apurinic site endonuclease
APEX	Ascorbic acid peroxidase
AP-site	Abasic site
ATM	Ataxia telangiectasia mutated
ATP	Adenosine triphosphate
ATR	Ataxia telangiectasia and Rad3 related
ATRIP	ATR-interacting protein
BARD1	BRCA1-associated RING domain protein 1
BER	Base Excision Repair
BMP	Bone morphogenetic protein
BP	Biological process
BRCA1/2	Breast cancer type 1/2 susceptibility protein
C	Carbon
C18	Octadodecyl alkane chains
CAA	Chloroacetamide
CAK	CDK-activating kinase
CBC	Cap binding complex
CC	Cellular component
Cdc6/20	Cell division cycle protein 6/20 homolog
Cdc25	Ras-specific guanine nucleotide-releasing factor 1
CDH1	Fizzy-related protein homolog
CDK	Cyclin-dependent kinases
Cdk9	Cyclin-dependent kinase 9
CDT1	DNA replication factor Cdt1
CENT2	Centrin-2
CHK1	Checkpoint kinase-1
CHK2	Checkpoint kinase-2
CID	Collision-induced dissociation
CKI	CDK inhibitor
Cln3	Battenin
COX2	Cyclooxygenases 2
CPDs	Cyclobutane Pyrimidine Dimers
CRL	Cullin-RING E3 ligases
CS	Cockayne syndrome
CSB	CS protein b
CTD	Carboxy-Terminal Domain
CtlP	CtBP-interacting protein
CTR	Control

Cu^{+}	Copper(I) ion
DDB2	DNA damage-binding protein 2
DDK	Dbf4-dependent protein kinase
DDR	DNA damage response
dHJ	Double HJ
D-loop	Displacement loop
DNA	Deoxyribonucleic acid
DNA-PKcs	DNA-dependent protein kinase catalytic subunit
DNA2	DNA replication ATP-dependent helicase/nuclease DNA2
dNTP	Deoxynucleotide
dNTPs	Deoxyribonucleotide triphosphates
DSB	Double strand break
DTT	Dithiothreitol
DUB	Deubiquitylase
ECM	Extracellular matrix
EGSEA	Ensemble Gene Set Enrichment Analysis
EGFR	Epidermal growth factor receptors
ER	Endoplasmic reticulum
ERKs	Extracellular signal-regulated kinases
EU	5-ethynyl uridine
EXO1	Exonuclease 1
FA	Formaldehyde
FAN1	Fanconi-associated nuclease 1
FC	Fold change
FDR	False discovery rate
Fe^{2+}	Iron(II) ion
G-phase	Gap phase
GG-NER	Global genome NER
GO	Gene ontology
GPCRs	G protein-coupled receptors
GRK	G protein-coupled receptor kinase
GSEA	Gene Set Enrichment Analysis
GTFs	General transcription factors
H_2O_2	Hydrogen peroxide
HEPES	4-(2-hydroxyethyl)-1-piperazineethanesulfonic acid
HJ	Holliday junction
HR	Homologous recombination
HSPCs	Hematopoietic stem and progenitor cells
ICL	Inter-strand crosslink
IDLs	Insertion-deletion loops
IF	Immunofluorescence
IKK	IκB kinase
IκB	Inhibitory κB
IL	Interleukin
IMB	Institute of Molecular Biology
IP	Immunoprecipitation
IR	Ionizing radiation
JNK	c-Jun NH2-terminal kinases
KD	Knock-down
KDa	Kilo Dalton
KEGG	Kyoto Encyclopedia of Genes and Genomes
LC50	Lethal concentration - killing 50% of cells

LC-MS/MS	Liquid chromatography and tandem mass spectrometry
LFQ	Label-free quantification
LIG1	Ligase 1
LLPS	Liquid-liquid phase separation
lncRNA	Long noncoding RNA
LysC	Endoproteinase LysC
m/z	Mass to charge
m6a	N6-methyladensine
MAD2	Mitotic spindle assembly checkpoint protein MAD2
MAPK	Mitogen-activated protein kinase
MAPKKs	MAP kinase kinases
MAP2K	MAPK kinase
MAP3K	MAPK kinase kinase
MAPKAPK	MAPK-activated protein kinase
MC	Molecular function
MCM	Minichromosome maintenance complex
MDC1	Mediator of DNA damage checkpoint protein 1
M- phase	Mitosis phase
Micro-SCX	Micro-tip based strong cation exchange chromatography
MMEJ	Microhomology-mediated end-joining
MMPs	Matrix metalloproteinases
MMR	Mismatch repair
MRC1	Mediator of the replication checkpoint 1
MRE11	Double-strand break repair protein MRE11
mRNA	Messenger RNA
MRN	MRE11-RAD50-NBS1
MS	Mass spectrometry
MS1	First stage of mass analysis / precursor spectrum
MS2	Second stage of mass analysis / fragment spectrum
NBS1	Nibrin
ncRNA	Non-coding RNA
NEIL1	Endonuclease 8-like 1
NELF	Negative elongation factor
NEM	N-ethylmaleimide
NER	Nucleotide excision repair
NFκB	Nuclear factor kappa B
NHEJ	Non-homologous end joining
NLS	Nuclear localization signal
O_2^-	Superoxide radical
OGG1	8-oxoguanine DNA glycosylase
OH*	Hydroxyl radical
p21 or cdkn1a	Cyclin-dependent kinase inhibitor 1A
PAK	p21-activated kinase
PARP	Poly [ADP-ribose] polymerase
PBS	Phosphate buffered saline
PCA	Principal component analysis
PCNA	Proliferating cell nuclear antigen
PCR	Polymerase chain reaction
PEI	Polyethylenimine
PEP	Posterior error probability
PER	Photoenzymatic repair
PGE2	Prostaglandin 2

PO_4	Phosphate group
Pol II	RNA polymerase II
Pol δ/ε/μ/η/ι/κ/ζ/ β/ λ/ θ/ ν	DNA polymerase δ/ε/μ/η/ι/κ/ζ/ β/ λ/ θ/ ν
PPP	Promoter-proximal pausing
PSP	Paraspeckels protein
P-TEFb	Positive transcription elongation factor b
PTM	Posttranslational modification
RAD23B	UV excision repair protein RAD23 homolog
RAD50	DNA repair protein RAD50
RBPs	RNA-binding proteins
RCT	Reactome
Rev1	DNA repair protein REV1
RFC	Replication factor C
RIPA	Radioimmunoprecipitation assay buffer
RNA	Ribonucleic acid
RNF8/14/168	E3 ubiquitin ligase
ROS	Reactive oxygen species
RPA	Replication protein A
RPCs	RNA-protein crosslinks
RP-HPLC	Reversed-phase high-performance chromatography
RPLs	60S ribosomal subunits
RPSs	40S ribosomal subunits
RQC	Ribosome-associated quality control
rRNA	Ribosomal RNA
RT	Room temperature (~22-23°C)
RTEL1	Regulator of telomere elongation helicase
S	Serine
S-phase	Synthesis phase
S/TQ motif	Serine or threonine residues followed by glutamine
SCX	Strong cation exchange
SDS-PAGE	Sodium dodecyl sulfate polyacrylamide gel electrophoresis
SSB	Single-stranded DNA break
siRNA	Short interfering RNA
ssDNA	Single stranded DNA
T (Protein)	Tyrosine
TBLs	Transcription blocking lesions
TC-NER	Transcription-coupled NER
TEAB	Triethylammonium bicarbonate
TF	Transcription factor
TFIIH/D	Multi-subunit transcription factor II H/D
TGF-β	Transforming growth factor
TGFβRI/II	TGF-β receptor type I/II
TGFR	Transforming growth factor receptor
TLR	Toll-like receptor
TiO2	Titanium dioxide
TLS	Translesion synthesis
TME	Tumor micro environment
TMT	Tandem mass tag
TNF	Tumor necrosis factor
TNFR	Tumor necrosis factor receptor
Top I	Topoisomerase I
Top II	Topoisomerase II

TOPBP1	Topoisomerase 2-binding protein 1
TOPOIII	Topoisomerase III
TP53BP1	TP53-binding protein 1
tRNA	Transfer RNA
TSS	Transcription start site
TTS	Transcription termination site
UAF1	WD repeat-containing protein 48
UBD	Ubiquitin-binding domain
UNG	Uracil-DNA glycosylase
USP1	Ubiquitin carboxyl-terminal hydrolase 1
UTR	Untranslated region
UV	Ultraviolet
UV-DDB	UV-damaged DNA-binding protein
VCP	Valosin-containing protein
WB	Western blot
WRN	Werner syndrome ATP-dependent helicase
WT	Wild type
XP	Xeroderma pigmentosum
XPA/B/C/D/E/F/G	Xeroderma pigmentosum protein A/B/C/D/E/F/G
YBX1/3	Y-box-binding protein 1/3
ZNF598	E3 ubiquitin-protein ligase ZNF598

6 References

[1] M. Tedetti *et al.*, "High penetration of ultraviolet radiation in the south east Pacific waters," *Geophys Res Lett*, vol. 34, no. 12, pp. 1–5, 2007, doi: 10.1029/2007GL029823.

[2] Z. Zeng, J. Richardson, D. Verduzco, D. L. Mitchell, and E. E. Patton, "Zebrafish have a competent p53-dependent nucleotide excision repair pathway to resolve ultraviolet B-induced DNA damage in the skin," *Zebrafish*, vol. 6, no. 4, pp. 405–415, Dec. 2009, doi: 10.1089/zeb.2009.0611.

[3] M. E. Borisova *et al.*, "P38-MK2 signaling axis regulates RNA metabolism after UV-light-induced DNA damage," *Nat Commun*, vol. 9, no. 1, Dec. 2018, doi: 10.1038/s41467-018-03417-3.

[4] M. Zhang, J. M. Berk, A. B. Mehrtash, J. Kanyo, and M. Hochstrasser, "A versatile new tool derived from a bacterial deubiquitylase to detect and purify ubiquitylated substrates and their interacting proteins," *PLoS Biol*, vol. 20, no. 6, Jun. 2022, doi: 10.1371/journal.pbio.3001501.

[5] G. Giglia-Mari, A. Zotter, and W. Vermeulen, "DNA damage response," *Cold Spring Harb Perspect Biol*, vol. 3, no. 1, pp. 1–19, 2011, doi: 10.1101/cshperspect.a000745.

[6] A. Ciccia and S. J. Elledge, "The DNA Damage Response: Making It Safe to Play with Knives," *Mol Cell*, vol. 40, no. 2, pp. 179–204, 2010, doi: 10.1016/j.molcel.2010.09.019.

[7] S. P. Jackson and J. Bartek, "The DNA-damage response in human biology and disease," *Nature*, vol. 461, no. 7267, pp. 1071–1078, 2009, doi: 10.1038/nature08467.

[8] J. X. Feng and N. C. Riddle, "Epigenetics and genome stability," *Mammalian Genome*, vol. 31, no. 5–6, pp. 181–195, 2020, doi: 10.1007/s00335-020-09836-2.

[9] J. T. Burgess *et al.*, "The Therapeutic Potential of DNA Damage Repair Pathways and Genomic Stability in Lung Cancer," *Front Oncol*, vol. 10, no. July, pp. 1–14, 2020, doi: 10.3389/fonc.2020.01256.

[10] L. Gibellini and L. Moro, "Programmed cell death in health and disease," *Cells*, vol. 10, no. 7, pp. 2–5, 2021, doi: 10.3390/cells10071765.

[11] F. R. De Gruijl, "Skin Cancer and Solar UV Radiation," *Eur J Cancer*, vol. 35, no. 14, pp. 2003–2009, 1999, doi: 10.1016/s0959-8049(99)00283-x.

[12] F. R. De Gruijl, H. J. Van Kranen, and L. H. F. Mullenders, "UV-induced DNA damage, repair, mutations and oncogenic pathways in skin cancer," *J Photochem Photobiol B*, vol. 63, pp. 19–27, 2001, doi: https://doi.org/10.1016/S1011-1344(01)00199-3.

[13] F. Liu-Smith, J. Jia, and Y. Zheng, "UV-Induced Molecular Signaling Differences in Melanoma and Non-melanoma Skin Cancer," in *Adv Exp Med Biol*, 2017, pp. 27–40. doi: 10.1007/978-3-319-56017-5_3.

[14] C. O'Connor, C. Courtney, and M. Murphy, "Shedding light on the myths of ultraviolet radiation in the COVID-19 pandemic," *Clin Exp Dermatol*, vol. 46, no. 1, pp. 187–188, 2021, doi: 10.1111/ced.14456.

[15] W. Strzałka, P. Zgłobicki, E. Kowalska, A. Bażant, D. Dziga, and A. K. Banaś, "The dark side of UV-induced DNA lesion repair," *Genes (Basel)*, vol. 11, no. 12, pp. 1–33, 2020, doi: 10.3390/genes11121450.

[16] F. R. De Gruijl and J. C. Van der Leun, “Environment and health: 3. Ozone depletion and ultraviolet radiation,” *Can Med Assoc J*, vol. 163, no. 7, pp. 851–855, 2000.

[17] R. P. Rastogi, Richa, A. Kumar, M. B. Tyagi, and R. P. Sinha, “Molecular mechanisms of ultraviolet radiation-induced DNA damage and repair,” *J Nucleic Acids*, vol. 2010, 2010, doi: 10.4061/2010/592980.

[18] J. Krutmann, A. Morita, and J. H. Chung, “Sun exposure: What molecular photodermatology tells us about its good and bad sides,” *Journal of Investigative Dermatology*, vol. 132, no. 3 PART 2, pp. 976–984, 2012, doi: 10.1038/jid.2011.394.

[19] A. Flo, A. C. Calpena, A. Díez-Noguera, A. del Pozo, and T. Cambras, “Daily Variation of UV-induced Erythema and the Action of Solar Filters,” *Photochemistry and Photobiology*, vol. 93, no. 2. Blackwell Publishing Inc., pp. 632–635, Mar. 01, 2017. doi: 10.1111/php.12670.

[20] E. D. Lephart, “Equol’s anti-aging effects protect against environmental assaults by increasing skin antioxidant defense and ECM proteins while decreasing oxidative stress and inflammation,” *Cosmetics*, vol. 5, no. 1, pp. 1–17, 2018, doi: 10.3390/cosmetics5010016.

[21] A. C. Mesa-Arango, S. V Flórez-Muñoz, and G. Sanclemente, “Mechanisms of skin aging,” *IATREIA*, vol. 25, no. 9, pp. 399–402, 2017, doi: 10.17533/udea.iatreia.v30n2a05.

[22] J. L. Ravanat, T. Douki, and J. Cadet, “Direct and indirect effects of UV radiation on DNA and its components,” *J Photochem Photobiol B*, vol. 63, no. 1–3, pp. 88–102, Oct. 2001, doi: 10.1016/S1011-1344(01)00206-8.

[23] A. Suryo Rahmanto *et al.*, “K6-linked ubiquitylation marks formaldehyde-induced RNA-protein crosslinks for resolution,” *Mol Cell*, vol. 83, no. 23, pp. 4272-4289.e10, 2023, doi: 10.1016/j.molcel.2023.10.011.

[24] Michael H. Patrick, “Studies on thymine-derived UV photoproducts in DNA--I. Formation and biological role of pyrimidine adducts in DNA,” *Photochem Photobiol*, vol. 25, no. 4, pp. 357–372, Apr. 1977.

[25] J. Cadet and T. Douki, “Formation of UV-induced DNA damage contributing to skin cancer development,” *Photochemical and Photobiological Sciences*, vol. 17, no. 12. Royal Society of Chemistry, pp. 1816–1841, 2018. doi: 10.1039/c7pp00395a.

[26] T. Douki, G. Vadesne-Bauer, and J. Cadet, “Formation of 2′-deoxyuridine hydrates upon exposure of nucleosides to gamma radiation and UVC-irradiation of isolated and cellular DNA,” *Photochemical & Photobiological Sciences*, vol. 1, no. 8, pp. 565–569, Aug. 2002, doi: 10.1039/b201612e.

[27] S. Kumar, N. D. Sharma, R. J. H. Davies, D. W. Phillipson, and J. A. McCloskey, “The isolation and characterisation of a new type of dimeric adenine photoproduct in UV-irradiated deoxyadenylates,” *Nucleic Acids Res*, vol. 15, no. 3, pp. 1199–1216, Feb. 1987, doi: 10.1093/nar/15.3.1199.

[28] N. Charlet-Berguerand *et al.*, “RNA polymerase II bypass of oxidative DNA damage is regulated by transcription elongation factors,” *EMBO Journal*, vol. 25, no. 23, pp. 5481–5491, 2006, doi: 10.1038/sj.emboj.7601403.

[29] S. Boeing *et al.*, “Multiomic Analysis of the UV-Induced DNA Damage Response,” vol. 7, no. 7, pp. 1597–1610, 2016.

[30] D. A. P. Rockx *et al.*, "UV-induced inhibition of transcription involves repression of transcription initiation and phosphorylation of RNA polymerase II," *Proc Natl Acad Sci U S A*, vol. 97, no. 19, pp. 10503–10508, 2000, doi: 10.1073/pnas.180169797.

[31] L. V. Mayne and A. R. Lehmann, "Failure of RNA synthesis to recover after UV irradiation: an early defect in cells from individuals with Cockayne's syndrome and Xeroderma Pigmentosum," *Cancer Res*, 1982, [Online]. Available: https://pubmed.ncbi.nlm.nih.gov/6174225/

[32] B. A. Donahue, S. Yin, J. S. Taylor, D. Reines, and P. C. Hanawalt, "Transcript cleavage by RNA polymerase II arrested by a cyclobutane pyrimidine dimer in the DNA template," *Proc Natl Acad Sci U S A*, vol. 91, no. 18, pp. 8502–8506, 1994, doi: 10.1073/pnas.91.18.8502.

[33] J. Cadet and J. Richard Wagner, "DNA base damage by reactive oxygen species, oxidizing agents, and UV radiation," *Cold Spring Harb Perspect Biol*, vol. 5, no. 2, pp. 1–18, 2013, doi: 10.1101/cshperspect.a012559.

[34] W. Dröge, "Free radicals in the physiological control of cell function," *Physiol Rev*, vol. 82, no. 1, pp. 47–95, 2002, doi: 10.1152/physrev.00018.2001.

[35] M. Genestra, "Oxyl radicals, redox-sensitive signalling cascades and antioxidants," *Cell Signal*, vol. 19, no. 9, pp. 1807–1819, 2007, doi: 10.1016/j.cellsig.2007.04.009.

[36] J. K. Willcox, S. L. Ash, and G. L. Catignani, "Antioxidants and prevention of chronic disease," *Crit Rev Food Sci Nutr*, vol. 44, no. 4, pp. 275–295, 2004, doi: 10.1080/10408690490468489.

[37] M. Valko, D. Leibfritz, J. Moncol, M. T. D. Cronin, M. Mazur, and J. Telser, "Free radicals and antioxidants in normal physiological functions and human disease," *International Journal of Biochemistry and Cell Biology*, vol. 39, no. 1, pp. 44–84, 2007, doi: 10.1016/j.biocel.2006.07.001.

[38] M. Valko, M. Izakovic, M. Mazur, C. J. Rhodes, and J. Telser, "Role of oxygen radicals in DNA damage and cancer incidence," *Mol Cell Biochem*, vol. 266, no. 1–2, pp. 37–56, 2004, doi: 10.1023/B:MCBI.0000049134.69131.89.

[39] J. Cadet, J. L. Ravanat, M. TavernaPorro, H. Menoni, and D. Angelov, "Oxidatively generated complex DNA damage: Tandem and clustered lesions," *Cancer Lett*, vol. 327, no. 1–2, pp. 5–15, 2012, doi: 10.1016/j.canlet.2012.04.005.

[40] B. Frei, "Reactive oxygen species and antioxidant vitamins: Mechanisms of action," *Am J Med*, vol. 97, no. 3, pp. 5–13, Sep. 1994.

[41] W. G. Chatterjee N, "Mechanisms of DNA Damage, Repair, and Mutagenesis," *Environ Mol Mutagen*, vol. 405, no. April, pp. 391–405, 2017, doi: 10.1002/em.

[42] A. R. Poetsch, "The genomics of oxidative DNA damage, repair, and resulting mutagenesis," *Comput Struct Biotechnol J*, vol. 18, pp. 207–219, 2020, doi: 10.1016/j.csbj.2019.12.013.

[43] B. Halliwell, "Free Radicals and Other Reactive Species in Disease," *Encyclopedia of Life Sciences*, pp. 1–7, 2005, doi: 10.1038/npg.els.0003913.

[44] M. Valko, H. Morris, and M. T. D. Cronin, "Metals, Toxicity and Oxidative Stress," *Curr Med Chem*, vol. 703, pp. 1161–1208, 2005, doi: 10.1016/j.scitotenv.2019.134798.

[45] D. Strumberg, A. A. Pilon, M. Smith, R. Hickey, L. Malkas, and Y. Pommier, "Conversion of Topoisomerase I Cleavage Complexes on the Leading Strand of Ribosomal DNA into 5′-

Phosphorylated DNA Double-Strand Breaks by Replication Runoff," *Mol Cell Biol*, vol. 20, no. 11, pp. 3977–3987, Jun. 2000, doi: 10.1128/MCB.20.11.3977-3987.2000.

[46] T. Ohnishi, E. Mori, and A. Takahashi, "DNA double-strand breaks: Their production, recognition, and repair in eukaryotes," *Mutation Research - Fundamental and Molecular Mechanisms of Mutagenesis*, vol. 669, no. 1–2, pp. 8–12, 2009, doi: 10.1016/j.mrfmmm.2009.06.010.

[47] J. P. Banáth and P. L. Olive, "Expression of phosphorylated histone H2AX as a surrogate of cell killing by drugs that create DNA double-strand breaks," *Cancer Res*, vol. 63, no. 15, pp. 4347–4350, 2003.

[48] T. Clouaire *et al.*, "Comprehensive Mapping of Histone Modifications at DNA Double-Strand Breaks Deciphers Repair Pathway Chromatin Signatures," *Mol Cell*, vol. 72, no. 2, pp. 250-262.e6, 2018, doi: 10.1016/j.molcel.2018.08.020.

[49] S. Juszkiewicz, G. Slodkowicz, Z. Lin, P. Freire-Pritchett, S. Y. Peak-Chew, and R. S. Hegde, "Ribosome collisions trigger cis-acting feedback inhibition of translation initiation," *Elife*, vol. 9, pp. 1–29, 2020, doi: 10.7554/eLife.60038.

[50] F. Li *et al.*, "Reanalysis of ribosome profiling datasets reveals a function of rocaglamide A in perturbing the dynamics of translation elongation via eIF4A," *Nat Commun*, vol. 14, no. 1, pp. 1–14, 2023, doi: 10.1038/s41467-023-36290-w.

[51] S. L. Leedom and K. C. Keiler, "Ribosome collisions: New ways to initiate ribosome rescue," *Current Biology*, vol. 32, no. 10, pp. R469–R472, 2022, doi: 10.1016/j.cub.2022.04.038.

[52] S. Meydan, N. R. Guydosh, and K. Diseases, "Pathways and Collision Types," vol. 67, no. 1, pp. 19–26, 2022, doi: 10.1007/s00294-020-01111-w.A.

[53] K. Best *et al.*, "Structural basis for clearing of ribosome collisions by the RQT complex," *Nat Commun*, vol. 14, no. 1, 2023, doi: 10.1038/s41467-023-36230-8.

[54] N. Ugajin, K. Imami, H. Takada, Y. Ishihama, S. Chiba, and Y. Mishima, "Znf598-mediated Rps10/eS10 ubiquitination contributes to the ribosome ubiquitination dynamics during zebrafish development," *Rna*, vol. 29, no. 12, pp. 1910–1927, 2023, doi: 10.1261/rna.079633.123.

[55] M. Shamsuzzaman *et al.*, "Inhibition of Ribosome Assembly and Ribosome Translation Has Distinctly Different Effects on Abundance and Paralogue Composition of Ribosomal Protein mRNAs in Saccharomyces cerevisiae," *mSystems*, vol. 8, no. 1, 2023, doi: 10.1128/msystems.01098-22.

[56] R. P. Boyce and P. Howard-Flanders, "Release of Ultraviolet Light-Induced Thymine Dimers From DNA in E. Coli," *Proceedings of the National Academy of Sciences of the United States of*, vol. 51, no. 1927, pp. 293–300, 1964, doi: 10.1073/pnas.51.2.293.

[57] C. Masutani *et al.*, "Purification and cloning of a nucleotide excision repair complex involving the xeroderma pigmentosum group C protein and a human homologue of yeast RAD23.," *EMBO J*, vol. 13, no. 8, pp. 1831–1843, Apr. 1994, doi: 10.1002/j.1460-2075.1994.tb06452.x.

[58] M. Araki *et al.*, "Centrosome Protein Centrin 2/Caltractin 1 Is Part of the Xeroderma Pigmentosum Group C Complex That Initiates Global Genome Nucleotide Excision Repair," *Journal of Biological Chemistry*, vol. 276, no. 22, pp. 18665–18672, Jun. 2001, doi: 10.1074/jbc.M100855200.

[59] F. Brueckner, U. Hennecke, T. Carell, and P. Cramer, “CPD Damage Recognition by Transcribing RNA Polymerase II,” *Science (1979)*, vol. 315, no. 5813, pp. 859–862, Feb. 2007, doi: 10.1126/science.1135400.

[60] B. A. Donahue, S. Yin, J. S. Taylor, D. Reines, and P. C. Hanawalt, “Transcript cleavage by RNA polymerase II arrested by a cyclobutane pyrimidine dimer in the DNA template.,” *Proceedings of the National Academy of Sciences*, vol. 91, no. 18, pp. 8502–8506, Aug. 1994, doi: 10.1073/pnas.91.18.8502.

[61] J. Xu *et al.*, “Structural basis for the initiation of eukaryotic transcription-coupled DNA repair,” *Nature*, vol. 551, no. 7682, pp. 653–657, Nov. 2017, doi: 10.1038/nature24658.

[62] Y. van der Weegen *et al.*, “The cooperative action of CSB, CSA, and UVSSA target TFIIH to DNA damage-stalled RNA polymerase II,” *Nat Commun*, vol. 11, no. 1, pp. 1–16, 2020, doi: 10.1038/s41467-020-15903-8.

[63] F. Coin, V. Oksenych, V. Mocquet, S. Groh, C. Blattner, and J. M. Egly, “Nucleotide Excision Repair Driven by the Dissociation of CAK from TFIIH,” *Mol Cell*, vol. 31, no. 1, pp. 9–20, 2008, doi: 10.1016/j.molcel.2008.04.024.

[64] J. A. Marteijn, H. Lans, W. Vermeulen, and J. H. J. Hoeijmakers, “Understanding nucleotide excision repair and its roles in cancer and ageing,” *Nature Reviews Molecular Cell Biology*, vol. 15, no. 7. Nature Publishing Group, pp. 465–481, 2014. doi: 10.1038/nrm3822.

[65] C. P. Selby and A. Sancar, “Human Transcription-Repair Coupling Factor CSB/ERCC6 Is a DNA-stimulated ATPase but Is Not a Helicase and Does Not Disrupt the Ternary Transcription Complex of Stalled RNA Polymerase II,” *Journal of Biological Chemistry*, vol. 272, no. 3, pp. 1885–1890, Jan. 1997, doi: 10.1074/jbc.272.3.1885.

[66] M. D. Wilson, M. Harreman, and J. Q. Svejstrup, “Ubiquitylation and degradation of elongating RNA polymerase II: The last resort,” *Biochim Biophys Acta Gene Regul Mech*, vol. 1829, no. 1, pp. 151–157, 2013, doi: 10.1016/j.bbagrm.2012.08.002.

[67] A. C. M. Cheung and P. Cramer, “Structural basis of RNA polymerase II backtracking, arrest and reactivation,” *Nature*, vol. 471, no. 7337, pp. 249–253, Mar. 2011, doi: 10.1038/nature09785.

[68] J.-P. Lainé and J.-M. Egly, “Initiation of DNA repair mediated by a stalled RNA polymerase IIO,” *EMBO J*, vol. 25, no. 2, pp. 387–397, Jan. 2006, doi: 10.1038/sj.emboj.7600933.

[69] G. Spivak, “Nucleotide excision repair in humans,” *DNA Repair (Amst)*, vol. 36, pp. 13–18, Dec. 2015, doi: 10.1016/j.dnarep.2015.09.003.

[70] S. Maynard, S. H. Schurman, C. Harboe, N. C. de Souza-Pinto, and V. A. Bohr, “Base excision repair of oxidative DNA damage and association with cancer and aging,” *Carcinogenesis*, vol. 30, no. 1, pp. 2–10, 2009, doi: 10.1093/carcin/bgn250.

[71] H. E. Krokan and M. Bjøra˚, “Base excision repair,” *Cold Spring Harbor Perspective in Biology*, pp. 23–64, 2013, doi: doi: 10.1101/cshperspect.a012583.

[72] K. Kurthkoti, P. Kumar, P. B. Sang, and U. Varshney, “Base excision repair pathways of bacteria: New promise for an old problem,” *Future Med Chem*, vol. 12, no. 4, pp. 339–355, 2020, doi: 10.4155/fmc-2019-0267.

[73] A. L. Jacobs and P. Schär, "DNA glycosylases: In DNA repair and beyond," *Chromosoma*, vol. 121, no. 1, pp. 1–20, 2012, doi: 10.1007/s00412-011-0347-4.

[74] S. S. Wallace, "Base excision repair: A critical player in many games," *DNA Repair (Amst)*, vol. 19, pp. 14–26, 2014, doi: 10.1016/j.dnarep.2014.03.030.

[75] J. Jiricny, "The multifaceted mismatch-repair system," *Nat Rev Mol Cell Biol*, vol. 7, no. 5, pp. 335–346, 2006, doi: 10.1038/nrm1907.

[76] G. M. Li, "Mechanisms and functions of DNA mismatch repair," *Cell Res*, vol. 18, no. 1, pp. 85–98, 2008, doi: 10.1038/cr.2007.115.

[77] A. A. Larrea, S. A. Lujan, and T. A. Kunkel, "SnapShot: DNA Mismatch Repair," *Cell*, vol. 141, no. 4, 2010, doi: 10.1016/j.cell.2010.05.002.

[78] L. Gu, Y. Hong, S. McCulloch, H. Watanabe, and G. M. Li, "ATP-dependent interaction of human mismatch repair proteins and dual role of PCNA in mismatch repair," *Nucleic Acids Res*, vol. 26, no. 5, pp. 1173–1178, 1998, doi: 10.1093/nar/26.5.1173.

[79] W. Strzalka and A. Ziemienowicz, "Proliferating cell nuclear antigen (PCNA): A key factor in DNA replication and cell cycle regulation," *Ann Bot*, vol. 107, no. 7, pp. 1127–1140, 2011, doi: 10.1093/aob/mcq243.

[80] H. Yajima, K.-J. Lee, S. Zhang, J. Kobayashi, and B. P. C. Chen, "DNA Double-Strand Break Formation upon UV-Induced Replication Stress Activates ATM and DNA-PKcs Kinases," *J Mol Biol*, vol. 385, no. 3, pp. 800–810, Jan. 2009, doi: 10.1016/j.jmb.2008.11.036.

[81] M. Srivastava and S. C. Raghavan, "DNA double-strand break repair inhibitors as cancer therapeutics," *Chem Biol*, vol. 22, no. 1, pp. 17–29, 2015, doi: 10.1016/j.chembiol.2014.11.013.

[82] J. R. Chapman, M. R. G. Taylor, and S. J. Boulton, "Playing the End Game: DNA Double-Strand Break Repair Pathway Choice," *Mol Cell*, vol. 47, no. 4, pp. 497–510, Aug. 2012, doi: 10.1016/j.molcel.2012.07.029.

[83] M. Zimmermann, F. Lottersberger, S. B. Buonomo, A. Sfeir, and T. de Lange, "53BP1 Regulates DSB Repair Using Rif1 to Control 5′ End Resection," *Science (1979)*, vol. 339, no. 6120, pp. 700–704, Feb. 2013, doi: 10.1126/science.1231573.

[84] C. Escribano-Díaz *et al.*, "A Cell Cycle-Dependent Regulatory Circuit Composed of 53BP1-RIF1 and BRCA1-CtIP Controls DNA Repair Pathway Choice," *Mol Cell*, vol. 49, no. 5, pp. 872–883, Mar. 2013, doi: 10.1016/j.molcel.2013.01.001.

[85] S. R. Williams, J. S. Williams, and J. A. Trainer, "Mre11–Rad50–Nbs1 is a keystone complex connecting DNA repair machinery, double-strand break signaling, and the chromatin template," *Biochemistry and Cell Biology*, vol. 85, no. 4, Aug. 2007, doi: DOI: 10.1139/O07-069.

[86] R. Pennisi, P. Ascenzi, and A. di Masi, "Hsp90: A new player in DNA Repair?," *Biomolecules*, vol. 5, no. 4. MDPI AG, pp. 2589–2618, Oct. 16, 2015. doi: 10.3390/biom5042589.

[87] S. Qiu and J. Huang, "MRN complex is an essential effector of DNA damage repair," *J Zhejiang Univ Sci B*, vol. 22, no. 1, pp. 31–37, 2021, doi: 10.1631/jzus.B2000289.

[88] E. Bolderson *et al.*, "Phosphorylation of Exo1 modulates homologous recombination repair of DNA double-strand breaks," *Nucleic Acids Res*, vol. 38, no. 6, pp. 1821–1831, 2010, doi: 10.1093/nar/gkp1164.

[89] A. Cruz-García, A. López-Saavedra, and P. Huertas, "BRCA1 accelerates CtIP-ediated DNA-end resection," *Cell Rep*, vol. 9, no. 2, pp. 451–459, 2014, doi: 10.1016/j.celrep.2014.08.076.

[90] Z. You and J. M. Bailis, "DNA damage and decisions: CtIP coordinates DNA repair and cell cycle checkpoints," *Trends Cell Biol*, vol. 20, no. 7, pp. 402–409, 2010, doi: 10.1016/j.tcb.2010.04.002.

[91] T. Helleday, J. Lo, D. C. van Gent, and B. P. Engelward, "DNA double-strand break repair: From mechanistic understanding to cancer treatment," *DNA Repair (Amst)*, vol. 6, no. 7, pp. 923–935, 2007, doi: 10.1016/j.dnarep.2007.02.006.

[92] W. D. Wright, S. S. Shah, and W. D. Heyer, "Homologous recombination and the repair of DNA double-strand breaks," *Journal of Biological Chemistry*, vol. 293, no. 27, pp. 10524–10535, 2018, doi: 10.1074/jbc.TM118.000372.

[93] W. Bussen, S. Raynard, V. Busygina, A. K. Singh, and P. Sung, "Holliday junction processing activity of the BLM-Topo IIIα-BLAP75 complex," *Journal of Biological Chemistry*, vol. 282, no. 43, pp. 31484–31492, 2007, doi: 10.1074/jbc.M706116200.

[94] A. Ciccia, N. McDonald, and S. C. West, "Structural and functional relationships of the XPF/MUS81 family of proteins," *Annu Rev Biochem*, vol. 77, pp. 259–287, 2008, doi: 10.1146/annurev.biochem.77.070306.102408.

[95] J. C. Muñoz, I. Beckerman, R. Choudhary, L. A. Bouvier, and M. J. Muñoz, "DNA Damage-Induced RNAPII Degradation and Its Consequences in Gene Expression," *Genes (Basel)*, vol. 13, no. 11, 2022, doi: 10.3390/genes13111951.

[96] K. Meek, V. Dang, and S. P. Lees-Miller, "DNA-PK: The Means to Justify the Ends?," *Adv Immunol*, vol. 99, pp. 33–58, 2008.

[97] A. J. Davis and D. J. Chen, "DNA double strand break repair via non-homologous end-joining," *Transl Cancer Res*, vol. 2, no. 3, pp. 130–143, 2013, doi: 10.3978/j.issn.2218-676X.2013.04.02.

[98] X. Wang, B. Hu, R. S. Weiss, and Y. Wang, "The effect of Hus1 on ionizing radiation sensitivity is associated with homologous recombination repair but is independent of nonhomologous end-joining," *Oncogene*, vol. 25, no. 13, pp. 1980–1983, Mar. 2006, doi: 10.1038/sj.onc.1209212.

[99] A. Bothmer, D. F. Robbiani, N. Feldhahn, A. Gazumyan, A. Nussenzweig, and M. C. Nussenzweig, "53BP1 regulates DNA resection and the choice between classical and alternative end joining during class switch recombination," *Journal of Experimental Medicine*, vol. 207, no. 4, pp. 855–865, 2010, doi: 10.1084/jem.20100244.

[100] P. Frit, V. Ropars, M. Modesti, J. B. Charbonnier, and P. Calsou, "Plugged into the Ku-DNA hub: The NHEJ network," *Prog Biophys Mol Biol*, vol. 147, pp. 62–76, 2019, doi: 10.1016/j.pbiomolbio.2019.03.001.

[101] P. Frit, N. Barboule, Y. Yuan, D. Gomez, and P. Calsou, "Alternative end-joining pathway(s): Bricolage at DNA breaks," *DNA Repair (Amst)*, vol. 17, pp. 81–97, 2014, doi: 10.1016/j.dnarep.2014.02.007.

[102] M. F. Goodman and R. Woodgate, “Translesion DNA polymerases,” *Cold Spring Harb Perspect Biol*, vol. 5, no. 10, 2013, doi: 10.1101/cshperspect.a010363.

[103] J. E. Sale, “Translesion DNA Synthesis and Mutagenesis in Eukaryotes,” *Cold Spring Harb Perspect Biol*, vol. 5, no. 12, 2013, doi: 10.1101/cshperspect.a012682.

[104] L. S. Waters, B. K. Minesinger, M. E. Wiltrout, S. D’Souza, R. V. Woodruff, and G. C. Walker, “Eukaryotic Translesion Polymerases and Their Roles and Regulation in DNA Damage Tolerance,” *Microbiology and Molecular Biology Reviews*, vol. 73, no. 1, pp. 134–154, 2009, doi: 10.1128/mmbr.00034-08.

[105] S. Sertic *et al.*, “Coordinated Activity of Y Family TLS Polymerases and EXO1 Protects Non-S Phase Cells from UV-Induced Cytotoxic Lesions,” *Mol Cell*, vol. 70, no. 1, pp. 34-47.e4, 2018, doi: 10.1016/j.molcel.2018.02.017.

[106] A. Hendel *et al.*, “PCNA ubiquitination is important, but not essential for translesion DNA synthesis in mammalian cells,” *PLoS Genet*, vol. 7, no. 9, 2011, doi: 10.1371/journal.pgen.1002262.

[107] J. Dunn, M. Potter, A. Rees, and T. M. Rünger, “Activation of the Fanconi anemia/BRCA pathway and recombination repair in the cellular response to solar ultraviolet light,” *Cancer Res*, vol. 66, no. 23, pp. 11140–11147, 2006, doi: 10.1158/0008-5472.CAN-06-0563.

[108] M. R. Hodskinson *et al.*, “Alcohol-derived DNA crosslinks are repaired by two distinct mechanisms,” *Nature*, vol. 579, no. 7800, pp. 603–608, 2020, doi: 10.1038/s41586-020-2059-5.

[109] J. Niraj, A. Färkkilä, and A. D. D’Andrea, “The Fanconi Anemia pathway in cancer,” *Annu Rev Cancer Biol*, vol. 3, no. 1, pp. 457–478, 2019, doi: 10.1146/annurev-cancerbio-030617-050422.

[110] C. C. Liang, Z. Li, D. Lopez-Martinez, W. V. Nicholson, C. Vénien-Bryan, and M. A. Cohn, “The FANCD2-FANCI complex is recruited to DNA interstrand crosslinks before monoubiquitination of FANCD2,” *Nat Commun*, vol. 7, 2016, doi: 10.1038/ncomms12124.

[111] R. Wang *et al.*, “ID complex,” vol. 580, no. 7802, pp. 278–282, 2020, doi: 10.1038/s41586-020-2110-6.DNA.

[112] D. Klein Douwel *et al.*, “XPF-ERCC1 Acts in Unhooking DNA Interstrand Crosslinks in Cooperation with FANCD2 and FANCP/SLX4,” *Mol Cell*, vol. 54, no. 3, pp. 460–471, 2014, doi: 10.1016/j.molcel.2014.03.015.

[113] P. Knipscheer *et al.*, “The Fanconi anemia pathway promotes replication-dependent DNA interstrand cross-link repair,” *Science (1979)*, vol. 326, no. 5960, pp. 1698–1701, 2009, doi: DOI: 10.1126/science.1182372.

[114] M. C. Kottemann and A. Smogorzewska, “Fanconi anemia and the repair of Watson and Crick crosslinks,” *Nature*, vol. 17, no. 7432, pp. 356–363, 2013, doi: doi: 10.1038/nature11863.

[115] M. Budzowska, T. G. Graham, A. Sobeck, and J. C. Shou Waga Walter, “Regulation of the Rev1–pol f complex during bypass of a DNA interstrand cross-link.” 2015.

[116] M. A. Cohn *et al.*, “A UAF1-Containing Multisubunit Protein Complex Regulates the Fanconi Anemia Pathway,” *Mol Cell*, vol. 28, no. 5, pp. 786–797, 2007, doi: 10.1016/j.molcel.2007.09.031.

[117] S. M. B. Nijman *et al.*, “The deubiquitinating enzyme USP1 regulates the fanconi anemia pathway,” *Mol Cell*, vol. 17, no. 3, pp. 331–339, 2005, doi: 10.1016/j.molcel.2005.01.008.

[118] N. Kitamura and J. J. Galligan, “A global view of the human post-translational modification landscape,” *Biochemical Journal*, vol. 480, no. 16. Portland Press Ltd, pp. 1241–1265, Aug. 01, 2023. doi: 10.1042/BCJ20220251.

[119] M. P. Stokes *et al.*, “Profiling of UV-induced ATM/ATR signaling pathways,” *Proc Natl Acad Sci U S A*, vol. 104, no. 50, pp. 19855–19860, 2007, doi: 10.1073/pnas.0707579104.

[120] B. M. Sirbu and D. Cortez, “DNA damage response: Three levels of DNA repair regulation,” *Cold Spring Harb Perspect Biol*, vol. 5, no. 8, 2013, doi: 10.1101/cshperspect.a012724.

[121] T. T. Paull, “Mechanisms of ATM activation,” *Annu Rev Biochem*, vol. 84, pp. 711–738, 2015, doi: 10.1146/annurev-biochem-060614-034335.

[122] A. Bensimon, R. Aebersold, and Y. Shiloh, “Beyond ATM: The protein kinase landscape of the DNA damage response,” *FEBS Lett*, vol. 585, no. 11, pp. 1625–1639, 2011, doi: 10.1016/j.febslet.2011.05.013.

[123] S. T. Kim, D. S. Lim, C. E. Canman, and M. B. Kastan, “Substrate specificities and identification of putative substrates of ATM kinase family members,” *Journal of Biological Chemistry*, vol. 274, no. 53, pp. 37538–37543, 1999, doi: 10.1074/jbc.274.53.37538.

[124] S. V. Kozlov *et al.*, “Autophosphorylation and ATM activation: Additional sites add to the complexity,” *Journal of Biological Chemistry*, vol. 286, no. 11, pp. 9107–9119, 2011, doi: 10.1074/jbc.M110.204065.

[125] M. T. Hayashi and and J. Karlseder, “DNA damage associated with mitosis and cytokinesis failure,” *Oncogene*, vol. 23, no. 1, pp. 1–7, 2013, doi: 10.1038/onc.2012.615.DNA.

[126] S. Liu *et al.*, “ATR Autophosphorylation as a Molecular Switch for Checkpoint Activation,” *Mol Cell*, vol. 43, no. 2, pp. 192–202, Jul. 2011, doi: 10.1016/j.molcel.2011.06.019.

[127] J. W. Harper and S. J. Elledge, “The DNA Damage Response: Ten Years After,” *Molecular Cell*, vol. 28, no. 5. Cell Press, pp. 739–745, Dec. 14, 2007. doi: 10.1016/j.molcel.2007.11.015.

[128] D. R. Raleigh and D. A. Haas-Kogan, “Molecular targets and mechanisms of radiosensitization using DNA damage response pathways,” *Future Oncology*, vol. 9, no. 2, Feb. 2013, doi: https://doi.org/10.2217/fon.12.185.

[129] F. Ribezzo, Y. Shiloh, and B. Schumacher, “Systemic DNA damage responses in aging and diseases,” *Semin Cancer Biol*, vol. 37–38, pp. 26–35, 2016, doi: 10.1016/j.semcancer.2015.12.005.

[130] G. K. Dasika, S. C. J. Lin, S. Zhao, P. Sung, A. Tomkinson, and E. Y. H. P. Lee, “DNA damage-induced cell cycle checkpoints and DNA strand break repair in development and tumorigenesis,” *Oncogene*, vol. 18, no. 55, pp. 7883–7899, 1999, doi: 10.1038/sj.onc.1203283.

[131] G. Goldstein, M. Scheid, U. Hammerling, D. H. Schlesinger, H. D. Niall, and E. A. Boyse, “Isolation of a polypeptide that has lymphocyte differentiating properties and is probably represented universally in living cells,” *Proc Natl Acad Sci U S A*, vol. 72, no. 1, pp. 11–15, 1975, doi: 10.1073/pnas.72.1.11.

[132] D. Komander and M. Rape, “The ubiquitin code,” *Annu Rev Biochem*, vol. 81, pp. 203–229, 2012, doi: 10.1146/annurev-biochem-060310-170328.

[133] P. D'Arcy and S. Linder, "Molecular pathways: Translational potential of deubiquitinases as drug targets," *Clinical Cancer Research*, vol. 20, no. 15, pp. 3908–3914, 2014, doi: 10.1158/1078-0432.CCR-14-0568.

[134] K. Sugasawa *et al.*, "UV-induced ubiquitylation of XPC protein mediated by UV-DDB-ubiquitin ligase complex," *Cell*, vol. 121, no. 3, pp. 387–400, 2005, doi: 10.1016/j.cell.2005.02.035.

[135] M. C. Thomas and C. M. Chiang, "The general transcription machinery and general cofactors.," *Crit Rev Biochem Mol Biol*, vol. 41, no. 3, pp. 105–178, 2006, doi: 10.1080/10409230600648736.

[136] A. Galloway and V. H. Cowling, "mRNA cap regulation in mammalian cell function and fate," *Biochimica et Biophysica Acta - Gene Regulatory Mechanisms*, vol. 1862, no. 3. Elsevier B.V., pp. 270–279, Mar. 01, 2019. doi: 10.1016/j.bbagrm.2018.09.011.

[137] Q. Zhou, T. Li, and D. H. Price, "RNA polymerase II elongation control," *Annu Rev Biochem*, vol. 81, pp. 119–143, 2012, doi: 10.1146/annurev-biochem-052610-095910.

[138] S. M. Vos *et al.*, "Architecture and RNA binding of the human negative elongation factor," *Elife*, vol. 5, no. JUNE2016, pp. 1–27, 2016, doi: 10.7554/eLife.14981.

[139] S. M. Vos *et al.*, "Structure of activated transcription complex Pol II–DSIF–PAF–SPT6," *Nature*, vol. 560, no. 7720, pp. 607–612, 2018, doi: 10.1038/s41586-018-0440-4.

[140] L. H. Williams *et al.*, "Pausing of RNA Polymerase II Regulates Mammalian Developmental Potential through Control of Signaling Networks," *Mol Cell*, vol. 58, no. 2, pp. 311–322, Apr. 2015, doi: 10.1016/j.molcel.2015.02.003.

[141] M. B. Ardehali and J. T. Lis, "Tracking rates of transcription and splicing in vivo," *Nat Struct Mol Biol*, vol. 16, no. 11, pp. 1123–1124, 2009, doi: 10.1038/nsmb1109-1123.

[142] K. Fujinaga, F. Huang, and B. M. Peterlin, "P-TEFb: The master regulator of transcription elongation," *Molecular Cell*, vol. 83, no. 3. Cell Press, pp. 393–403, Feb. 02, 2023. doi: 10.1016/j.molcel.2022.12.006.

[143] A. Kumar, M. Clerici, L. M. Muckenfuss, L. A. Passmore, and M. Jinek, "Mechanistic insights into mRNA 3′-end processing," *Curr Opin Struct Biol*, vol. 59, pp. 143–150, 2019, doi: 10.1016/j.sbi.2019.08.001.

[144] Y. Sun, K. Hamilton, and L. Tong, "Recent molecular insights into canonical pre-mRNA 3'-end processing," *Transcription*, vol. 11, no. 2, pp. 83–96, 2020, doi: 10.1080/21541264.2020.1777047.

[145] J. B. Rodríguez-Molina, S. West, and L. A. Passmore, "Knowing when to stop: Transcription termination on protein-coding genes by eukaryotic RNAPII," *Mol Cell*, vol. 83, no. 3, pp. 404–415, 2023, doi: 10.1016/j.molcel.2022.12.021.

[146] L. H. Gregersen and J. Q. Svejstrup, "The Cellular Response to Transcription-Blocking DNA Damage," *Trends in Biochemical Sciences*, vol. 43, no. 5. Elsevier Ltd, pp. 327–341, May 01, 2018. doi: 10.1016/j.tibs.2018.02.010.

[147] M. D. Lavigne, D. Konstantopoulos, K. Z. Ntakou-Zamplara, A. Liakos, and M. Fousteri, "Global unleashing of transcription elongation waves in response to genotoxic stress restricts somatic mutation rate," *Nat Commun*, vol. 8, no. 1, Dec. 2017, doi: 10.1038/s41467-017-02145-4.

[148] L. Williamson *et al.*, "UV Irradiation Induces a Non-coding RNA that Functionally Opposes the Protein Encoded by the Same Gene," *Cell*, vol. 168, no. 5, pp. 843-855.e13, 2017, doi: 10.1016/j.cell.2017.01.019.

[149] L. C. Andrade-Lima, A. Veloso, and M. Ljungman, "Transcription blockage leads to new beginnings," *Biomolecules*, vol. 5, no. 3, pp. 1600–1617, 2015, doi: 10.3390/biom5031600.

[150] A. Bugai *et al.*, "P-TEFb Activation by RBM7 Shapes a Pro-survival Transcriptional Response to Genotoxic Stress," *Mol Cell*, vol. 74, no. 2, pp. 254-267.e10, 2019, doi: 10.1016/j.molcel.2019.01.033.

[151] M. E. Borisova *et al.*, "P38-MK2 signaling axis regulates RNA metabolism after UV-light-induced DNA damage," *Nat Commun*, vol. 9, no. 1, 2018, doi: 10.1038/s41467-018-03417-3.

[152] H. Lans, J. H. J. Hoeijmakers, W. Vermeulen, and J. A. Marteijn, "The DNA damage response to transcription stress," *Nature Reviews Molecular Cell Biology*, vol. 20, no. 12. Nature Research, pp. 766–784, Dec. 01, 2019. doi: 10.1038/s41580-019-0169-4.

[153] H. Lans, J. A. Marteijn, B. Schumacher, J. H. J. Hoeijmakers, G. Jansen, and W. Vermeulen, "Involvement of global genome repair, transcription coupled repair, and chromatin remodeling in UV DNA damage response changes during developm," *PLoS Genet*, vol. 6, no. 5, p. 41, 2010, doi: 10.1371/journal.pgen.1000941.

[154] Y. Nakazawa *et al.*, "Ubiquitination of DNA Damage-Stalled RNAPII Promotes Transcription-Coupled Repair," *Cell*, vol. 180, no. 6, pp. 1228-1244.e24, 2020, doi: 10.1016/j.cell.2020.02.010.

[155] A. Tufegdžić Vidaković *et al.*, "Regulation of the RNAPII Pool Is Integral to the DNA Damage Response," *Cell*, vol. 180, no. 6, pp. 1245-1261.e21, 2020, doi: 10.1016/j.cell.2020.02.009.

[156] Y. Y. Chiou, J. Hu, A. Sancar, and C. P. Selby, "RNA polymerase II is released from the DNA template during transcription-coupled repair in mammalian cells," *Journal of Biological Chemistry*, vol. 293, no. 7, pp. 2476–2486, 2018, doi: 10.1074/jbc.RA117.000971.

[157] D. C. Di Giammartino, K. Nishida, and J. L. Manley, "Mechanisms and consequences of alternative polyadenylation," *Mol Cell.*, vol. 23, no. 1, pp. 1–7, 2011, doi: 10.1016/j.molcel.2011.08.017.Mechanisms.

[158] D. Chowdhury, Y. E. Choi, and M. E. Brault, "Charity begins at home: Non-coding RNA functions in DNA repair," *Nat Rev Mol Cell Biol*, vol. 14, no. 3, pp. 181–189, 2013, doi: 10.1038/nrm3523.

[159] C. Ohle, R. Tesorero, G. Schermann, N. Dobrev, I. Sinning, and T. Fischer, "Transient RNA-DNA Hybrids Are Required for Efficient Double-Strand Break Repair," *Cell*, vol. 167, no. 4, pp. 1001-1013.e7, 2016, doi: 10.1016/j.cell.2016.10.001.

[160] S. F. Mansilla *et al.*, "Cyclin Kinase-independent role of p21CDKN1A in the promotion of nascent DNA elongation in unstressed cells," *Elife*, vol. 5, pp. 1–26, 2016, doi: 10.7554/eLife.18020.

[161] F. Ardito, M. Giuliani, D. Perrone, G. Troiano, and L. Lo Muzio, "The crucial role of protein phosphorylation in cell signalingand its use as targeted therapy (Review)," *Int J Mol Med*, vol. 40, no. 2, pp. 271–280, 2017, doi: 10.3892/ijmm.2017.3036.

[162] X. Li, M. Wilmanns, J. Thornton, and M. Köhn, "Elucidating Human Phosphatase-Substrate Networks," pp. 1–14, 2013, doi: DOI: 10.1126/scisignal.2003203.

[163] F. Sacco, L. Perfetto, L. Castagnoli, and G. Cesareni, “The human phosphatase interactome: An intricate family portrait,” *FEBS Letters*, vol. 586, no. 17. pp. 2732–2739, Aug. 14, 2012. doi: 10.1016/j.febslet.2012.05.008.

[164] A. M. Bode and Z. Dong, “Mitogen-activated protein kinase activation in UV-induced signal transduction.,” *Sci STKE*, vol. 2003, no. 167, pp. 38–40, 2003, doi: 10.1126/scisignal.1672003re2.

[165] V. Muthusamy and T. J. Piva, “The UV response of the skin: A review of the MAPK, NFκB and TNFα signal transduction pathways,” *Arch Dermatol Res*, vol. 302, no. 1, pp. 5–17, 2010, doi: 10.1007/s00403-009-0994-y.

[166] D. Kitagawa *et al.*, “Activation of extracellular signal-regulated kinase by ultraviolet is mediated through Src-dependent epidermal growth factor receptor phosphorylation. Its implication in an anti-apoptotic function,” *Journal of Biological Chemistry*, vol. 277, no. 1, pp. 366–371, 2002, doi: 10.1074/jbc.M107110200.

[167] M. Cargnello and P. P. Roux, “Activation and Function of the MAPKs and Their Substrates, the MAPK-Activated Protein Kinases,” *Microbiology and Molecular Biology Reviews*, vol. 75, no. 1, pp. 50–83, 2011, doi: 10.1128/mmbr.00031-10.

[168] K. Szoltysek, A. Walaszczyk, P. Janus, M. Kimmel, and P. Widlak, “Irradiation with UV-C inhibits TNF-α-dependent activation of the NF-κB pathway in a mechanism potentially mediated by reactive oxygen species,” *Genes to Cells*, vol. 22, no. 1, pp. 45–58, Jan. 2017, doi: 10.1111/gtc.12455.

[169] A. A. Alafiatayo, K. S. Lai, S. Ahmad, M. Mahmood, and N. A. Shaharuddin, “RNA-Seq analysis revealed genes associated with UV-induced cell necrosis through MAPK/TNF-α pathways in human dermal fibroblast cells as an inducer of premature photoaging,” *Genomics*, vol. 112, no. 1, pp. 484–493, 2020, doi: 10.1016/j.ygeno.2019.03.011.

[170] Winter-Vann and and Johnson, “Integrated Activation of MAP3Ks Balances Cell Fate in Response to Stress.” 2007.

[171] A. Zeke, M. Misheva, A. Reményi, and M. A. Bogoyevitch, “JNK Signaling: Regulation and Functions Based on Complex Protein-Protein Partnerships,” *Microbiology and Molecular Biology Reviews*, vol. 80, no. 3, pp. 793–835, 2016, doi: 10.1128/mmbr.00043-14.

[172] C. R. Weston and R. J. Davis, “The JNK signal transduction pathway,” *Curr Opin Cell Biol*, vol. 19, no. 2, pp. 142–149, 2007, doi: 10.1016/j.ceb.2007.02.001.

[173] C. López-Camarillo, E. A. Ocampo, M. L. Casamichana, C. Pérez-Plasencia, E. Álvarez-Sánchez, and L. A. Marchat, “Protein kinases and transcription factors activation in response to UV-radiation of skin: Implications for carcinogenesis,” *Int J Mol Sci*, vol. 13, no. 1, pp. 142–172, 2012, doi: 10.3390/ijms13010142.

[174] P. C. Calses *et al.*, “DGCR8 Mediates Repair of UV-Induced DNA Damage Independently of RNA Processing,” *Cell Rep*, vol. 19, no. 1, pp. 162–174, 2017, doi: 10.1016/j.celrep.2017.03.021.

[175] E. D. Gallagher, S. Xu, C. Moomaw, C. A. Slaughter, and M. H. Cobb, “Binding of JNK/SAPK to MEKK1 is regulated by phosphorylation,” *Journal of Biological Chemistry*, vol. 277, no. 48, pp. 45785–45792, 2002, doi: 10.1074/jbc.M207702200.

[176] L. Jinlian, Z. Yingbin, and W. Chunbo, “p38 MAPK in regulating cellular responses to ultraviolet radiation.,” *J Biomed Sci*, vol. 14, no. 3, pp. 303–312, 2007, doi: 10.1007/s11373-007-9148-4.

[177] Z. Miyake, M. Takekawa, Q. Ge, and H. Saito, "Activation of MTK1/MEKK4 by GADD45 through Induced N-C Dissociation and Dimerization-Mediated trans Autophosphorylation of the MTK1 Kinase Domain," *Molecular and Cell Biology*, pp. 2765–2776, Aug. 2007, doi: https://doi.org/10.1128/MCB.01435-06.

[178] M. Takekawa and H. Saito, "A family of stress-inducible GADD45-like proteins mediate activation of the stress-responsive MTK1/MEKK4 MAPKKK," *Cell*, vol. 95, no. 4, pp. 521–530, 1998, doi: 10.1016/S0092-8674(00)81619-0.

[179] M. Raman, S. Earnest, K. Zhang, Y. Zhao, and M. H. Cobb, "TAO kinases mediate activation of p38 in response to DNA damage," *EMBO Journal*, vol. 26, no. 8, pp. 2005–2014, Apr. 2007, doi: 10.1038/sj.emboj.7601668.

[180] L. Courtial *et al.*, "The c-Jun N-terminal kinase prevents oxidative stress induced by UV and thermal stresses in corals and human cells," *Sci Rep*, vol. 7, no. March, pp. 1–10, 2017, doi: 10.1038/srep45713.

[181] H. C. Ding M, Li J, Leonard SS, Shi X, Costa M, Castranova V, Vallyathan V, "Differential role of hydrogen peroxide in UV-induced signal transduction," *Mol Cell Biochem*, 2002, [Online]. Available: https://pubmed.ncbi.nlm.nih.gov/12162463/

[182] I. Dolado, A. Swat, N. Ajenjo, G. De Vita, A. Cuadrado, and A. R. Nebreda, "p38α MAP Kinase as a Sensor of Reactive Oxygen Species in Tumorigenesis," *Cancer Cell*, vol. 11, no. 2, pp. 191–205, 2007, doi: 10.1016/j.ccr.2006.12.013.

[183] L. Lu, L. Wang, and B. Shell, "UV-Induced Signaling Pathways Associated with Corneal Epithelial Cell Apoptosis," *Invest Ophthalmol Vis Sci*, vol. 44, no. 12, pp. 5102–5109, 2003, doi: 10.1167/iovs.03-0591.

[184] B. Fuller, "Role of PGE-2 and Other Inflammatory Mediators in Skin Aging and Their Inhibition by Topical Natural Anti-Inflammatorie," *Cosmetics*, vol. 6, no. 1, 2019, doi: 10.3390/cosmetics6010006.

[185] A. Kammeyer and R. M. Luiten, "Oxidation events and skin aging," *Ageing Res Rev*, vol. 21, pp. 16–29, 2015, doi: 10.1016/j.arr.2015.01.001.

[186] M. Ichihashi *et al.*, "UV-induced skin damage," *Toxicology*, vol. 189, no. 1–2, pp. 21–39, 2003, doi: 10.1016/S0300-483X(03)00150-1.

[187] M. Piepkorn, H. Predd, R. Underwood, and P. Cook, "Proliferation-differentiation relationships in the expression of heparin-binding epidermal growth factor-related factors and erbB receptors by normal and psoriatic human keratinocytes," *Arch Dermatol Res*, vol. 295, no. 3, pp. 93–101, 2003, doi: 10.1007/s00403-003-0391-x.

[188] H. Matsuura, F. Myokai, J. Arata, S. Noji, and S. Taniguchi, "Expression of type II transforming growth factor-β receptor mRNA in human skin, as revealed by in situ hybridization," *J Dermatol Sci*, vol. 8, no. 1, pp. 25–32, 1994, doi: 10.1016/0923-1811(94)90317-4.

[189] P. Schmid, P. Itin, and T. H. Rufli, "In situ analysis of transforming growth factors-β (TGF-β1, TGF-β2, TGF-β3) and TGF-β type II receptor expression in basal cell carcinomas," *British Journal of Dermatology*, vol. 134, no. 6, pp. 1044–1051, 1996, doi: 10.1111/j.1365-2133.1996.tb07940.x.

[190] N. Iram *et al.*, "Age-related changes in expression and function of toll-like receptors in human skin," *Development (Cambridge)*, vol. 139, no. 22, pp. 4210–4219, 2012, doi: 10.1242/dev.083477.

[191] T. S. Kupper, "Immune and inflammatory processes in cutaneous tissues: Mechanisms and speculations," *Journal of Clinical Investigation*, vol. 86, no. 6, pp. 1783–1789, 1990, doi: 10.1172/jci114907.

[192] R. T. Lee, W. H. Briggs, G. C. Cheng, H. B. Rossiter, P. Libby, and T. Kupper, "Mechanical deformation promotes secretion of IL-1 alpha and IL-1 receptor antagonist.," *The Journal of Immunology*, vol. 159, no. 10, pp. 5084–5088, Nov. 1997, doi: 10.4049/jimmunol.159.10.5084.

[193] T. B. El-Abaseri, B. Hammiller, S. K. Repertinger, and L. A. Hansen, "The Epidermal Growth Factor Receptor Increases Cytokine Production and Cutaneous Inflammation in Response to Ultraviolet Irradiation," *ISRN Dermatol*, vol. 2013, pp. 1–11, Jun. 2013, doi: 10.1155/2013/848705.

[194] A. L. Kim *et al.*, "Role of p38 MAPK in UVB-induced inflammatory responses in the skin of SKH-1 hairless mice," *Journal of Investigative Dermatology*, vol. 124, no. 6, pp. 1318–1325, 2005, doi: 10.1111/j.0022-202X.2005.23747.x.

[195] G. Bonizzi and M. Karin, "The two NF-κB activation pathways and their role in innate and adaptive immunity," *Trends Immunol*, vol. 25, no. 6, pp. 280–288, 2004, doi: 10.1016/j.it.2004.03.008.

[196] S. Basak *et al.*, "A Fourth IκB Protein within the NF-κB Signaling Module," *Cell*, vol. 128, no. 2, pp. 369–381, 2007, doi: 10.1016/j.cell.2006.12.033.

[197] N. Parameswaran *et al.*, "Arrestin-2 and G protein-coupled receptor kinase 5 interact with NFκB1 p105 and negatively regulate lipopolysaccharide-stimulated ERK1/2 activation in macrophages," *Journal of Biological Chemistry*, vol. 281, no. 45, pp. 34159–34170, 2006, doi: 10.1074/jbc.M605376200.

[198] P. K. Chaudhary and S. Kim, "The grks reactome: Role in cell biology and pathology," *International Journal of Molecular Sciences*, vol. 22, no. 7. MDPI, Apr. 01, 2021. doi: 10.3390/ijms22073375.

[199] S. Patial, J. Luo, K. J. Porter, J. L. Benovic, and N. Parameswaran, "G-protein-coupled-receptor kinases mediate TNFα-induced NF-κB signalling via direct interaction with and phosphorylation of IκBα," *Biochemical Journal*, vol. 425, no. 1, pp. 169–178, Jan. 2010, doi: 10.1042/BJ20090908.

[200] S. H. Cant and J. A. Pitcher, "G Protein-coupled Receptor Kinase 2–mediated Phosphorylation of Ezrin Is Required for G Protein- coupled Receptor–dependent Reorganization of the Actin Cytoskeleton," *Mol Biol Cell*, vol. 16, no. 7, pp. 3088–3099, 2005, doi: https://doi.org/10.1091/mbc.e04-10-0877.

[201] G. M. Barton and R. Medzhitov, "Toll-Like Receptor Signaling Pathways," *Science (1979)*, vol. 300, pp. 1524–1525, Jun. 2003, doi: DOI: 10.1126/science.1085536.

[202] X. Wang, Z. Bi, Y. Wang, and Y. Wang, "Increased MAPK and NF-κB expression of Langerhans cells is dependent on TLR2 and TLR4, and increased IRF-3 expression is partially dependent on TLR4 following UV exposure," *Mol Med Rep*, vol. 4, no. 3, pp. 541–546, May 2011, doi: 10.3892/mmr.2011.450.

[203] T. M. Ansary, M. R. Hossain, K. Kamiya, M. Komine, and M. Ohtsuki, "Inflammatory molecules associated with ultraviolet radiation-mediated skin aging," *Int J Mol Sci*, vol. 22, no. 8, 2021, doi: 10.3390/ijms22083974.

[204] E. Batlle and J. Massagué, “Transforming Growth Factor-β Signaling in Immunity and Cancer,” *Immunity*, vol. 50, no. 4, pp. 924–940, 2019, doi: 10.1016/j.immuni.2019.03.024.

[205] J. Massagué, “How cells read TGF-β signals,” *Nat Rev Mol Cell Biol*, vol. 1, pp. 169–178, 2000, doi: DOI: 10.1038/35043051.

[206] T. Quan, E. Little, H. Quan, Z. Qin, J. J. Voorhees, and G. J. Fisher, “Elevated Matrix Metalloproteinases and Collagen Fragmentation in Photodamaged Human Skin: Impact of Altered Extracellular Matrix Microenvironment on Dermal Fibroblast Function Taihao,” *Nature*, vol. 133, no. 5, pp. 1362–1366, 2013, doi: 10.1038/jid.2012.509.Elevated.

[207] K. E. Hoot, M. Oka, G. Han, E. Bottinger, Q. Zhang, and X. J. Wang, “HGF upregulation contributes to angiogenesis in mice with keratinocyte-specific Smad2 deletion,” *Journal of Clinical Investigation*, vol. 120, no. 10, pp. 3606–3616, 2010, doi: 10.1172/JCI43304.

[208] T. H. Quan, T. Y. He, S. Kang, J. J. Voorhees, and G. J. Fisher, “Ultraviolet irradiation alters transforming growth factor β/Smad pathway in human skin in vivo,” *Journal of Investigative Dermatology*, vol. 119, no. 2, pp. 499–506, 2002, doi: 10.1046/j.1523-1747.2002.01834.x.

[209] G. Han *et al.*, “Distinct mechanisms of TGF-β1-mediated epithelial-to- mesenchymal transition and metastasis during skin carcinogenesis,” *Journal of Clinical Investigation*, vol. 115, no. 7, pp. 1714–1723, 2005, doi: 10.1172/JCI24399.

[210] K. E. Hoot *et al.*, “Keratinocyte-specific Smad2 ablation results in increased epithelial-mesenchymal transition during skin cancer formation and progression,” *Journal of Clinical Investigation*, vol. 118, no. 8, pp. 2722–2732, 2008, doi: 10.1172/JCI33713.

[211] P. Cammareri *et al.*, “Inactivation of TGFβ receptors in stem cells drives cutaneous squamous cell carcinoma,” *Nat Commun*, vol. 7, pp. 1–14, 2016, doi: 10.1038/ncomms12493.

[212] D. Xu *et al.*, “The effect of ultraviolet radiation on the transforming growth factor beta 1/Smads pathway and p53 in actinic keratosis and normal skin,” *Arch Dermatol Res*, vol. 305, no. 9, pp. 777–786, 2013, doi: 10.1007/s00403-013-1361-6.

[213] Z. Wang, “Regulation of cell cycle progression by growth factor-induced cell signaling,” *Cells*, vol. 10, no. 12, 2021, doi: 10.3390/cells10123327.

[214] A. Panagopoulos and M. Altmeyer, “The Hammer and the Dance of Cell Cycle Control,” *Trends Biochem Sci*, vol. 46, no. 4, pp. 301–314, 2021, doi: 10.1016/j.tibs.2020.11.002.

[215] N. Hustedt and D. Durocher, “The control of DNA repair by the cell cycle,” *Nat Cell Biol*, vol. 19, no. 1, pp. 1–9, 2017, doi: 10.1038/ncb3452.

[216] S. M. Jones and A. Kazlauskas, “Growth factor-dependent signaling and cell cycle progression,” *FEBS Lett*, vol. 490, no. 3, pp. 110–116, 2001, doi: 10.1016/S0014-5793(01)02113-5.

[217] D. Killander and A. Zetterberg, “Quantitative cytochemical studies on interphase growth. I. Determination of DNA, RNA and mass content of age determined mouse fibroblasts in vitro and of intercellular variation in generation time,” *Exp Cell Res*, vol. 38, no. 2, pp. 272–284, 1965, doi: 10.1016/0014-4827(65)90403-9.

[218] D. Killander and A. Zetterberg, “A quantitative cytochemical investigation of the relationship between cell mass and initiation of DNA synthesis in mouse fibroblasts in vitro,” *Exp Cell Res*, vol. 40, no. 1, pp. 12–20, 1965, doi: 10.1016/0014-4827(65)90285-5.

[219] R. Nash, G. Tokiwa, S. Anand, K. Erickson, and A. B. Futcher, "The WHI1+ gene of Saccharomyces cerevisiae tethers cell division to cell size and is a cyclin homolog.," *EMBO J*, vol. 7, no. 13, pp. 4335–4346, 1988, doi: 10.1002/j.1460-2075.1988.tb03332.x.

[220] P. Jorgensen, J. L. Nishikawa, B. J. Breitkreutz, and M. Tyers, "Systematic identification of pathways that couple cell growth and division in yeast," *Science (1979)*, vol. 297, no. 5580, pp. 395–400, 2002, doi: 10.1126/science.1070850.

[221] S. Pavey, T. Russell, and B. Gabrielli, "G2 phase cell cycle arrest in human skin following UV irradiation," *Oncogene*, vol. 20, no. 43, pp. 6103–6110, 2001, doi: 10.1038/sj.onc.1204707.

[222] T. A. Weinert and L. H. Hartwell, "The RAD9 gene controls the cell cycle response to DNA damage in saccharomyces cerevisiae," *Science (1979)*, vol. 241, no. 4863, pp. 317–322, 1988, doi: 10.1126/science.3291120.

[223] M. J. O'Connell, N. C. Walworth, and A. M. Carr, "The G2-phase DNA-damage checkpoint," *Trends Cell Biol*, vol. 10, no. 7, pp. 296–303, 2000, doi: 10.1016/S0962-8924(00)01773-6.

[224] F. Al-Khodairy and A. M. Carr, "DNA repair mutants defining G2 checkpoint pathways in Schizosaccharomyces pombe.," *EMBO J*, vol. 11, no. 4, pp. 1343–1350, 1992, doi: 10.1002/j.1460-2075.1992.tb05179.x.

[225] C. Tapia-Alveal, T. M. Calonge, and M. J. O'Connell, "Regulation of Chk1," *Cell Div*, vol. 4, pp. 3–9, 2009, doi: 10.1186/1747-1028-4-8.

[226] C. Latif, N. R. den Elzen, and M. J. O'Connell, "DNA damage checkpoint maintenance through sustained Chk1 activity," *J Cell Sci*, vol. 117, no. 16, pp. 3489–3498, 2004, doi: 10.1242/jcs.01204.

[227] F. Al-Khodairy, E. Fotou, K. S. Sheldrick, D. J. F. Griffiths, A. R. Lehmann, and A. M. Carr, "Identification and characterization of new elements involved in checkpoint and feedback controls in fission yeast," *Mol Biol Cell*, vol. 5, no. 2, pp. 147–160, 1994, doi: 10.1091/mbc.5.2.147.

[228] C. A. MacDougall, T. S. Byun, C. Van, M. C. Yee, and K. A. Cimprich, "The structural determinants of checkpoint activation," *Genes Dev*, vol. 21, no. 8, pp. 898–903, 2007, doi: 10.1101/gad.1522607.

[229] M. J. O'Connell and K. A. Cimprich, "G2 damage checkpoints: What is the turn-on?," *J Cell Sci*, vol. 118, no. 1, pp. 1–6, 2005, doi: 10.1242/jcs.01626.

[230] X. Lu, B. Nannenga, and L. a Donehower, "PPM1D dephosphorylates Chk1 and p53 and abrogates cell cycle checkpoints," *Genes Dev*, vol. 19, no. 10, pp. 1162–1174, 2005, doi: DOI: 10.1101/gad.1291305.

[231] N. Den Elzen, A. Kosoy, H. Christopoulos, and M. J. O'Connell, "Resisting arrest: Recovery from checkpoint arrest through dephosphorylation of Chk1 by PP1," *Cell Cycle*, vol. 3, no. 5, pp. 529–533, 2004, doi: 10.4161/cc.3.5.820.

[232] L. E. Giono and J. J. Manfredi, "The p53 Tumor Suppressor Participates in Multiple Cell Cycle Checkpoints," *Journal Cellular Physiology*, vol. 211(3), no. May, pp. 736–747, 2006, doi: 10.1002/JCP.

[233] L. A. Carvajal, P. J. Hamard, C. Tonnessen, and J. J. Manfredi, "E2F7, a novel target, is up-regulated by p53 and mediates DNA damage-dependent transcriptional repression," *Genes Dev*, vol. 26, no. 14, pp. 1533–1545, 2012, doi: 10.1101/gad.184911.111.

[234] S. S. Clair *et al.*, "DNA damage-induced downregulation of Cdc25C is mediated by p53 via two independent mechanisms: One involves direct binding to the cdc25C promoter," *Mol Cell*, vol. 16, no. 5, pp. 725–736, 2004, doi: 10.1016/j.molcel.2004.11.002.

[235] L. A. Carvajal and J. J. Manfredi, "Another fork in the road - Life or death decisions by the tumour suppressor p53," *EMBO Rep*, vol. 14, no. 5, pp. 414–421, 2013, doi: 10.1038/embor.2013.25.

[236] W. Nordstrom and J. M. Abrams, "Guardian ancestry: Fly p53 and damage-inducible apoptosis," *Cell Death Differ*, vol. 7, no. 11, pp. 1035–1038, 2000, doi: 10.1038/sj.cdd.4400766.

[237] K. Sugasawa, "Xeroderma Pigmentosum genes: Functions inside and outside DNA repair," *Carcinogenesis*, vol. 29, no. 3, pp. 455–465, 2008, doi: 10.1093/carcin/bgm282.

[238] O. G. Liu, X. Y. Xiong, C. M. Li, X. S. Zhou, and S. S. Li, "Role of xeroderma pigmentosum group D in cell cycle and apoptosis in cutaneous squamous cell carcinoma A431 cells," *Medical Science Monitor*, vol. 24, pp. 453–460, 2018, doi: 10.12659/MSM.905319.

[239] P. R. Musich, Z. Li, and Y. Zou, "Xeroderma Pigmentosa Group A (XPA), Nucleotide Excision Repair and Regulation by ATR in Response to Ultraviolet Irradiation," 2017, pp. 41–54. doi: 10.1007/978-3-319-56017-5_4.

[240] M. Morino *et al.*, "Mitotic UV irradiation induces a DNA replication-licensing defect that potentiates G1 arrest response," *PLoS One*, vol. 10, no. 3, pp. 1–18, 2015, doi: 10.1371/journal.pone.0120553.

[241] T. Wittmann, A. Hyman, and A. Desai, "The spindle: A dynamic assembly of microtubules and motors," *Nat Cell Biol*, vol. 3, no. 1, 2001, doi: 10.1038/35050669.

[242] J. R. McLean, D. Chaix, M. D. Ohi, and K. L. Gould, "State of the APC/C: Organization, function, and structure," *Crit Rev Biochem Mol Biol*, vol. 46, no. 2, pp. 118–136, 2011, doi: 10.3109/10409238.2010.541420.

[243] M. J. O'Connell, M. J. E. Krien, and T. Hunter, "Never say never. The NIMA-related protein kinases in mitotic control," *Trends Cell Biol*, vol. 13, no. 5, pp. 221–228, 2003, doi: 10.1016/S0962-8924(03)00056-4.

[244] M. Malumbres and M. Barbacid, "Cell cycle kinases in cancer," *Curr Opin Genet Dev*, vol. 17, no. 1, pp. 60–65, 2007, doi: 10.1016/j.gde.2006.12.008.

[245] H. Nishitani and Z. Lygerou, "DNA Replication Licensing," *Bioscience*, vol. 1, no. 7, pp. 2115–2132, Sep. 2004, doi: https://doi.org/10.2741/1315.

[246] Y. J. Xu, M. Davenport, and T. J. Kelly, "Two-stage mechanism for activation of the DNA replication checkpoint kinase Cds1 in fission yeast," *Genes Dev*, vol. 20, no. 8, pp. 990–1003, 2006, doi: 10.1101/gad.1406706.

[247] J. M. Bailis, D. D. Luche, T. Hunter, and S. L. Forsburg, "Minichromosome Maintenance Proteins Interact with Checkpoint and Recombination Proteins To Promote S-Phase Genome Stability," *Mol Cell Biol*, vol. 28, no. 5, pp. 1724–1738, 2008, doi: 10.1128/mcb.01717-07.

[248] B. E. Stead, C. J. Brandl, M. K. Sandre, and M. J. Davey, "Mcm2 phosphorylation and the response to replicative stress," *BMC Genet*, vol. 13, pp. 1–11, 2012, doi: 10.1186/1471-2156-13-36.

[249] K. Y. Lee and K. Myung, "PCNA modifications for regulation of post-replication repair pathways," *Mol Cells*, vol. 26, no. 1, pp. 5–11, 2008, doi: 10.1016/s1016-8478(23)13956-2.

[250] Y. Zeng, K. C. Forbes, Z. Wu, S. Moreno, H. Piwnica-Worms, and T. Enoch, "Replication checkpoint requires phosphorylation of the phosphatase Cdc25 by Cds1 or Chk1," *Nature*, vol. 395, no. 6701, pp. 507–510, 1998, doi: 10.1038/26766.

[251] B. Furnari, A. Blasina, M. N. Boddy, C. H. McGowan, and P. Russell, "Cdc25 inhibited in vivo and in vitro by checkpoint kinases Cds1 and Chk1," *Mol Biol Cell*, vol. 10, no. 4, pp. 833–845, 1999, doi: 10.1091/mbc.10.4.833.

[252] H. Nishitani and P. Nurse, "p65cdc18 Plays a major role controlling the initiation of DNA replication in fission yeast," *Cell*, vol. 83, no. 3, pp. 397–405, 1995, doi: 10.1016/0092-8674(95)90117-5.

[253] M. J. O'Connell and P. Nurse, "How cells know they are in G1 or G2," *Curr Opin Cell Biol*, vol. 6, no. 6, pp. 867–871, 1994, doi: 10.1016/0955-0674(94)90058-2.

[254] K. Bambino and J. Chu, *Zebrafish in Toxicology and Environmental Health*, 1st ed., vol. 124. Elsevier Inc., 2017. doi: 10.1016/bs.ctdb.2016.10.007.

[255] S. Sieber *et al.*, "Zebrafish as a preclinical in vivo screening model for nanomedicines," *Adv Drug Deliv Rev*, vol. 151–152, pp. 152–168, 2019, doi: 10.1016/j.addr.2019.01.001.

[256] C. B. Kimmel, W. W. Ballard, S. R. Kimmel, B. Ullmann, and T. F. Schilling, "Stages of embryonic development of the zebrafish," *Developmental Dynamics*, vol. 203, no. 3, pp. 253–310, 1995, doi: 10.1002/aja.1002030302.

[257] M. Giannaccini, A. Cuschieri, L. Dente, and V. Raffa, "Non-mammalian vertebrate embryos as models in nanomedicine," *Nanomedicine*, vol. 10, no. 4, pp. 703–719, 2014, doi: 10.1016/j.nano.2013.09.010.

[258] Y. J. Dai *et al.*, "Zebrafish as a model system to study toxicology," *Environ Toxicol Chem*, vol. 33, no. 1, pp. 11–17, 2014, doi: 10.1002/etc.2406.

[259] L. C. Chien, Y. H. Wu, T. N. Ho, Y. Y. Huang, and T. Hsu, "Heat stress modulates nucleotide excision repair capacity in zebrafish (Danio rerio) early and mid-early embryos via distinct mechanisms," *Chemosphere*, vol. 238, p. 124653, 2020, doi: 10.1016/j.chemosphere.2019.124653.

[260] S. Chakravarthy, S. Sadagopan, A. Nair, and S. K. Sukumaran, "Zebrafish as an in vivo high-throughput model for genotoxicity," *Zebrafish*, vol. 11, no. 2, pp. 154–166, 2014, doi: 10.1089/zeb.2013.0924.

[261] D. S. Pei and P. R. Strauss, "Zebrafish as a model system to study DNA damage and repair," *Mutation Research - Fundamental and Molecular Mechanisms of Mutagenesis*, vol. 743–744, pp. 151–159, 2013, doi: 10.1016/j.mrfmmm.2012.10.003.

[262] Y. Chang, W. Y. Lee, Y. J. Lin, and T. Hsu, "Mercury (II) impairs nucleotide excision repair (NER) in zebrafish (Danio rerio) embryos by targeting primarily at the stage of DNA incision," *Aquatic Toxicology*, vol. 192, pp. 97–104, 2017, doi: 10.1016/j.aquatox.2017.09.001.

[263] S. R. Costa, R. R. Velasques, M. L. M. Hoff, M. M. Souza, and J. Z. Sandrini, "Characterization of different DNA repair pathways in hepatic cells of Zebrafish (Danio rerio)," *DNA Repair (Amst)*, vol. 83, Nov. 2019, doi: 10.1016/j.dnarep.2019.102695.

[264] J. Z. Sandrini, G. S. Trindade, L. E. M. Nery, and L. F. Marins, "Time-course expression of DNA repair-related genes in hepatocytes of zebrafish (Danio rerio) after UV-B exposure," *Photochem Photobiol*, vol. 85, no. 1, pp. 220–226, Jan. 2009, doi: 10.1111/j.1751-1097.2008.00422.x.

[265] S. P. G. Moore, J. Kruchten, K. J. Toomire, and P. R. Strauss, “Transcription factors and DNA repair enzymes compete for damaged promoter sites,” *Journal of Biological Chemistry*, vol. 291, no. 11, pp. 5452–5460, Mar. 2016, doi: 10.1074/jbc.M115.672733.

[266] A. Kienzler, S. Bony, and A. Devaux, “DNA repair activity in fish and interest in ecotoxicology: A review,” *Aquatic Toxicology*, vol. 134–135. pp. 47–56, Jun. 05, 2013. doi: 10.1016/j.aquatox.2013.03.005.

[267] S. Fortier, X. Yang, Y. Wang, R. A. O. Bennett, and P. R. Strauss, “Base excision repair in early zebrafish development: Evidence for DNA polymerase switching and standby AP endonuclease activity,” *Biochemistry*, vol. 48, no. 23, pp. 5396–5404, Jun. 2009, doi: 10.1021/bi900253d.

[268] D. S. Pei, P. P. Jia, J. J. Luo, W. Liu, and P. R. Strauss, “AP endonuclease 1 (Apex1) influences brain development linking oxidative stress and DNA repair,” *Cell Death Dis*, vol. 10, no. 5, May 2019, doi: 10.1038/s41419-019-1578-1.

[269] L. Yan *et al.*, “8-Oxoguanine DNA glycosylase 1 (ogg1) maintains the function of cardiac progenitor cells during heart formation in zebrafish,” *Exp Cell Res*, vol. 319, no. 19, pp. 2954–2963, Nov. 2013, doi: 10.1016/j.yexcr.2013.07.012.

[270] C. L. Bladen, S. Navarre, W. S. Dynan, and D. J. Kozlowski, “Expression of the Ku70 subunit (XRCC6) and protection from low dose ionizing radiation during zebrafish embryogenesis,” *Neurosci Lett*, vol. 422, no. 2, pp. 97–102, 2007, doi: 10.1016/j.neulet.2007.05.045.

[271] C. L. Bladen, W. K. Lam, W. S. Dynan, and D. J. Kozlowski, “DNA damage response and Ku80 function in the vertebrate embryo,” *Nucleic Acids Res*, vol. 33, no. 9, pp. 3002–3010, 2005, doi: 10.1093/nar/gki613.

[272] M. Hagmann *et al.*, “Homologous Recombination and DMA-End Joining Reactions in Zygotes and Early Embryos of Zebrafish (Danio rerio) and Drosophila melanogaster,” 1998. doi: DOI:10.1515/bchm.1998.379.6.673.

[273] L. Fan, J. Moon, J. Crodian, and P. Collodi, “Homologous recombination in zebrafish ES cells,” *Transgenic Res*, vol. 15, no. 1, pp. 21–30, 2006, doi: 10.1007/s11248-005-3225-0.

[274] J. Vierstraete, A. Willaert, P. Vermassen, P. J. Coucke, A. Vral, and K. B. M. Claes, “Accurate quantification of homologous recombination in zebrafish: Brca2 deficiency as a paradigm,” *Sci Rep*, vol. 7, no. 1, pp. 1–10, 2017, doi: 10.1038/s41598-017-16725-3.

[275] N. Kumar, N. C. Moreno, B. C. Feltes, C. F. M. Menck, and B. Van Houten, “Cooperation and interplay between base and nucleotide excision repair pathways: From DNA lesions to proteins,” *Genetics and Molecular Biology*, vol. 43, no. 1. Brazilian Journal of Genetics, 2020. doi: 10.1590/1678-4685-GMB-2019-0104.

[276] T. Hsu, C. S. Cheng, C. Y. Shih, and F. L. Yeh, “Detection and partial characterization of a UV-damaged-DNA binding activity highly expressed in zebrafish (Danio rerio) embryos,” 2002.

[277] S. Weber, “Light-driven enzymatic catalysis of DNA repair: A review of recent biophysical studies on photolyase,” *Biochimica et Biophysica Acta - Bioenergetics*, vol. 1707, no. 1 SPEC. ISS. Elsevier, pp. 1–23, Feb. 25, 2005. doi: 10.1016/j.bbabio.2004.02.010.

[278] A. Sancar, “Structure and function of DNA photolyase and cryptochrome blue-light photoreceptors,” *Chem Rev*, vol. 103, no. 6, pp. 2203–2237, Jun. 2003, doi: 10.1021/cr0204348.

[279] Q. Dong, K. Svoboda, T. R. Tiersch, and W. Todd Monroe, “Photobiological effects of UVA and UVB light in zebrafish embryos: Evidence for a competent photorepair system,” *J Photochem Photobiol B*, vol. 88, no. 2–3, pp. 137–146, Sep. 2007, doi: 10.1016/j.jphotobiol.2007.07.002.

[280] C. Yi and C. He, “DNA Repair by Reversal of DNA Damage,” *Cold Spring Harb Perspect Biol*, vol. 5, no. 1, pp. a012575–a012575, Jan. 2013, doi: 10.1101/cshperspect.a012575.

[281] F. G. Kapp *et al.*, “Protection from UV light is an evolutionarily conserved feature of the haematopoietic niche,” 2018. doi: DOI: 10.1038/s41586-018-0213-0.

[282] A. R. Osborn *et al.*, “De novo synthesis of a sunscreen compound in vertebrates,” *Elife*, vol. 4, no. MAY, May 2015, doi: 10.7554/eLife.05919.

[283] J. Kimi and D. Patel, “Contrasting structural impacts induced by cis-syn cyclobutane dimer and (6-4) adduct in DNA duplex decamers: implication in mutagenesis and repair activity,” 1995. doi: doi: 10.1111/j.1751-1097.1995.tb05236.x.

[284] A. S. Balajee and V. A. Bohr, “Genomic heterogeneity of nucleotide excision repair,” *Gene*, vol. 250, no. 1–2. pp. 15–30, May 30, 2000. doi: 10.1016/S0378-1119(00)00172-4.

[285] H. Luze, S. P. Nischwitz, I. Zalaudek, R. Müllegger, and L. P. Kamolz, “DNA repair enzymes in sunscreens and their impact on photoageing—A systematic review,” *Photodermatol Photoimmunol Photomed*, vol. 36, no. 6, pp. 424–432, 2020, doi: 10.1111/phpp.12597.

[286] K. Howe *et al.*, “The zebrafish reference genome sequence and its relationship to the human genome,” *Nature*, vol. 496, no. 7446, pp. 498–503, Apr. 2013, doi: 10.1038/nature12111.

[287] J. F. Amatruda and E. E. Patton, “Chapter 1 Genetic Models of Cancer in Zebrafish,” *International Review of Cell and Molecular Biology*, vol. 271, no. C. pp. 1–34, 2008. doi: 10.1016/S1937-6448(08)01201-X.

[288] P. Mao, J. J. Wyrick, S. A. Roberts, and M. J. Smerdon, “UV-Induced DNA Damage and Mutagenesis in Chromatin,” *Photochemistry and Photobiology*, vol. 93, no. 1. Blackwell Publishing Inc., pp. 216–228, Jan. 01, 2017. doi: 10.1111/php.12646.

[289] J. Hu, O. Adebali, S. Adar, and A. Sancar, “Dynamic maps of UV damage formation and repair for the human genome,” *Proc Natl Acad Sci U S A*, vol. 114, no. 26, pp. 6758–6763, 2017, doi: 10.1073/pnas.1706522114.

[290] L. J. Kuo and L. X. Yang, “γ-H2AX- A novel biomaker for DNA double-strand breaks,” *In Vivo (Brooklyn)*, vol. 22, no. 3, pp. 305–310, 2008.

[291] S. Banerjee and M. Leptin, “Systemic Response to Ultraviolet Radiation Involves Induction of Leukocytic IL-1β and Inflammation in Zebrafish,” *The Journal of Immunology*, vol. 193, no. 3, pp. 1408–1415, Aug. 2014, doi: 10.4049/jimmunol.1400232.

[292] T. Suganuma *et al.*, “The ATAC Acetyltransferase Complex Coordinates MAP Kinases to Regulate JNK Target Genes,” *Cell*, vol. 142, no. 5, pp. 726–736, Sep. 2010, doi: 10.1016/j.cell.2010.07.045.

[293] A. C. Gingras *et al.*, “Hierarchical phosphorylation of the translation inhibitor 4E-BP1,” *Genes Dev*, vol. 15, no. 21, pp. 2852–2864, Nov. 2001, doi: 10.1101/gad.912401.

[294] J. E. Dawson *et al.*, "Non-cooperative 4E-BP2 folding with exchange between eIF4E-binding and binding-incompatible states tunes cap-dependent translation inhibition," *Nat Commun*, vol. 11, no. 1, Dec. 2020, doi: 10.1038/s41467-020-16783-8.

[295] T. O'Neill *et al.*, "Utilization of oriented peptide libraries to identify substrate motifs selected by ATM," *Journal of Biological Chemistry*, vol. 275, no. 30, pp. 22719–22727, Jul. 2000, doi: 10.1074/jbc.M001002200.

[296] N. Wlodarchak, R. Tariq, and R. Striker, "Comparative analysis of the human and zebrafish kinomes: focus on the development of kinase inhibitors HHS Public Access," *Trends Cell Mol Biol*, vol. 10, pp. 49–75, 2015.

[297] K. Watari, M. Nakaya, and H. Kurose, "Multiple functions of G protein-coupled receptor kinases," *Journal of Molecular Signaling*, vol. 9, no. 1. Ubiquity Press Ltd, Mar. 06, 2014. doi: 10.1186/1750-2187-9-1.

[298] E. R. Weiss, M. H. Ducceschi, T. J. Horner, A. Li, C. M. Craft, and S. Osawa, "Species-Specific Differences in Expression of G-Protein-Coupled Receptor Kinase (GRK) 7 and GRK1 in Mammalian Cone Photoreceptor Cells: Implications for Cone Cell Phototransduction," 2001. [Online]. Available: http://www.ncbi.nlm.nih.gov/genome/guide/human/

[299] C. H. Heldin, K. Miyazono, and P. T. Dijke, "TGF-signalling from cell membrane to nucleus through SMAD proteins," 1997. doi: doi: 10.1038/37284.

[300] A. Hemmati-Brivanlou and G. H. Thomsen, "Ventral mesodermal patterning in Xenopus embryos: Expression patterns and activities of BMP-2 and BMP-4," *Developmental Genetics*, vol. 17, no. 1. pp. 78–89, 1995. doi: 10.1002/dvg.1020170109.

[301] R. N. Wang *et al.*, "Bone Morphogenetic Protein (BMP) signaling in development and human diseases," *Genes Dis*, vol. 1, no. 1, pp. 87–105, 2014, doi: 10.1016/j.gendis.2014.07.005.

[302] D. Yadin, P. Knaus, and T. D. Mueller, "Structural insights into BMP receptors: Specificity, activation and inhibition," *Cytokine Growth Factor Rev*, vol. 27, pp. 13–34, 2016, doi: 10.1016/j.cytogfr.2015.11.005.

[303] K. Tsuji *et al.*, "BMP2 activity, although dispensable for bone formation, is required for the initiation of fracture healing," *Nat Genet*, vol. 38, no. 12, pp. 1424–1429, Dec. 2006, doi: 10.1038/ng1916.

[304] K. Bobacz, R. Gruber, A. Soleiman, L. Erlacher, J. S. Smolen, and W. B. Graninger, "Expression of bone morphogenetic protein 6 in healthy and osteoarthritic human articular chondrocytes and stimulation of matrix synthesis in vitro," *Arthritis Rheum*, vol. 48, no. 9, pp. 2501–2508, Sep. 2003, doi: 10.1002/art.11248.

[305] S. Xie *et al.*, "Genotoxic stress-induced activation of Plk3 is partly mediated by Chk2.," *Cell Cycle*, vol. 1, no. 6, pp. 424–429, 2002, doi: 10.4161/cc.1.6.271.

[306] A. Ward and J. W. Hudson, "P53-Dependent and Cell Specific Epigenetic Regulation of the Polo-Like Kinases Under Oxidative Stress," *PLoS One*, vol. 9, no. 1, pp. 1–12, 2014, doi: 10.1371/journal.pone.0087918.

[307] R. Kumar, R. Sanawar, X. Li, and F. Li, "Structure, biochemistry, and biology of PAK kinases," *Gene*, vol. 605. Elsevier B.V., pp. 20–31, Mar. 20, 2017. doi: 10.1016/j.gene.2016.12.014.

[308] J. Roig and J. A. Traugh, “p21-activated Protein Kinase-PAK Is Activated by Ionizing Radiation and Other DNA-damaging Agents,” 1999. doi: DOI:https://doi.org/10.1074/jbc.274.44.31119.

[309] X. Wang, W. R. Chen, and D. Xing, “A pathway from JNK through decreased ERK and Akt activities for FOXO3a nuclear translocation in response to UV irradiation,” *J Cell Physiol*, vol. 227, no. 3, pp. 1168–1178, 2012, doi: 10.1002/jcp.22839.

[310] M. A. Kim *et al.*, “Akt2, but not Akt1, is required for cell survival by inhibiting activation of JNK and p38 after UV irradiation,” *Oncogene*, vol. 28, no. 9, pp. 1241–1247, 2009, doi: 10.1038/onc.2008.487.

[311] J. Yu *et al.*, “Phosphorylation switches protein disulfide isomerase activity to maintain proteostasis and attenuate ER stress,” *EMBO J*, vol. 39, no. 10, pp. 1–21, 2020, doi: 10.15252/embj.2019103841.

[312] P. Walter and D. Ron, “The Unfolded Protein Response: From Stress Pathway to Homeostatic Regulation,” 2011. [Online]. Available: https://www.science.org

[313] H. Nishitoh *et al.*, “ASK1 is essential for endoplasmic reticulum stress-induced neuronal cell death triggered by expanded polyglutamine repeats,” *Genes Dev*, vol. 16, no. 11, pp. 1345–1355, Jun. 2002, doi: 10.1101/gad.992302.

[314] F. Urano *et al.*, “Coupling of Stress in the ER to Activation of JNK Protein Kinases by Transmembrane Protein Kinase IRE1,” *Science (1979)*, vol. 287, pp. 664–666, 2000, doi: 10.1126/science.287.5453.664.

[315] G. S. Hotamisligil and R. J. Davis, “Cell signaling and stress responses,” *Cold Spring Harb Perspect Biol*, vol. 8, no. 10, 2016, doi: 10.1101/cshperspect.a006072.

[316] W. Leung *et al.*, “FANCD2-dependent mitotic DNA synthesis relies on PCNA K164 ubiquitination,” *Cell Rep*, vol. 42, no. 12, p. 113523, 2023, doi: 10.1016/j.celrep.2023.113523.

[317] W. Leung, R. M. Baxley, G. L. Moldovan, and A. K. Bielinsky, “Mechanisms of DNA damage tolerance: post-translational regulation of PCNA,” *Genes*, vol. 10, no. 1. MDPI AG, Jan. 01, 2019. doi: 10.3390/genes10010010.

[318] M. B. Kastan and J. Bartek, “Cell-cycle checkpoints and cancer,” *Nature*, vol. 432, no. 7015, pp. 316–323, Nov. 2004, doi: 10.1038/nature03097.

[319] E. P. Rogakou, C. Boon, C. Redon, and W. M. Bonner, “Megabase chromatin domains involved in DNA double-strand breaks in vivo,” *Journal of Cell Biology*, vol. 146, no. 5, pp. 905–915, 1999, doi: 10.1083/jcb.146.5.905.

[320] I. M. Ward and J. Chen, “Histone H2AX Is Phosphorylated in an ATR-dependent Manner in Response to Replicational Stress,” *Journal of Biological Chemistry*, vol. 276, no. 51, pp. 47759–47762, 2001, doi: 10.1074/jbc.C100569200.

[321] A. Maréchal and L. Zou, “DNA damage sensing by the ATM and ATR kinases,” *Cold Spring Harb Perspect Biol*, vol. 5, no. 9, Sep. 2013, doi: 10.1101/cshperspect.a012716.

[322] S. Matsuoka *et al.*, “ATM and ATR substrate analysis reveals extensive protein networks responsive to DNA damage,” *Science (1979)*, vol. 316, no. 5828, pp. 1160–1166, 2007, doi: 10.1126/science.1140321.

[323] J. Shao, “Ser784 phosphorylation: a clinically relevant enhancer of VCP function in the DNA damage response,” *Mol Cell Oncol*, vol. 7, no. 5, pp. 1–4, 2020, doi: 10.1080/23723556.2020.1796179.

[324] M. Livingstone *et al.*, “Valosin-containing protein phosphorylation at Ser784 in response to DNA damage,” *Cancer Res*, vol. 65, no. 17, pp. 7533–7540, Sep. 2005, doi: 10.1158/0008-5472.CAN-04-3729.

[325] C. Zhu *et al.*, “Phospho-Ser784-VCP Is Required for DNA Damage Response and Is Associated with Poor Prognosis of Chemotherapy-Treated Breast Cancer,” *Cell Rep*, vol. 31, no. 10, Jun. 2020, doi: 10.1016/j.celrep.2020.107745.

[326] A. N. Blackford and S. P. Jackson, “ATM, ATR, and DNA-PK: The Trinity at the Heart of the DNA Damage Response,” *Molecular Cell*, vol. 66, no. 6. Cell Press, pp. 801–817, Jun. 15, 2017. doi: 10.1016/j.molcel.2017.05.015.

[327] A. C. Parplys *et al.*, “NUCKS1 is a novel RAD51AP1 paralog important for homologous recombination and genome stability,” *Nucleic Acids Res*, vol. 43, no. 20, pp. 9817–9834, 2015, doi: 10.1093/nar/gkv859.

[328] S. Panier and S. J. Boulton, “Double-strand break repair: 53BP1 comes into focus,” *Nat Rev Mol Cell Biol*, vol. 15, no. 1, pp. 7–18, 2014, doi: 10.1038/nrm3719.

[329] M. Winter *et al.*, “Deciphering the acute cellular phosphoproteome response to irradiation with X-rays, protons and carbon ions,” *Molecular and Cellular Proteomics*, vol. 16, no. 5, pp. 855–872, 2017, doi: 10.1074/mcp.M116.066597.

[330] M. Di Virgilio *et al.*, “Rif1 prevents resection of DNA breaks and promotes immunoglobulin class switching,” *Science (1979)*, vol. 339, no. 6120, pp. 711–715, 2013, doi: 10.1126/science.1230624.

[331] J. Kang *et al.*, “Functional Interaction of H2AX, NBS1, and p53 in ATM-Dependent DNA Damage Responses and Tumor Suppression,” *Mol Cell Biol*, vol. 25, no. 2, pp. 661–670, 2005, doi: 10.1128/mcb.25.2.661-670.2005.

[332] R. S. Tibbetts *et al.*, “A role for ATR in the DNA damage-induced phosphorylation of p53,” *Genes Dev*, vol. 13, no. 2, pp. 152–157, 1999, doi: 10.1101/gad.13.2.152.

[333] H. C. Reinhardt and M. B. Yaffe, “Kinases that control the cell cycle in response to DNA damage: Chk1, Chk2, and MK2,” *Current Opinion in Cell Biology*, vol. 21, no. 2. pp. 245–255, Apr. 2009. doi: 10.1016/j.ceb.2009.01.018.

[334] H. Christian Reinhardt and M. B. Yaffe, “Phospho-Ser/Thr-binding domains: Navigating the cell cycle and DNA damage response,” *Nat Rev Mol Cell Biol*, vol. 14, no. 9, pp. 563–580, 2013, doi: 10.1038/nrm3640.

[335] Y. Wang and L. L. Chen, “Organization and function of paraspeckles,” *Essays in Biochemistry*, vol. 64, no. 6. Portland Press Ltd, pp. 875–882, Dec. 01, 2020. doi: 10.1042/EBC20200010.

[336] S. Cardinale, B. Cisterna, P. Bonetti, C. Aringhieri, M. Biggiogera, and S. M. L. Barabino, “Subnuclear Localization and Dynamics of the Pre-mRNA 3 End Processing Factor Mammalian Cleavage Factor I 68-kDa Subunit □ D,” *Mol Biol Cell*, vol. 18, pp. 1282–1292, 2007, doi: 10.1091/mbc.E06.

[337] D. M. Mitrea and R. W. Kriwacki, “Phase separation in biology; Functional organization of a higher order Short linear motifs - The unexplored frontier of the eukaryotic proteome,” *Cell Communication and Signaling*, vol. 14, no. 1. BioMed Central Ltd., Jan. 05, 2016. doi: 10.1186/s12964-015-0125-7.

[338] E. Taiana *et al.*, “Long non-coding RNA NEAT1 targeting impairs the DNA repair machinery and triggers anti-tumor activity in multiple myeloma,” *Leukemia*, vol. 34, no. 1, pp. 234–244, Jan. 2020, doi: 10.1038/s41375-019-0542-5.

[339] H. Sunwoo, M. E. Dinger, J. E. Wilusz, P. P. Amaral, J. S. Mattick, and D. L. Spector, “Men ε/β nuclear-retained non-coding RNAs are up-regulated upon muscle differentiation and are essential components of paraspeckles,” *Genome Res*, vol. 19, no. 3, pp. 347–359, Mar. 2009, doi: 10.1101/gr.087775.108.

[340] L. L. Chen and G. G. Carmichael, “Altered Nuclear Retention of mRNAs Containing Inverted Repeats in Human Embryonic Stem Cells: Functional Role of a Nuclear Noncoding RNA,” *Mol Cell*, vol. 35, no. 4, pp. 467–478, Aug. 2009, doi: 10.1016/j.molcel.2009.06.027.

[341] T. Naganuma, S. Nakagawa, A. Tanigawa, Y. F. Sasaki, N. Goshima, and T. Hirose, “Alternative 3′-end processing of long noncoding RNA initiates construction of nuclear paraspeckles,” *EMBO Journal*, vol. 31, no. 20, pp. 4020–4034, Oct. 2012, doi: 10.1038/emboj.2012.251.

[342] A. H. Fox, Y. W. Lam, A. K. L. Leung, C. E. Lyon, J. Andersen, and M. Mann, “Paraspeckles: A Novel Nuclear Domain,” 2002. doi: https://doi.org/10.1016/S0960-9822(01)00632-7.

[343] K. V. Prasanth *et al.*, “Regulating gene expression through RNA nuclear retention,” *Cell*, vol. 123, no. 2, pp. 249–263, Oct. 2005, doi: 10.1016/j.cell.2005.08.033.

[344] C. M. Borini Etichetti, A. Tenaglia, M. N. Arroyo, and J. E. Girardini, “Expression of zebrafish cpsf6 in embryogenesis and role of protein domains on subcellular localization,” *Gene Expression Patterns*, vol. 36, no. April, p. 119114, 2020, doi: 10.1016/j.gep.2020.119114.

[345] S. Liu, H. Mizu, and H. Yamauchi, “Photoinflammatory responses to UV-irradiated ketoprofen mediated by the induction of ROS generation, enhancement of cyclooxygenase-2 expression, and regulation of multiple signaling pathways,” *Free Radic Biol Med*, vol. 48, no. 6, pp. 772–780, 2010, doi: 10.1016/j.freeradbiomed.2009.12.014.

[346] J. P. Annes, J. S. Munger, and D. B. Rifkin, “Making sense of latent TGFβ activation,” *Journal of Cell Science*, vol. 116, no. 2. pp. 217–224, Jan. 15, 2003. doi: 10.1242/jcs.00229.

[347] E. Gazzerro and E. Canalis, “Bone morphogenetic proteins and their antagonists,” *Rev Endocr Metab Disord*, vol. 7, no. 1–2, pp. 51–65, 2006, doi: 10.1007/s11154-006-9000-6.

[348] B. Li, “Bone Morphogenetic Protein-Smad Pathway as Drug Targets for Osteoporosis and Cancer Therapy,” *Endocrine, Metabolic & Immune Disorders-Drug Targets*, vol. 8, no. 3, pp. 208–219, 2008, doi: 10.2174/187153008785700127.

[349] Y. G. Chen and A. M. Meng, “Negative regulation of TGF-β signaling in development,” 2004. [Online]. Available: http://www.cell-research.com

[350] C. G. Hart and S. Karimi-Abdolrezaee, “Bone morphogenetic proteins: New insights into their roles and mechanisms in CNS development, pathology and repair,” *Exp Neurol*, vol. 334, no. August, p. 113455, 2020, doi: 10.1016/j.expneurol.2020.113455.

[351] K. Harnisch *et al.*, “Myelination in multiple sclerosis lesions is associated with regulation of bone morphogenetic protein 4 and its Antagonist Noggin,” *Int J Mol Sci*, vol. 20, no. 1, Jan. 2019, doi: 10.3390/ijms20010154.

[352] V. Sahni *et al.*, “BMPR1a and BMPR1b signaling exert opposing effects on gliosis after spinal cord injury,” *Journal of Neuroscience*, vol. 30, no. 5, pp. 1839–1855, Feb. 2010, doi: 10.1523/JNEUROSCI.4459-09.2010.

[353] J. K. Sabo, T. D. Aumann, D. Merlo, T. J. Kilpatrick, and H. S. Cate, “Remyelination is altered by bone morphogenic protein signaling in demyelinated lesions,” *Journal of Neuroscience*, vol. 31, no. 12, pp. 4504–4510, Mar. 2011, doi: 10.1523/JNEUROSCI.5859-10.2011.

[354] M. K. H. T. K. and Y. H. Yukihito Kabuyama1, “Early signaling events induced by 280-nm UV irradiation,” vol. 269. pp. 664–670, 2002.

[355] P. P. Roux and J. Blenis, “ERK and p38 MAPK-Activated Protein Kinases: a Family of Protein Kinases with Diverse Biological Functions,” *Microbiology and Molecular Biology Reviews*, vol. 68, no. 2, pp. 320–344, Jun. 2004, doi: 10.1128/mmbr.68.2.320-344.2004.

[356] S. F. G. Krens, S. He, H. P. Spaink, and B. E. Snaar-Jagalska, “Characterization and expression patterns of the MAPK family in zebrafish,” *Gene Expression Patterns*, vol. 6, no. 8, pp. 1019–1026, Oct. 2006, doi: 10.1016/j.modgep.2006.04.008.

[357] M. A. Bogoyevitch and N. W. Court, “Counting on mitogen-activated protein kinases - ERKs 3, 4, 5, 6, 7 and 8,” *Cellular Signalling*, vol. 16, no. 12. pp. 1345–1354, Dec. 2004. doi: 10.1016/j.cellsig.2004.05.004.

[358] G. L. Johnson, H. G. Dohlman, and L. M. Graves, “MAPK kinase kinases (MKKKs) as a target class for small-molecule inhibition to modulate signaling networks and gene expression,” *Current Opinion in Chemical Biology*, vol. 9, no. 3. pp. 325–331, Jun. 2005. doi: 10.1016/j.cbpa.2005.04.004.

[359] T. P. Garrington and G. L. Johnson, “Organization and regulation of mitogen-activated protein kinase signaling pathways,” *Curr Opin Cell Biol*, vol. 11, no. 2, pp. 211–218, 1999, doi: https://doi.org/10.1016/S0955-0674(99)80028-3.

[360] R. E. Chen and J. Thorner, “Function and regulation in MAPK signaling pathways: Lessons learned from the yeast Saccharomyces cerevisiae,” *Biochimica et Biophysica Acta (BBA) - Molecular Cell Research*, vol. 1773, no. 8, pp. 1311–1340, Aug. 2007, doi: 10.1016/j.bbamcr.2007.05.003.

[361] P. Coulombe and S. Meloche, “Atypical mitogen-activated protein kinases: Structure, regulation and functions,” *Biochim Biophys Acta Mol Cell Res*, vol. 1773, no. 8, pp. 1376–1387, 2007, doi: 10.1016/j.bbamcr.2006.11.001.

[362] P. Déléris *et al.*, “Activation loop phosphorylation of ERK3/ERK4 by group I p21-activated kinases (PAKs) defines a novel PAK-ERK3/4-MAPK-activated protein kinase 5 signaling pathway,” *Journal of Biological Chemistry*, vol. 286, no. 8, pp. 6470–6478, 2011, doi: 10.1074/jbc.M110.181529.

[363] A. De La Mota-Peynado, J. Chernoff, and A. Beeser, “Identification of the atypical MAPK Erk3 as a novel substrate for p21-activated Kinase (Pak) activity,” *Journal of Biological Chemistry*, vol. 286, no. 15, pp. 13603–13611, Apr. 2011, doi: 10.1074/jbc.M110.181743.

[364] L. Elkhadragy, H. Alsaran, M. Morel, and W. Long, “Activation loop phosphorylation of ERK3 is important for its kinase activity and ability to promote lung cancer cell invasiveness,” *Journal of Biological Chemistry*, vol. 293, no. 42, pp. 16193–16205, 2018, doi: 10.1074/jbc.RA118.003699.

[365] Q. Cai *et al.*, “MAPK6-AKT signaling promotes tumor growth and resistance to mTOR kinase blockade,” 2021.

[366] L. New *et al.*, “PRAK, a novel protein kinase regulated by the p38 MAP kinase,” *EMBO Journal*, vol. 17, no. 12, pp. 3372–3384, 1998, doi: 10.1093/emboj/17.12.3372.

[367] U. Moens and S. Kostenko, “Structure and function of MK5/PRAK: The loner among the mitogen-activated protein kinase activated protein kinases,” *Biol Chem*, vol. 394, no. 9, pp. 1115–1132, 2013, doi: 10.1515/hsz-2013-0149.

[368] M. Perander *et al.*, “Regulation of atypical MAP kinases ERK3 and ERK4 by the phosphatase DUSP2,” *Sci Rep*, vol. 7, pp. 1–13, 2017, doi: 10.1038/srep43471.

[369] V. A. Klenchint, P. D. Calverttll, and M. Deric Bowndsjj, “Inhibition of rhodopsin kinase by recoverin. Further evidence for a negative feedback system in phototransduction,” 1995. doi: doi: 10.1074/jbc.270.27.16147.

[370] E. N. Gorodovikova, I. I. Senin, and P. P. Philippov, “Calcium-sensitive control of rhodopsin phosphorylation in the reconstituted system consisting of photoreceptor membranes, rhodopsin kinase and recoverin,” *FEBS Lett*, vol. 353, no. 2, pp. 171–172, Oct. 1994, doi: 10.1016/0014-5793(94)01030-7.

[371] S. Kawamura, “Rhodopsin phosphorylation as a mechanism of cyclic GMP phosphodiesterase regulation by S-modulin,” 1993. doi: DOI: 10.1038/362855a0.

[372] N. Ahrens, D. Elbers, H. Greb, U. Janssen-Bienhold, and K. W. Koch, “Interaction of G protein-coupled receptor kinases and recoverin isoforms is determined by localization in zebrafish photoreceptors,” *Biochim Biophys Acta Mol Cell Res*, vol. 1868, no. 4, p. 118946, 2021, doi: 10.1016/j.bbamcr.2020.118946.

[373] O. Rinner, Y. V. Makhankov, O. Biehlmaier, and S. C. F. Neuhauss, “Knockdown of cone-specific kinase GRK7 in larval zebrafish leads to impaired cone response recovery and delayed dark adaptation,” *Neuron*, vol. 47, no. 2, pp. 231–242, Jul. 2005, doi: 10.1016/j.neuron.2005.06.010.

[374] Y. Wada, J. Sugiyama, T. Okano, and Y. Fukada, “GRK1 and GRK7: Unique cellular distribution and widely different activities of opsin phosphorylation in the zebrafish rods and cones,” *J Neurochem*, vol. 98, no. 3, pp. 824–837, Aug. 2006, doi: 10.1111/j.1471-4159.2006.03920.x.

[375] S. Gumeni, Z. Evangelakou, V. G. Gorgoulis, and I. P. Trougakos, “Proteome stability as a key factor of genome integrity,” *International Journal of Molecular Sciences*, vol. 18, no. 10. MDPI AG, Oct. 01, 2017. doi: 10.3390/ijms18102036.

[376] M. González-Quiroz *et al.*, “Proteostasis Meets the DNA Damage Response,” *Trends Cell Biol*, vol. 30, no. 11, pp. 881–891, 2020, doi: 10.1016/j.tcb.2020.09.002ï.

[377] E. Dufey *et al.*, “Genotoxic stress triggers the activation of IRE1α-dependent RNA decay to modulate the DNA damage response,” *Nat Commun*, vol. 11, no. 1, Dec. 2020, doi: 10.1038/s41467-020-15694-y.

[378] J. Son, S. Mogre, F. E. Chalmers, J. Ibinson, S. Worrell, and A. B. Glick, "The Endoplasmic Reticulum Stress Sensor IRE1α Regulates the UV DNA Repair Response through the Control of Intracellular Calcium Homeostasis," *Journal of Investigative Dermatology*, vol. 142, no. 6, pp. 1682-1691.e7, 2022, doi: 10.1016/j.jid.2021.11.010.

[379] E. M. Bahassi, D. L. Myer, R. J. McKenney, R. F. Hennigan, and P. J. Stambrook, "Priming phosphorylation of Chk2 by polo-like kinase 3 (Plk3) mediates its full activation by ATM and a downstream checkpoint in response to DNA damage," *Mutation Research - Fundamental and Molecular Mechanisms of Mutagenesis*, vol. 596, no. 1-2 SPEC. ISS., pp. 166–176, 2006, doi: 10.1016/j.mrfmmm.2005.12.002.

[380] M. Sang *et al.*, "Plk3 inhibits pro-apoptotic activity of p73 through physical interaction and phosphorylation," *Genes to Cells*, vol. 14, pp. 775–788, 2009, doi: https://doi.org/10.1111/j.1365-2443.2009.01309.x.

[381] L. Wang, J. Gao, W. Dai, and L. Lu, "Activation of polo-like kinase 3 by hypoxic stresses," *Journal of Biological Chemistry*, vol. 283, no. 38, pp. 25928–25935, 2008, doi: 10.1074/jbc.M801326200.

[382] Q. Wang *et al.*, "Cell Cycle Arrest and Apoptosis Induced by Human Polo-Like Kinase 3 Is Mediated through Perturbation of Microtubule Integrity," *Mol Cell Biol*, vol. 22, no. 10, pp. 3450–3459, 2002, doi: 10.1128/mcb.22.10.3450-3459.2002.

[383] N. G. Howlett, T. Taniguchi, S. G. Durkin, A. D. D'Andrea, and T. W. Glover, "The Fanconi anemia pathway is required for the DNA replication stress respone and for the regulation of common fragile site stability," *Hum Mol Genet*, vol. 14, no. 5, pp. 693–701, 2005, doi: 10.1093/hmg/ddi065.

[384] M. Ishiai *et al.*, "FANCI phosphorylation functions as a molecular switch to turn on the Fanconi anemia pathway," *Nat Struct Mol Biol*, vol. 15, no. 11, pp. 1138–1146, 2008, doi: 10.1038/nsmb.1504.

[385] L. Geng, C. J. Huntoon, and L. M. Karnitz, "RAD18-mediated ubiquitination of PCNA activates the Fanconi anemia DNA repair network," *Journal of Cell Biology*, vol. 191, no. 2, pp. 249–257, Oct. 2010, doi: 10.1083/jcb.201005101.

[386] N. G. Howlett, J. A. Harney, M. A. Rego, F. W. Kolling IV, and T. W. Glover, "Functional interaction between the fanconi anemia D2 protein and proliferating cell nuclear antigen (PCNA) via a conserved putative PCNA interaction motif," *Journal of Biological Chemistry*, vol. 284, no. 42, pp. 28935–28942, Oct. 2009, doi: 10.1074/jbc.M109.016352.

[387] J. Cox and M. Mann, "MaxQuant enables high peptide identification rates, individualized p.p.b.-range mass accuracies and proteome-wide protein quantification," *Nat Biotechnol*, vol. 26, no. 12, pp. 1367–1372, Dec. 2008, doi: 10.1038/nbt.1511.

[388] J. Cox, N. Neuhauser, A. Michalski, R. A. Scheltema, J. V. Olsen, and M. Mann, "Andromeda: A Peptide Search Engine Integrated into the MaxQuant Environment," *J Proteome Res*, vol. 10, no. 4, pp. 1794–1805, Apr. 2011, doi: 10.1021/pr101065j.

[389] J. E. Elias and S. P. Gygi, "Target-decoy search strategy for increased confidence in large-scale protein identifications by mass spectrometry," *Nat Methods*, vol. 4, no. 3, pp. 207–214, Mar. 2007, doi: 10.1038/nmeth1019.

[390] F. J. Martin *et al.*, "Ensembl 2023," *Nucleic Acids Res*, vol. 51, no. 1 D, pp. D933–D941, Jan. 2023, doi: 10.1093/nar/gkac958.

[391] A. Dobin *et al.*, “STAR: Ultrafast universal RNA-seq aligner,” *Bioinformatics*, vol. 29, no. 1, pp. 15–21, Jan. 2013, doi: 10.1093/bioinformatics/bts635.

[392] Y. Liao, G. K. Smyth, and W. Shi, “FeatureCounts: An efficient general purpose program for assigning sequence reads to genomic features,” *Bioinformatics*, vol. 30, no. 7, pp. 923–930, Apr. 2014, doi: 10.1093/bioinformatics/btt656.

[393] M. I. Love, W. Huber, and S. Anders, “Moderated estimation of fold change and dispersion for RNA-seq data with DESeq2,” *Genome Biol*, vol. 15, no. 12, Dec. 2014, doi: 10.1186/s13059-014-0550-8.

[394] W. Huber *et al.*, “Orchestrating high-throughput genomic analysis with Bioconductor,” *Nat Methods*, vol. 12, no. 2, pp. 115–121, Jan. 2015, doi: 10.1038/nmeth.3252.

[395] G. Yu, L. G. Wang, Y. Han, and Q. Y. He, “ClusterProfiler: An R package for comparing biological themes among gene clusters,” *OMICS*, vol. 16, no. 5, pp. 284–287, May 2012, doi: 10.1089/omi.2011.0118.

[396] G. Yu and Q. Y. He, “ReactomePA: An R/Bioconductor package for reactome pathway analysis and visualization,” *Mol Biosyst*, vol. 12, no. 2, pp. 477–479, 2016, doi: 10.1039/c5mb00663e.

[397] S. Sayols, “rrvgo: a Bioconductor package for interpreting lists of Gene Ontology terms,” 2023. doi: 10.17912/micropub.biology.000811.

[398] M. Kciuk, B. Marciniak, M. Mojzych, and R. Kontek, “Focus on uv-induced DNA damage and repair—disease relevance and protective strategies,” *Int J Mol Sci*, vol. 21, no. 19, pp. 1–33, 2020, doi: 10.3390/ijms21197264.

[399] A. Canedo and T. L. Rocha, “Zebrafish (Danio rerio) using as model for genotoxicity and DNA repair assessments: Historical review, current status and trends,” *Science of the Total Environment*, vol. 762, p. 144084, 2021, doi: 10.1016/j.scitotenv.2020.144084.